LINEAR LIBRARY
C01 0068 2887

VOIDS IN THE DISTRIBUTION OF GALAXIES: an assessment of their significance and implications for large-scale structure formation theories

Guinevere Kauffmann

Thesis submitted for the degree of
Master of Science
at the University of Cape Town
March 1990

The University of Cape Town has been given the right to reproduce this thesis in whole or in part. Copyright is held by the author.

The copyright of this thesis vests in the author. No quotation from it or information derived from it is to be published without full acknowledgement of the source. The thesis is to be used for private study or non-commercial research purposes only.

Published by the University of Cape Town (UCT) in terms of the non-exclusive license granted to UCT by the author.

University of Cape Town

ACKNOWLEDGEMENTS

First and foremost, I must thank my supervisor, Professor Tony Fairall, who introduced me to extragalactic astronomy and thereby influenced not only my choice of Masters degree project, but my preferred research direction as well. His kindness, willingness to listen, and invariably sound advice were very much appreciated and will not be forgotten.

I also say thank you to Lev Kofman, whom I have not yet had the privilege of meeting. His fascinating theory of adhesion and his question: "Can one obtain a spectrum of void sizes?" were the two sources of inspiration that led me to choose the topic of my thesis.

I am grateful to John Huchra for the use of ZCAT (1987), a database that was crucial in that it enabled me to derive a spectrum of void sizes.

There are a number of "behind the scenes" people who have helped me out a great deal. In particular, I am grateful to Graeme Pendock who helped me overcome my natural aversion to computers and turned me into a reasonably competent "hacker". He also helped me draw some of the diagrams appearing in this thesis. I am also indebted to my father, Ken Kauffmann, for lots of useful suggestions and to Archie Maurellis, for numerous enlightening conversations.

TABLE OF CONTENTS

INTRODUCTION

Voids in Extragalactic Astronomy

The reader unacquainted with modern extragalactic astronomy may be forgiven for feeling distinctly puzzled by the title of this thesis. The conventional definition of a void, after all, brings to mind images of nothingness, of regions where no data of any kind exists. Scientists, on the other hand, are generally not interested in nothingness. Scientists are well known for their propensity to want to measure as many things in as many ways as possible. It thus may seem almost paradoxical to learn that the study of empty regions in the sky may be crucial to unravelling some of the mysteries of the Big Bang and explaining the origin of structure in the universe.

In extragalactic astronomy, the three-dimensional region that constitutes a void is transparent and empty, or nearly empty of galaxies. Voids were not immediately recognized in the sky distribution of galaxies because they tend to be overlaid by superimposed background and foreground galaxies. In order to recognize a void, one needs to know the three-dimensional distribution of galaxies in large homogeneous samples. To an approximation that neglects the peculiar motions of galaxies, distances can be estimated from redshifts, using the Hubble relation between redshift and distance. Hubble discovered that there is a linear relation between the redshift of a galaxy cz, and its luminosity distance d_L, with slope H_o which has been estimated to be in the range 50 km/s $Mpc^{-1} < H_o <$ 100 km/s Mpc^{-1}. The observational requirement for determining the three dimensional distribution of galaxies thus reduces to obtaining redshifts from Doppler-shifted spectral lines of galaxies in large homogeneous samples.

In the 1920s it took several nights of observation to accumulate the necessary exposure time for the spectrographic determination of the redshift of a bright galaxy. By the 1950's improvements in the photographic emulsions had reduced the time to about one hour. Then in the 1970s equipment was developed that, at the telescope, continuously subtracts off the contribution from the night sky, electronically integrates the spectrum during the exposure, and then, after only a matter of minutes, transfers the spectrum directly onto magnetic tape for computer utilization, where the final reductions can be performed quickly and as automatically as desired. With modern reduction techniques, Doppler velocities are derived with a typical accuracy of 30 km/s. The techniques of 21 cm astronomy achieve typical accuracies of 10 km/s.

These advances have led to a spectacular growth in the field of extragalactic astronomy. Observational workers have embarked on a systematic and dedicated attack on the problem of determining the direct three-dimensional distribution of galaxies. Theoretical workers have begun to use results from the new data to constrain parameters in old, revised and new models invented for the purpose of explaining the astrophysical origin and evolution of large-scale structure in the universe.

The existence of large superclusters of galaxies has been the subject of many years of controversial discussion, but seems now beyond doubt. The cluster of galaxies near the north galactic pole, with a diameter of 10°, is the Virgo cluster of which our Local Group of galaxies is a part. Long extensions to the right, and across the pole to the left are, together with the Virgo cluster, parts of a supercluster which contains almost all of the bright galaxies in the northern hemisphere. This "Local Supercluster" appears to be a highly non-spherical, disc-like structure with a radius of about 15 Mpc and an axial ratio of about 1:6 [Tully, 1982]. The great number of redshifts that have been measured with large telescopes in recent years have provided clear evidence for other such large-scale structures. [Gregory et al, 1980; Huchra et al,1983; Davis et al, 1982; Tully, 1986]

Perhaps the first use of the term "void" in the extragalactic literature occurred in an article by Chincarini and Rood [1980] describing the stream of research that led to the discovery of superclusters and areas empty of galaxies from early redshift surveys of the Coma and Hercules regions of the sky. "Void" is a natural contraction of the phrase "region devoid of galaxies", which had in fact been used earlier (see for example [Gregory & Thompson 1978] and [Tifft & Gregory 1976]).

The next very exciting and important development in our picture of the universe was the discovery of a "frothy", sheetlike appearance to the distribution of galaxies ([Haynes & Giovanelli 1986], [Fairall et al 1985]). One very well-known depiction of this frothy structure is the famous "slice of the universe", a systematic collection of redshifts of all galaxies of apparent magnitude $m < 15.5$ in a region of the sky measuring 6° by 117° [de Lapparent et al, 1986]. The map of this slice is displayed in figure 1. A slice from an independent survey of galaxies in the Southern Hemisphere [Fairall & Jones 1988] is displayed in figure 2 for comparison. Both plots give an impression of strong clustering of galaxies into thin sheets, filaments, or ridges, whilst space is dominated by large, apparently empty quasi-spherical voids. In other words, *the universe appears to have a bubbly, foam-like*

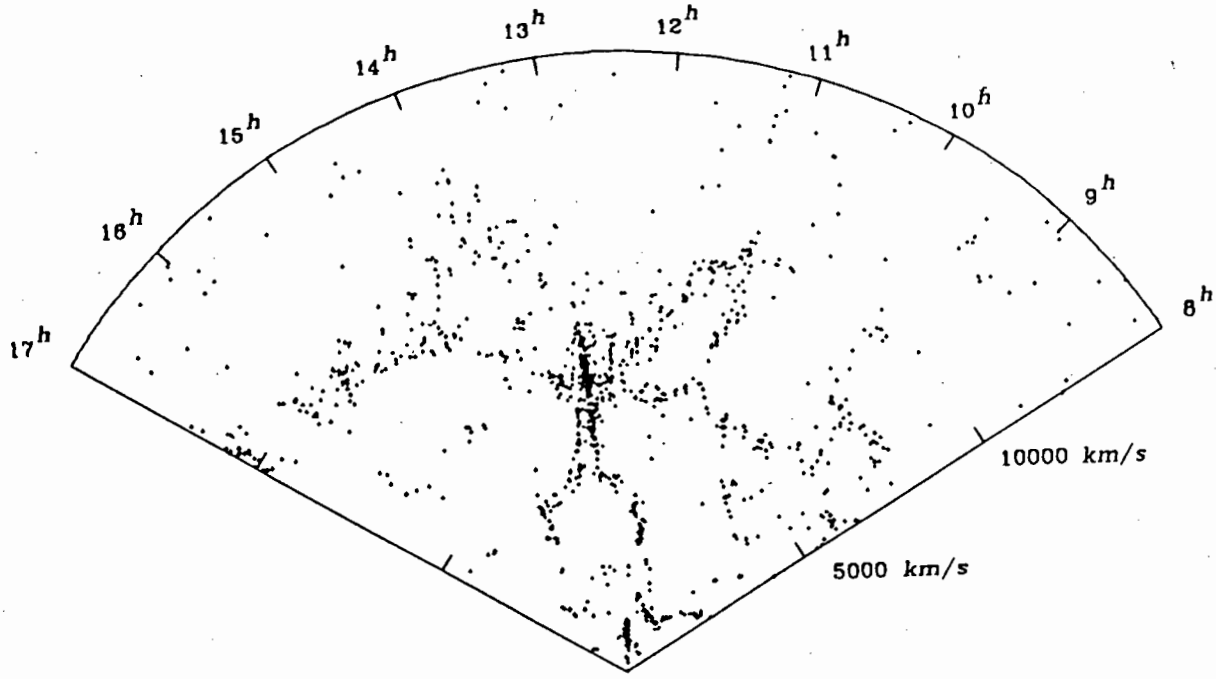

Figure 1 *The CfA "slice of the universe". Map of the observed velocity plotted vs. right ascension in the declination wedge 26.5° ≤ δ ≤ 32.5°.*

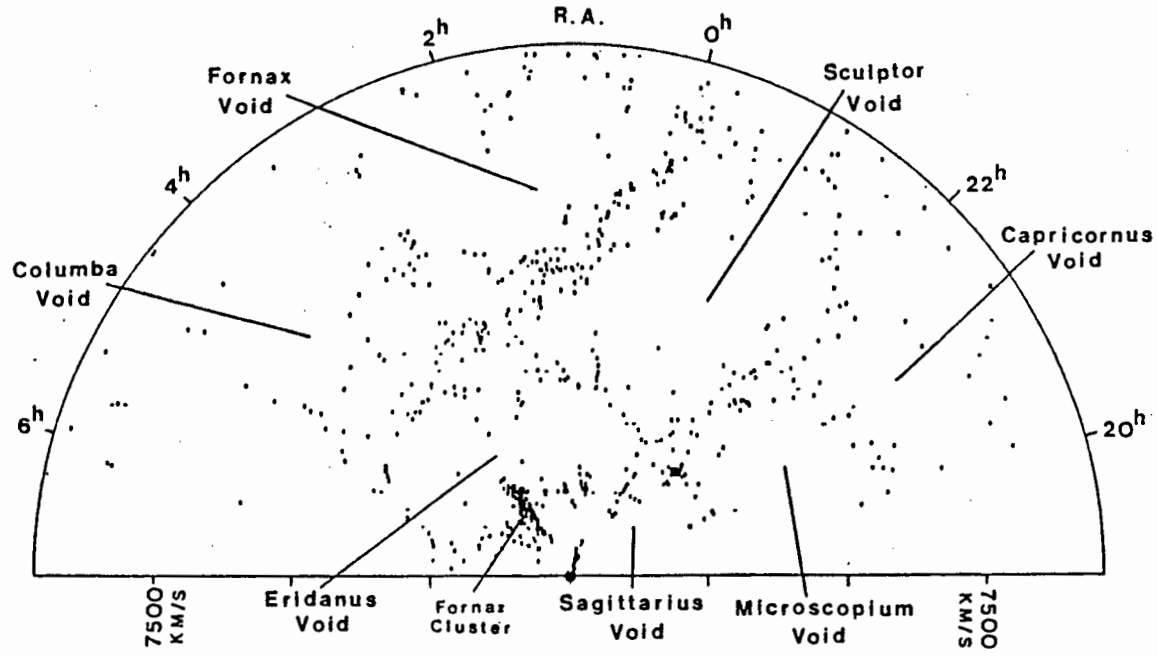

Figure 2 *A slice from the Southern Redshifts Catalogue (1988). The declination limits are -17.5° to -47.5°.*

structure. The large Bootes void - a 50 Mpc hole that does not contain any luminous galaxies - which created much discussion when it was discovered [Kirshner et al, 1981] - is not an exception; structures like it are the rule.

How then should one proceed in analyzing and interpreting the data at hand in order to gain some insight into the origins of the structure described above? Up to now, the standard method has been to study the distribution of the galaxies themselves. Much work has been done in analyzing two-point correlation functions which provide a measure of how galaxies are clustered (see later). Another approach has been to try to incorporate some of the advantages of pattern recognition by using the techniques of percolation and mapping theory. [Doroshkevich et al 1982]

In this thesis, an alternative approach will be presented - the study and analysis of voids; in other words,regions that are empty of galaxies. In a bubbly or foamy universe, voids would intuitively seem to be the fundamental objects to investigate. In the following chapters, it will be shown how the properties and statistics of voids do indeed provide important links between astronomical observations and theories of large scale structure formation.

Chapter I gives an overview of the current well-known theoretical models of large-scale structure formation and explains how the predictions of these models can be tested by the investigation of voids in the distribution of galaxies.

Chapter II reviews work that has already been done on the statistics and properties of voids. In particular, attention is focussed on the establishment of a new statistic, the void probability function, which is sensitive to the presence of voids and is intimately linked to the hierarchy of N-point correlation functions derived by Peebles [1980]. Chapter II also contains a brief review of the work done by Gott on point-smoothing analysis and the use of the topological genus parameter to distinguish between various theoretical models of structure formation.

Chapters III and IV present the original work done by the author in establishing a method of surveying all important voids in the available data. A systematic search for all voids out to a redshift of about 15000 km/s is described. Methods of assessing the significance of these voids are discussed. Upon applying these methods, a list of "statistically significant" voids is constructed and this list is used to derive a spectrum of void sizes. Finally, these chapters illustrate how this new technique of studying voids might serve as an important tool in determining the origins of the large-scale structure observed in the universe today.

CHAPTER I

THEORETICAL MODELS OF LARGE-SCALE STRUCTURE FORMATION

The aim of modern theories of the structure of the universe is to explain the extreme inhomogeneities observed at present - the sizes and shapes of galaxies, the clustering hierarchy of galaxies into groups, clusters and superclusters and the presence of large voids in the distribution of galaxies.

At present there are two main classes of theoretical models. The first class is comprised of the so-called "standard" Gaussian fluctuation models. These models assume that the present large-scale structure is the result of the growth by gravitational interaction of initially small perturbations in a smooth background density. For reasons that will be elaborated on later, these models are not compatible with a universe which contains only baryons. This has led to the development of the Dark Matter models in which the initial density perturbations occur on a non-baryonic background.

The second class of models is comprised of non-Gaussian fluctuation models. The two main contenders are the cosmic string and explosion models. Cosmic strings are curvature singularities predicted by a number of the Grand Unified Theories (GUTs) developed by particle physicists. These curvature singularities turn into closed loops and matter is accreted onto the loops to form galaxies and clusters. In the explosion model, structure is not produced by small density fluctuations in the early universe, but rather from explosions of first-generation objects, which help gravity in forming further galaxies and clusters.

It should be stressed that no single elegant model has yet been proposed that can explain all the observations. Biased cold dark matter models are presently in vogue, but whether the theory will be able to stand up to the latest observational results is still an open question.

The aim of this chapter is to provide an introduction to galaxy formation theory and to present a concise description of some of the current standard theories. This chapter also highlights how these models might be tested by the investigation of voids in the distribution of galaxies.

1.1)Jeans Theory

The first serious theory of galaxy formation was proposed by Sir James Jeans early in this century [Jeans 1902,1928]. Jeans supposed the universe to be filled with a non-relativistic fluid, with mass-density ρ , pressure p, velocity **v** and gravitational field **g**, governed by the equation of continuity

$$\partial_t \rho + \nabla.(\rho \mathbf{v}) = 0 \tag{1}$$

the Euler equation

$$\partial_t \mathbf{v} + (\mathbf{v}.\nabla)\mathbf{v} = (-1/\rho)\nabla p + \mathbf{g} \tag{2}$$

and the gravitational field equations

$$\nabla \times \mathbf{g} = 0 \tag{3}$$

$$\nabla . \mathbf{g} = -4\pi G\rho \tag{4}$$

Introducing into these Newtonian equations small perturbations p_1, ρ_1, $\mathbf{v}_1$ and $\mathbf{g}_1$ and linearizing the equations on the homogeneous background yields:

$$\partial_t \rho_1 + \rho_0 \nabla.\mathbf{v}_1 = 0 \tag{5}$$

$$\partial_t \mathbf{v}_1 = (-c_s^2/\rho_0)\nabla\rho_1 + \mathbf{g}_1 \tag{6}$$

$$\nabla \times \mathbf{g}_1 = 0 \tag{7}$$

$$\nabla.\mathbf{g}_1 = -4\pi G\rho_1 \tag{8}$$

where $c_s^2 = p_1/\rho_1$.

For such adiabatic perturbations ($p_1 = \rho_1 c_s^2$) one finally obtains a wave equation for ρ_1:

$$\partial_{tt}\rho_1 = c_s^2.v\rho_1 + 4\pi G\rho_o\rho_1 \tag{9}$$

An ansatz of the form $\exp[i(\mathbf{k}.\mathbf{x} - \omega t)]$ leads to a dispersion equation

$$\omega^2 = \mathbf{k}^2 - c_s^2 - 4\pi G\rho_0 . \qquad (10)$$

ω is imaginary for wave numbers below the critical value

$$k_j = (4\pi G\rho_0/c_s^2)^{1/2} \qquad (11)$$

so that ρ_1 can grow exponentially. For wave numbers greater than k_j, ω is real and the disturbances propagate as acoustic waves.

Unfortunately, Jeans theory is not applicable to the formation of galaxies in an expanding universe, because Jeans assumed a static medium. The first satisfactory theory of the instabilities in an expanding universe was given by Lifshitz [1946]. Remarkably, many of the results of the Jeans theory still apply. Disturbances at wave numbers below k_j still grow, not exponentially, but like a power of t.

Thus, there are two, distinct, limiting cases. For a long-wavelength perturbation, gravity plays the primary role. Gravity is responsible for the instability of a uniform matter distribution and for the existence of growing density perturbations. For short-wavelength perturbations, however, pressure plays the dominant role. A density perturbation is accompanied by a pressure perturbation which leads to the propagation of an acoustic wave.

The boundary beyond which gravitational instability occurs is determined by the condition $k = k_j$ or $\lambda = 2\pi/k = \lambda_j = 2\pi/k_j$, i.e. this boundary is at the Jeans length. One often speaks of the "Jeans mass", that is the mass contained in the volume $(\lambda_j/2)^3$ -

$$M_j = (\lambda_j/2)^3 . \rho_0 \qquad (12)$$

This is the smallest mass for which the pressure cannot prevent growth in the density under the action of gravity. It is therefore assumed that in the course of time, a homogeneous distribution of matter will separate into discrete objects, each with a mass not less than M_j. The particular masses into which the medium fragments depends on the spectrum of small initial perturbations, about which more will be said later.

1.2) Thermal History of the Early Universe

Particle physicists believe that they have a fairly sound understanding of the physical processes that must have taken place after the first few milliseconds of the big bang. A knowledge of the thermal history of the early universe, together with a theory of gravitational instability as outlined above, enables one to form a picture of how initial density perturbations would have evolved at early times.

Since some knowledge of the thermal history of the early universe will be useful throughout our discussion of galaxy formation theories, a brief summary is presented below.

A) At very early times, when the temperature T was above 10^{12} K, the universe contained a great variety of particles in thermal equilibrium, including photons, leptons, mesons and nucleons and their antiparticles.

B) At the time when $T \approx 10^{12}$ K, the universe contained photons, muons, antimuons, electrons, positrons, neutrinos and antineutrinos. In addition, there was a very small nucleonic contamination, with neutrons and protons in equal numbers. All of these particles were in thermal equilibrium.

C) As the temperature dropped below 10^{12} K, the muons and antimuons began to annihilate. After almost all the muons were gone, the neutrinos and antineutrinos decoupled from the other particles, leaving $e\pm$, photons and a few nucleons in thermal equilibrium, with $T \propto R^{-1}$.

D) As the temperature dropped below 10^{11} K ($t \approx 0.01$ sec), the neutron-proton mass difference began to shift the small nucleonic contamination towards more protons and fewer neutrons.

E) As the temperature dropped below 5×10^9 K ($t \approx 4$ sec), the electron-positron pairs began to annihilate, leaving as the dominant constituents of the universe only photons, neutrinos and antineutrinos, with the photon temperature 40.1% higher than the neutrino temperature. At the same time, the cooling of the neutrinos and antineutrinos, and the disappearance of the electrons and positrons, froze the neutron-proton ratio at about 1:5.

F) At a temperature of about 10^9 K (t ≈ 180 sec), the neutrons rapidly began to fuse with protons into heavier nuclei, leaving an ionized gas of hydrogen and He^4, with about 27% helium by weight, and a trace of He^3 and other elements.

G) The free expansion of photons, neutrinos and antineutrinos continued. The ionized gas temperature remained locked to the photon temperature until hydrogen recombined at T ≈ 4000°K.

H) At some temperature between 10^3 K and 10^5 K, the energy density of the photons, neutrinos and antineutrinos dropped below the rest-mass density of hydrogen and helium, and we entered upon the matter-dominated era.

1.3) The Evolution of the Jeans Mass

Using our knowledge of the thermal history of the universe, it is possible to calculate the evolution of the Jeans mass throughout the early history of the universe. The details are not given here (see [Weinberg 1972]), but figure 3 gives a plot of Jeans mass as a function of radiation temperature.

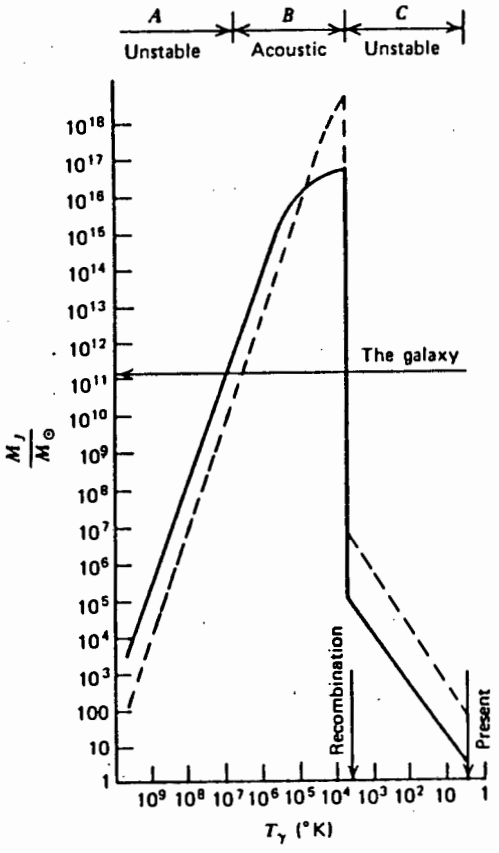

Figure 3 *Jeans mass as a function of radiation temperature. Solid line is for a present mean mass density in the universe of* 3×10^{-29} *g/cm*^{3}. *Dashed line is for a density of* 10^{-30} *g/cm*^{3}.

If we fix our attention on a particular fluctuation whose mass M has the value $M_G \approx 10^{11}$ solar masses of a typical good-sized present galaxy, we may distinguish three phases in its growth.

A) The Jeans mass will be less than the galactic mass until the temperature drops to about 10^7 K. During this period, the amplitude of the fluctuation will have a chance to grow under the influence of its own gravitation. Since the total energy density is dominated in this early phase by radiation, this is a relativistic problem, and the growth rate must be calculated in a general-relativistic formalism.

B) From the time T drops below 10^7 K until the recombination of hydrogen at T ≈ 4000 K, the Jeans mass will be larger than the galactic mass, so the protogalactic disturbance will behave like a packet of ordinary sound waves. No growth is possible during this phase.

C) From the time of recombination until the present, the Jeans mass will be much smaller than the galactic mass, so the fluctuation amplitude can again grow. The total energy density in this phase is dominated by hydrogen rest-mass, so this is a non-relativistic problem, and the growth rate can be treated by Newtonian methods.

There is one disappointing aspect of this general picture. Nothing so far gives any clue to the reason for the observed galactic mass distribution. The Jeans mass just before recombination is very much larger than any galactic mass, whereas the Jeans mass just after recombination appears to be related to the mass of a globular cluster rather than a galaxy.

A partial answer to this puzzle has appeared in calculations of the damping of protogalactic fluctuations while they are undergoing acoustic oscillations in phase B described above.

1.4) The Adiabatic Damping Scale

During the phase when the wavelength of a fluctuation is less than the Jeans length, the fluctuation will undergo acoustic oscillations which can be damped by dissipative processes [Peebles 1980; Weinberg 1971; Silk 1968]. Dissipative effects arise as deviations from thermal equilibrium, for instance when the mean free time between collisions of particles is longer than the expansion time.

For epochs before recombination, the main interaction mechanism between particles is Thomson-scattering of non-relativistic electrons. This scattering of the electrons by the radiation makes any displacement of the electrons through the radiation much like moving through cold, viscous molasses. The viscosity of the fluid therefore inhibits the growth of gravitational instabilities that might be caused by the accretion of matter alone.

Furthermore, just as sound waves in the air die out in a few tens of meters because the particles that make up the pressure waves are scattered and their coherent motion is dissipated as heat, sound waves in the cosmic medium set up by fluctuations lose their energy and die away at all but the longest wavelengths.

It is a requirement of grand unified theories that the ratio of the density of photons to the density of matter always remains the same. Therefore, in the compression phase of a fluctuation sound wave, the compression of photons must match the compression of particles with mass. If the distance covered by a photon in the time since the start of the big bang is greater than the distance across the compressed region of a fluctuation, the photon will in effect not take part in the compression, but will instead dissipate its share of the energy of the fluctuation. Since the photons greatly outnumber the particles with mass, they carry almost all the energy of the fluctuations and so fluctuations on a scale smaller than the average radial displacement of a photon since the start of the big bang are damped out.

In spite of being scattered by electrons, the photons diffuse radially outwards through the medium so fast that they dissipate the energy of all but the longest fluctuations. By the time of recombination, the photons have diffused through a region of the universe whose mass is 10^{14} solar masses. All initial fluctuations that encompass a mass smaller than this are therefore erased.

1.5) The Horizon Scale

It should be noted that there is an upper limit to the size of fluctuation that can be perceived by any observer at a given time. That limit is the spatial horizon of the observer, which is a sphere, centred on the observer, whose radius is equal to the distance light can travel since the time of the Big Bang. Fluctuations undetectable in the early universe become detectable later on, because they begin to be encompassed by the observer's ever-widening horizon.

1.6) The Primeval Fluctuation Spectrum

Up to now, we have only discussed the evolution and behaviour of discrete density perturbations. What concerns us in practice is the entire spectrum of density perturbations, i.e. the evolution of fluctuations on all mass scales.

Up to recently, the general belief amongst theorists has been that at some very early epoch, some unspecified physical process produced fluctuations of sufficient amplitude to result in the inhomogeneities observed today. What form the spectrum of initial fluctuations should take was an unsolved problem. Astrophysicists just postulated a spectrum of perturbations. The convention was to define a spectrum of fluctuations as they cross the horizon, i.e. as $\lambda = ct$,

$$\delta_H = \kappa \, (M_H / M_*)^{-\alpha} \qquad (13)$$

where M_H is the mass of the fluctuation as it crosses the horizon, and α and M_* are free parameters.

A suggestion by Zel'dovich [1970] is favoured : $\alpha = 0$, $\kappa = 10^{-4}$. The amplitude $\kappa = 10^{-4}$ is set so as to avoid problems with the observational constraints from the observed high degree of isotropy of the 3-K microwave background radiation (more on this later). The scale-free $\alpha = 0$ spectrum seems reasonable, because for $\alpha < 0$, the perturbations would diverge on large scales, and for $\alpha > 0$ divergences on small scales would occur.

At the time of Zel'dovich's proposal, there was no compelling physical reason for adopting such a fluctuation spectrum. Recently, however, it has been shown [Brandenburger and Kahn 1984] that the model of the "inflationary universe" predicts a spectrum with $\alpha = 0$. Unfortunately the amplitude k comes out too large in the models discused with $\kappa \approx 50$ instead of $\kappa \approx 10^{-4}$.

1.7) The Limits of the Linear Theory

So far, our theory of the evolution of large scale structure in the universe seems relatively straightforward. We have established a likely form for a spectrum of initial density perturbations and we seem to have all the necessary physical tools to draw conclusions about the evolution of the spectrum and about the development of incipient astronomical objects.

However, we are forgetting that astronomical objects result from strong non-linearities - they are characterized by $\delta\rho/\rho >> 1$. For example, $\delta\rho/\rho \approx 100$ for the least dense objects which are clusters of galaxies. This means that the linear theory is no longer valid since the approximation equations (5) through (8) no longer apply.

Immediately after recombination, the radiation pressure drops, and fluctuations that have survived the previous era of radiation-dominated interactions are no longer inhibited from being amplified. Thereafter, gravitational instability proceeds with full vigour, density contrasts exceed the limits of the linear theory, and the formation of astronomical objects must now be described by a non-linear theory.

1.8) Zel'dovich's Non-linear Theory (Pancaking)

Non-linear problems in physics are on the whole extremely difficult to solve. One way of dealing with them, is the construction of an approximation method that extrapolates the linear solution to the general case. This method is very powerful, but it is always necessary to remember the limits of its accuracy.

Let us first consider the simplest possible, relevant case: the one-dimensional motion of a zero-temperature, collisionless, continuous medium. Its motion is easily described in Lagrangian coordinates. The actual position (i.e. Eulerian coordinates x) of a particular particle is given as a function of its initial (Lagrangian) coordinates q and time t by:

$$x(t,q) = q + t.v_0(q) \qquad (14)$$

where $v_0(q)$ is the initial velocity field of the particle. Let us further suppose that at the initial time t = 0, the density of matter is homogeneous, i.e. $\rho(x,0) = \rho_0$.

At $t>0$, the density of matter becomes inhomogeneous. Using the mass-conservation law $\rho(x,t)dx = \rho_0 dq$, we can calculate the distribution of density as a function of the Lagrangian coordinate q,

$$\rho(q,t) = \rho_0 / (1 + t.\alpha(q)) \qquad (15)$$

where $\alpha(q) = dv_0/dq$.

Equation (15) predicts that at the time

$$t(q) = -1/\alpha(q) \qquad (16)$$

the density at the point with Lagrangian coordinates q becomes infinite. In corresponding points of Eulerian space, there are caustics or density singularities.

One can easily see from equation (16) that the first singularities arise locally at the negative minima of $\alpha(q)$. Immediately after that, two neighbouring points achieve infinite density and become the boundaries of the caustic region.

The explanation for these density singularities is as follows. In a collisionless medium of weakly interacting particles, multistream configurations may form. This means that at a point with Eulerian coordinates x, there are particles that have arrived from different points in Lagrangian space with coordinates q_1, q_2, ... q_n. These particles have different velocities v_1, v_2 ... v_n. It is the result of the differing velocities of the particles that after some time, the rapidly moving particles will catch up and outstrip the slow ones. In the vicinity of a negative minimum of $\alpha(q)$, two neighbouring points exchange their positions for the first time. As a result, a density singularity arises in Eulerian space at the corresponding time.

Let us now turn our attention to the three-dimensional case.
After recombination, the matter in the universe can be fairly well described as cold dust moving under the action of gravity alone. It is thus worthwhile to investigate the effect of non-linear perturbations in a zero-temperature, zero-pressure medium. In the assumed approximate solution [Zel'dovich 1970], the Eulerian coordinates **r** are expressed in terms of the Lagrangian coordinates **q** as follows:

$$\mathbf{r} = a(t)\,[\,\mathbf{q} - b(t).s(\mathbf{q})] \qquad (17)$$

The first term (a(t)**q**) corresponds to unperturbed motion and is, of course, the Hubble expansion law. The Lagrangian coordinates **q** are thus defined as the comoving coordinates of the unperturbed motion.

The second term in equation (17) describes perturbations. The formula is exact (see "Relativistic Astrophysics", vol.2, by Zel'dovich) in the case of small, growing perturbations. Zel'dovich uses it for finite and even larger density contrasts. If we make a simple transformation

$$\mathbf{x} = \mathbf{r} / a(t) \ , \quad \tau = b(t) \quad \text{and} \quad v(\mathbf{q}) = -s(\mathbf{q})$$

we obtain instead of (17),

$$\mathbf{x} = \mathbf{q} + \tau . v(\mathbf{q}) \tag{18}$$

Since equation (18) is of the same form as equation (14), some features of the motion of non-interacting matter in accordance with (15) persist in the case of gravitating systems. Moreover, since accelerations in gravitating systems are caused by gradients of the gravitational potential, one can assume that the velocity is of the potential type, i.e.

$$\mathbf{v} = \nabla\Phi .$$

If rotations were initially present, they would be strongly damped due to the expansion. This makes the analysis more definite.

In analogy to what we have done before, we can obtain an explicit expression for the density as a function of the Lagrangian coordinates and time in the three-dimensional case:

$$\rho(t,\mathbf{q}) = \rho_o / \det (\delta_{ik} + \tau . (\partial v_i / \partial q_k) \tag{19}$$

Equation (19) can be written in terms of the eigenvalues,
$-\alpha(\mathbf{q})$, $-\beta(\mathbf{q})$ and $-\gamma(\mathbf{q})$ of the symmetric tensor

$$d_{ik} = \partial v_i / \partial q_k$$

We assume that the eigenvalues are ordered at every point in Lagrangian space, i.e.

$$\alpha(\mathbf{q}) \geq \beta(\mathbf{q}) \quad \text{and} \quad \beta(\mathbf{q}) \geq \gamma(\mathbf{q}) .$$

Equation (19) then becomes

$$\rho(t,\mathbf{q}) = \rho_0 / ([1 - \tau\alpha(\mathbf{q})] [1 - \tau\beta(\mathbf{q})] [1 - \tau\gamma(\mathbf{q})]) .$$

The eigenvalues α, β and γ govern the local contraction or expansion of matter along three orthogonal directions corresponding to the eigenvectors.

Locally, the first singularity arises at the positive maximum α_m of the function $\alpha(\mathbf{q})$ at the time $t = 1/\alpha_m$. This represents a one-dimensional contraction of matter along an axis and in three dimensions, these caustics or density singularities are referred to as "pancakes". It should be remembered that Zel'dovich's model assumes a zero-temperature, zero-pressure medium. It can be shown that in the case of positive temperatures and pressures, all density singularities are erased. Pancaking still occurs, but the pancakes have a definite thickness (see [Zel'dovich 1970]).

Work done by Zel'dovich [1970] and others ([Centrella & Melott 1983] ; [Shapiro et al 1983]) has shown that at first pancakes develop in isolated regions, but they soon grow into thin sheets that intersect and form a cellular type of structure. Initially, the prediction of cellular structure by the pancake model was taken as very welcome news, as observational studies had begun to uncover the presence of large voids in the universe. However, there were soon discovered to be very serious difficulties with the model as it is described above. These difficulties will be described in the next section.

1.9) So What's Wrong With Baryonic Galaxy Formation?

The main difficulty with baryonic galaxy formation is the observed high degree of isotropy of the cosmic microwave background radiation. Because the background radiation has propagated freely ever since the photons and the electrons ceased to interact, i.e. after recombination, the variation in the temperature of the radiation across the sky reflects primordial inhomogeneities in the distribution of matter. Experiments have set the anisotropy

limit on the microwave background to be $\Delta T/T < 10^{-4}$ on a 4.5' scale ([Urson & Wilkinson, 1984], [Davies et al 1987])

Another difficulty is that the estimated density of luminous matter in the universe is less than about two percent of the density needed to close the universe. This means that on a cosmic scale the force of gravity would have been so weak in recent epochs that fluctuations must have completed their growth and collapsed at a much earlier time, when the density of matter was much greater than it is today. The amplitude of such fluctuations, however, would have been much to large to have been compatible with the observed uniformity in the microwave background. On the other hand, if the initial fluctuations had been small enough to be compatible with the radiation background, the birth of galaxies would have been practically impossible.

If the universe is dense enough for the amplitude of the fluctuations to be reconciled with the uniformity of the background, the universe must be made up predominantly of dark matter. Furthermore, this dark matter cannot be baryonic in nature. This is because of upper limits that are placed on baryon density by theories of nucleosynthesis in the early universe. In order for the predictions of current theoretical models of nucleosynthesis to agree with the present-day abundances of light elements, the total density of baryons that could have been present at the time of nucleosynthesis is constrained so highly that these particles' current density must be less than 20% of the density required for closure. This density is still not sufficient for baryonic galaxy formation to work.

These arguments have led theorists to develop non-baryonic galaxy formation theories.

1.10) Other Evidence for Dark Matter in the Universe

The best-documented evidence for the presence for the presence of dark matter is based on the velocities of rotation of spiral galaxies [Rubin et al 1985]. The Doppler frequency shift makes it possible to determine how quickly stars in the arms of a spiral galaxy are rotating. According to Newton's laws, the orbital velocity of objects far from a central concentration of mass should drop off in proportion to the reciprocal of the square root of their distance from the centre of rotation. Extensive surveys of stars and hot gas in the outer regions of spiral galaxies have shown that the rotational velocities of these objects remain constant, rather than dropping off, out to distances greater than 30 kiloparsecs from the galactic core.

It had already been suggested by Ostriker and Peebles [1973] that there might be some unseen mass in spiral galaxies, because otherwise gravitational instabilities would cause the galaxies to collapse into bar-shaped formations. The stability of spiral galaxies, as well as the rates of rotation of their outer arms, could be explained if the galaxies were each embedded in a large, roughly spherical distribution of dark matter.

There is other dynamical evidence for dark matter. A well-known theorem of classical mechanics called the virial theorem establishes a relation between the average kinetic and gravitational potential energies of objects in stable, gravitationally bound systems that have reached dynamical equilibrium. It should therefore be possible to estimate the total mass of such a system (which is related to its total gravitational potential energy) by measuring the relative velocities of a large number of pairs of objects within the system. This method has yielded evidence of dark matter in a wide variety of systems, ranging from dwarf spheroidal galaxies to clusters (see for example [Press and Davis 1982]).

Another method pioneered by Peebles and his coworkers [Davis and Peebles 1983], relies on the statistical analysis of large numbers of galaxies. Peebles showed that it is possible to relate the mean relative velocity of a large number of pairs of galaxies to the mean mass density of the universe, assuming that the regions probed contain stable dynamical systems.

It is striking that all available methods yield essentially the same result: if the distribution of galaxies traces the distribution of mass in the universe, then the universe contains less than about 20 to 30 percent of the mean mass density that would be necessary for closure. Note that this figure matches the upper limit placed on the baryon density by theories of early-universe nucleosynthesis.

1.11) The Flatness Problem

At the moment, the conventional wisdom amongst theorists is that the universe is flat. In other words, most theorists do not choose to believe what the observations tell them - that the universe has a density of only about 20% of the critical density.

The reason for this, now called the flatness problem, was first pointed out by Dicke and Peebles. The essential point is that any deviation from an exactly flat universe should increase linearly with time. If the universe had even a small non-zero curvature at the time of

nucleosynthesis, the deviation from flatness would by today have increased by a factor of about 10^{12}. Since the mass density in the present-day universe is within a factor 10 of the mass density of a closed universe (i.e. the universe is very close to being flat), at nucleosynthesis the universe must have either been exactly flat or curved to an extremely small degree: it must have been flat to an accuracy of within one part in a million million.

If the universe is measurably curved today, cosmologists must accept the miraculous fact that this is so for the first time in the 10^{10}-year history of the universe; if it had been measurably non-flat at much earlier times, it would be much more obviously curved than it is today.

This line of reasoning suggests that the universe is exactly flat, that it contains precisely the critical amount of mass. The development and wide acceptance of the inflationary model of the universe, which solves the flatness problem by means of a period of exponential expansion at very early times, has further strengthened the belief that the universe is exactly flat. Since normal matter probably accounts for only 20 to 30 percent of the critical density, some form of more exotic matter must be present in the universe.

1.12) Massive Neutrinos, Hot Dark Matter, and Galaxy Formation

What might the dark, exotic, undetected matter in the universe be made of? One of the earliest proposals was that the dark matter is composed of neutrinos. It was originally thought that neutrinos were massless, but there is no theoretical reason for supposing they might not have some mass. Stringent experimental limits have been set on the maximum possible neutrino mass and it is very small indeed - less than about 20 eV. Nonetheless theorists were hopeful. If the neutrino did indeed turn out to have a small mass, might it not prove to be the necessary ingredient both to make up the critical density of the universe, and to salvage the pancake theory of galaxy formation?

As dark-matter candidates, neutrinos have two strong advantages over other contenders. First of all, they are known to exist. Second, primordial nucleosynthesis calculations suggest that neutrinos must be as abundant as photons in the universe today. Thus, as Cowsik and McLelland first estimated (see [Cowsik 1986] for details), if neutrinos have a mass in the range of 10^{-4} to 10^{-5} times the mass of the electron, they could account for enough mass to close the universe.

If we refer back to our discussion of the thermal history of the universe, we will remember that in the first second of the big bang, the primordial soup included an abundance of neutrinos. Being very light and interacting very weakly with other particles, the neutrinos moved at relativistic speeds - hence the label "hot" which is used to describe them.

Collisionless relativistic particles define another damping scale, which is different to the adiabatic damping scale for non-relativistic particles discussed previously. Directional dispersion [Peebles 1980; Bond & Szalay 1983] is the effect by which a wave pattern in three dimensions decays. Waves travelling in different directions interfere destructively on average, and consequently the amplitudes decay. This kind of damping is very effective for extremely relativistic particles. It leads to a damping $\propto t^{-1}$ of fluctuation amplitudes.

Fluctuations of relativistic particles are also damped by free streaming i.e. the effect that as long as the particles are relativistic, and thus not bound gravitationally to any real degree, they move freely away from a compression region. The velocity dispersion of the particles is then responsible for the disappearance of the compression region. These processes have the consequence that collisionless relativistic particles damp out all fluctuations on scales less than the horizon.

As the universe expanded, the neutrinos cooled and slowed down. Shortly before recombination, neutrinos having masses in the appropriate range to close the universe would have become non-relativistic and would have begun to make up the primary component of the energy density of the universe. Analytic calculations show that only after this time could they have clumped together gravitationally. At any earlier times, as we have mentioned, fluctuations on scales smaller than the horizon would have been erased because the neutrinos, being relativistic, would not have been bound to dense regions.

The first scale that allows growth of fluctuations is thus the horizon size at the epoch when the particles become non-relativistic. This scale corresponds to a present distance of 10^8 light years and a mass of 10^{15} to 10^{16} solar masses. The agreement with the size and mass of galaxy superclusters that are now observed is striking. Figure 4 shows the spectrum of density fluctuations for a neutrino model at the beginning of recombination.

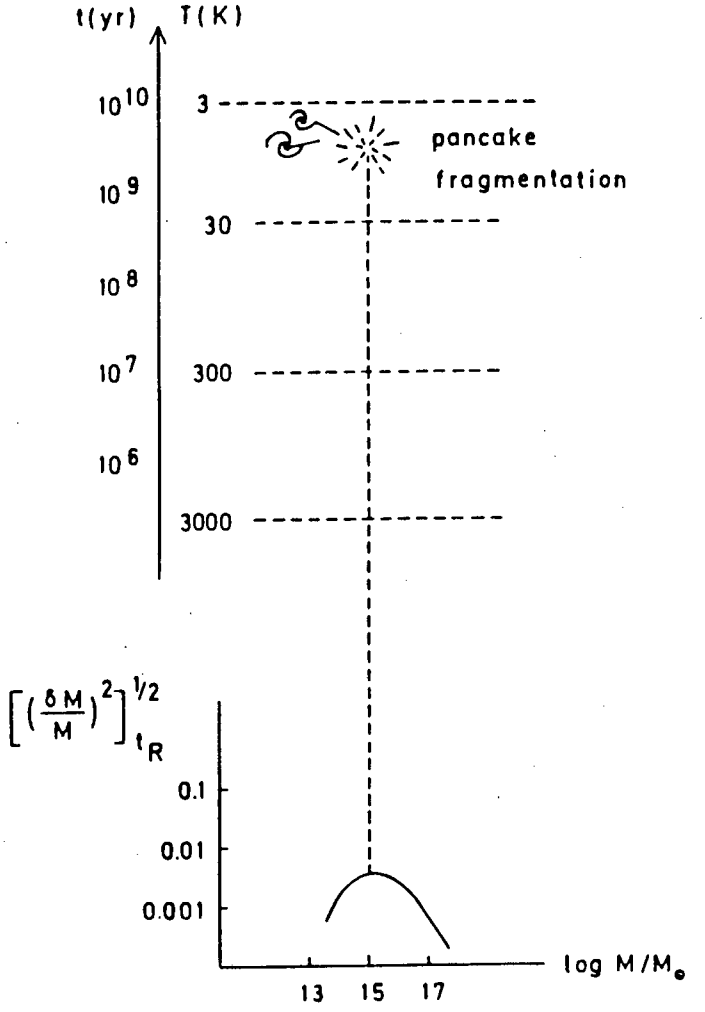

Figure 4 *The density fluctuation spectrum at the time of recombination and the subsequent collapse of large scale structures in a neutrino model of galaxy formation.*

How can such fluctuations be compatible with the observed uniformity of the background radiation? The neutrinos cease their erasure of the fluctuations before recombination, but unlike the electrons their motions are not inhibited by the viscosity of the fluid, as they interact so weakly with photons and electrons. Gravitational instabilities among the neutrinos can accordingly begin to develop before recombination, and so they can grow over a much longer time than the fluctuations of ordinary matter can. The initial amplitude of the neutrino fluctuations needed to account for the present inhomogeneities of matter could therefore have been much smaller than the amplitude of fluctuations needed in a mixture of radiation and ordinary matter. With massive neutrinos, the anisotropy of the background radiation required to generate the observed inhomogeneities is reduced by an order of magnitude or more.

The inclusion of massive neutrinos leads to an extended version of the pancake theory. [Centrella & Melott 1983]. The initial collapse of a pancake distributes most of the neutrinos widely, because most of them are accelerated by the collapse to large velocities. Such neutrinos are destined to fill the dark regions of intergalactic space. Other neutrinos, however, move more slowly because they are initially closer to the central plane of the pancake and do not undergo large accelerations. The thin layer of gas in the vicinity of the central plane condenses and breaks up to form protogalaxies. The slow-moving neutrinos are gathered together by aggregates of ordinary matter, and the matter near the centre of the protogalaxy continues to condense and form stars. Neutrinos at the periphery of the protogalaxy, however, are gravitationally shared and never condense; they become the dark matter in the galactic halo. Again, a cellular type structure of galaxies is formed by the merging and intersections of pancakes. Galaxy formation in the neutrino model is often referred to as "top-down" formation because of the development of the large structures before the smaller ones.

1.13) Disadvantages of the Hot Dark Matter Model

The scenario of a neutrino-dominated universe is attractive in many ways. It would have led to a system of filament-shaped superclusters and large voids that resemble features identified in current surveys of large-scale clustering. (see figure 5) In addition, it seems to resolve the anisotropy problem.

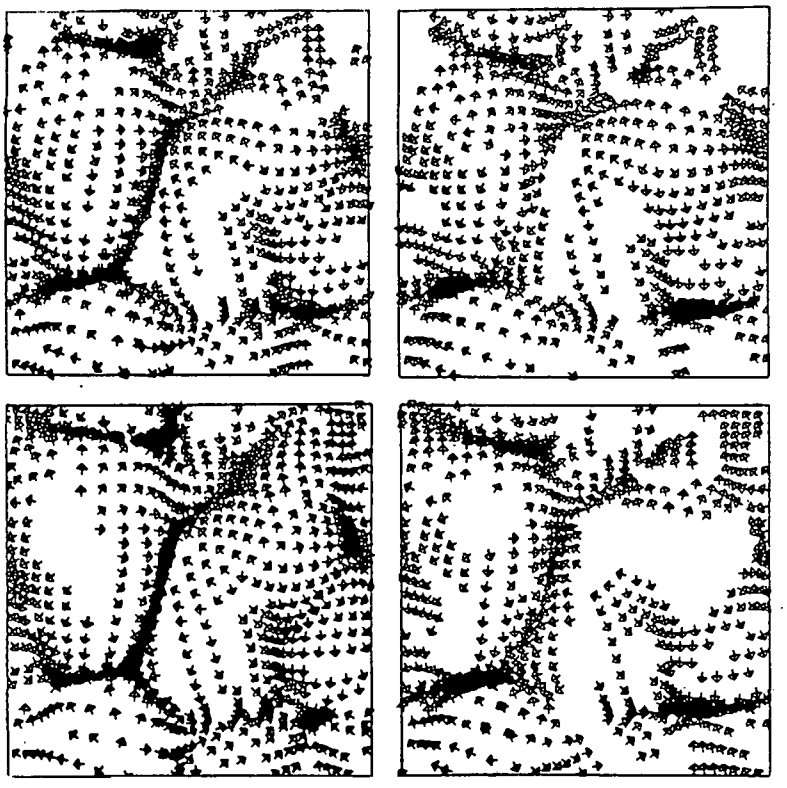

Figure 5 *Four consecutive, two-dimensional space slices of the 3D neutrino distribution at a late non-linear epoch as predicted by N -body simulations.*

These attractive features led Frenk, White and Davis [1983] and independently, Centrella and Melott [1983] to develop numerical models investigating the details of gravitational clumping in a neutrino-dominated universe. (see section on N-body simulations later on) The investigators encountered serious difficulties when they tried to recreate the clustering that has actually been observed.

Essentially they found that in a neutrino-dominated universe the fragmenting of clusters into galaxies and the formation of galaxies would have to have occurred relatively recently (when the universe was at least half its present age) in order to match the currently observed levels of clustering. This conclusion is hard to reconcile with the existence of such structures as quasars, which formed in much earlier eras.

On the other hand, in order to produce galaxies at high enough redshift, clusters and large scale structures would have to be much less diffuse than they are actually observed to be. In other words, hot dark matter models result in the overproduction of clusters if galaxies are to be formed at early enough times.

This and other difficulties have led most theorists to abandon the hot dark matter models and to turn to other types of dark matter for inspiration.

1.14) Cold Dark Matter and Galaxy Formation

A way out of the problems with neutrino models seems clear. Find models in which galaxies can form significantly earlier than larger structures do. This suggests the need for what has become known as cold dark matter: dark matter that was so cold (that is, moving so slowly) that it was non-relativistic significantly earlier than neutrinos were and could therefore cluster gravitationally much earlier.

Recall that the time at which a class of particles becomes non-relativistic is a key factor in determining the size of structure that can be formed by that class of particles. At times before the particles become non-relativistic, structures on scales smaller than the horizon would break up. Hence, in order for galaxies to form before larger structures, cold dark matter would have to have been non-relativistic by the time the horizon reached the scale size of galaxies.

A popular cold dark matter (from now on, CDM) candidate is the axion. The existence of axions follows from a theoretical approach developed to explain a special relation that links, in the strong interactions between quarks, the two kinds of symmetry known as charge conjugation and parity.[Ipser & Sikivie 1983]

Another candidate for CDM comes from the theoretical framework known as supersymmetry. In the theory of supersymmetry, for every particle now known there exists a "supersymmetric partner": a particle identical in most respects except spin. The most promising CDM candidate of the supersymmetric partners is the supersymmetric photon - the massive photino.[Ellis et al 1984]

A third CDM candidate are black holes of mass between 10^{-16} and 10^{6} solar masses, the lower limit implied by the non-observation of gamma rays from black hole decay by Hawking radiation, and the upper limit required to avoid disruption of galactic disks and star clusters. [Stecker & Shafi 1983]

There is thus no shortage of CDM candidate particles - although there is no direct evidence that any of them actually exists. Numerous experiments have been proposed to try to detect CDM particles in the universe. [Krauss 1986] Until these yield any positive results, CDM theories by necessity remain a bit pie in the sky.

The characteristic property of CDM is the absence of the free streaming mass limit; this limit is less than 10^{8} solar masses for all the possible different CDM candidates and it is therefore negligible for the problem of galaxy formation.

Blumenthal and Primack were the first to consider a universe consisting of CDM, photons, neutrinos and ordinary matter. [Primack & Blumenthal 1983] Fluctuations having mass less than about 10^{15} solar masses cross the horizon when the universe is still radiation dominated. After such fluctuations cross the horizon, their neutrino components dissipate by free-streaming, and the remaining photon and charged particle perturbations oscillate as an acoustic wave, whose amplitude is ultimately damped by photon diffusion. (see sections (1.4) and (1.12)) The CDM fluctuations are also not able to grow much during this period because of the dominance of the radiation energy. This effect is known as the Zel'dovich-Meszaros effect. This stagnation in the growth of CDM fluctuations between the epochs of horizon crossing and matter domination is commonly referred to as "stagspansion".

Because fluctuations with mass less than 10^{15} solar masses grow very little during the stagspansion era and as fluctuations on all scales grow at essentially the same rate after the universe becomes matter-dominated, the initial density fluctuation spectrum evolves to a much flatter spectrum by the time of recombination. In figure 6, the density fluctuation spectrum for CDM at the time of recombination is plotted.

After recombination, the density contrasts grow to be bigger than one and non-linear gravitational effects become important. However, it is possible to get an idea of how clustering will proceed by examining the spectrum in figure 6.

Since the spectrum has the largest amplitude for small masses, these masses will first undergo collapse. Pancaking occurs, but on the scale of galaxies rather than superclusters. Smaller mass fluctuations are themselves typically clustered within larger mass perturbations, which go non-linear later. It is thus evident that the spectrum in figure 6 will lead to a hierarchical clustering picture, or a "bottom-up" formation scenario, in which galaxies form first and clusters and superclusters form at later times by the gravitational attraction of the galaxies and clusters.

1.15) Problems with Cold Dark Matter Theories

As we have mentioned, a real problem is the question of the existence of any CDM particle. Another problem is the existence of large voids such as that in Bootes, where the number-density of galaxies is at least a factor of 4 lower than the average density.

CDM scenarios, as described above, have almost the exact opposite problem to the one that hot dark matter (hereafter, HDM) scenarios must contend with. Recall that HDM models produce an overabundance of clusters if galaxy formation is to have taken place at high enough redshift. CDM models, on the other hand, simply do not produce enough clusters and voids by the present epoch.

Although CDM models work quite well on small scales, predicting roughly the observed mass range of galaxies and the existence of galactic haloes and clusters, they have trouble accounting for the very large-scale structures that are observed by astronomers in the universe today.

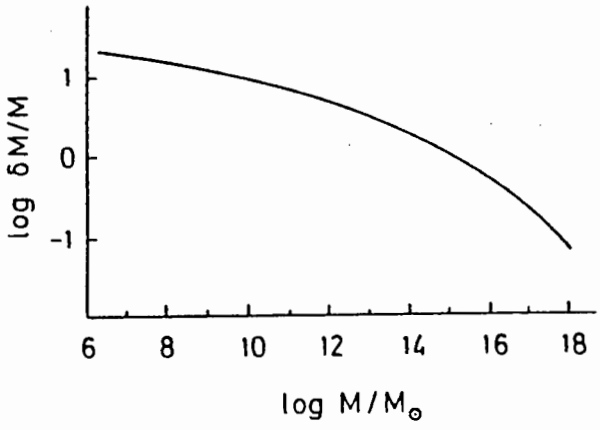

Figure 6 *The density fluctuation spectrum at the time of recombination for a cold dark matter model.*

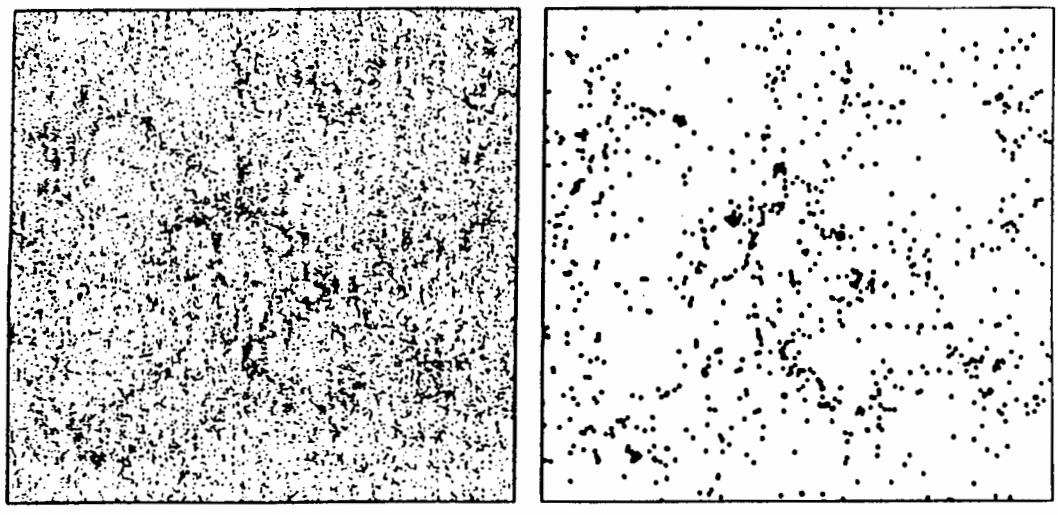

Figure 7 *The projected distribution of all particles (left) and of the biased galaxies (right) in a CDM N -body simulation. "Galaxies" correspond to the 2.5σ peaks of the linear density distribution.*

1.16) Biasing and Hybrid Models

Simulations of the two most popular models in which the universe is either dominated by cold dark matter or by massive neutrinos, have led to the conclusion that if the universe is flat, neither can reproduce the observed large-scale distribution of galaxies unless galaxy formation is biased. This implies that the luminous galaxies do not accurately mirror the distribution of the dark matter on large scales.

In the CDM models, an enhanced clustering of galaxies over the background matter could arise if galaxies formed only from exceptionally high peaks of the density distribution. If a threshold
υ_G for galaxy formation is introduced, such that only density peaks with at least υ_G times the root-mean-square density-fluctuations are identified as galaxies, and followed in their evolution, then a picture such as that shown in figure 7 emerges.

The distribution of "biased" galaxies is compared with the dark matter distribution. It can be seen that the "galaxies" follow the clustering of the dark matter but with greatly enhanced amplitude. Underdense regions or voids are also seen to be enhanced in the biased picture.

The crucial question is what astrophysical mechanism prevents lower-υ peaks from also turning into galaxies, thereby neutralizing the effect. Answers to this question have been proposed, but they are still at the speculative stage.One mechanism for biasing has been proposed by Rees. [Rees 1987] What he proposes is as follows:

The high-υ peaks of the density distribution would collapse earlier, and have a higher density at turnaround, than the more typical fluctuations. They may, for this reason alone, form galaxies more readily and thereby create the biasing. Collapse and fragmentation of gas within protogalaxies are highly sensitive to the ratio of the cooling time to the collapse time: these processes occur more rapidly when this ratio is small. Moreover, if the high-υ perturbations collapsed at $z \geq 10$,Compton scattering of the microwave background would guarantee efficient cooling. This process, whose efficiency is proportional to $(1 + z)^4$ would be unimportant for lower-υ systems collapsing at late times.

The formation of galaxies from lower-υ perturbations may be further impeded owing to some kind of negative feedback induced by the first galaxies. These first galaxies might photo-ionize, or shock heat, regions that were collapsing more slowly to high temperatures, thus preventing such regions from completing the process of galaxy formation.

In the neutrino models, some form of anti-biasing is required. Galaxy formation needs to be suppressed in high-density regions. For instance, galaxies might form preferentially in the flat sheet-like pancakes and not in the denser filaments and clusters. Although an anti-biasing like this can eliminate the timing-scaling problems in HDM models, one has to worry about reconciling it with the indications for a positive bias discussed earlier.

An alternative resolution is to appeal to hybrid scenarios. Hybrid scenarios attempt to combine CDM models on small scales and HDM models on large scales. The hybrid models can be successful where the dark matter models fail: for example, in reproducing simultaneously the observed structure on galactic scales and on supergalactic scales.

The theoretical work on biasing and hybrid models is still in an early and highly speculative stage. Some scientists look down on these mechanisms as essentially ad hoc ways of fine-tuning parameters in order to save theoretical models which are fundamentally flawed. Biased CDM models have been in fashion the past few years, as they have been the most successful in

matching observations. However, considerable evidence for structure on scales greater than $30h^{-1}$Mpc has now been accumulated by a number of investigators. This large-scale structure cannot be matched by these models, which do not produce enough power on scales greater than $20h^{-1}$Mpc. If these results are confirmed by new and deeper observations, it will be damaging to biased CDM models.

1.17) The Link from Theoretical Models to Astronomical Observations

In order to gauge the validity of a theoretical model by comparing its predictions to actual astronomical observations, some method must be found of evolving the model up to the present time. For this reason, many attempts have been made to simulate the evolution of an expanding universe on computers, and then to extract the observable statistical properties from the numerical results.

a) N - body simulations on the computer

The simulations are always concerned with a cubic volume of the universe with periodic boundary conditions in all three spatial directions. Within this volume, N galaxies or particles move under the influence of their relative gravitational force. The purpose of the N-body simulation is to keep track of the individual trajectories and velocities of each of the N particles. An N-body simulation can be divided into the following procedures.:

i) *Establishment of initial conditions.* N- body simulations are generally started at the onset of non-linearity, when the density contrasts in the universe $\delta\rho/\rho$ exceed unity. The initial conditions are conventionally described in terms of the power spectrum of density fluctuations at the onset of non-linearity. This power spectrum will differ from theoretical model to theoretical model, of course. The establishment of initial conditions in an N-body simulation amounts to finding a representation for the power spectrum in terms of a three-dimensional distribution of particles at the start of the model. Methods for doing this are described by Efstathiou et al [1985].

ii) *Calculation of the force on each particle.* The force F_i' on each particle may be obtained from a summation over all pair interactions

$$F_i' = - \sum_{j \neq i} G m_j \frac{x_i' - x_j'}{|x_i' - x_j'|}$$

This method is very time-consuming, however. A more popular method is to divide the cubic volume into a fine lattice. A mass is ascribed to each lattice point by means of an interpolation formula from the disordered points (particles) to the grid. The Poisson equation is solved on the lattice and the gravitational force at the lattice points is then computed. The force is then interpolated for the intermediate positions of each of the N particles.

iii) *Integration of the equations of motion.* The equations of motion are solved by a numerical difference method, whereby the positions and velocities of each particle are evaluated at small time intervals δt. The forces on the particles must of course be recalculated after each time interval.

The above description is a rather sketchy and simplified view of the N -body simulation procedure. However, our main interest lies in what we can learn from N -body simulations as opposed to the numerical techniques that are needed to construct them.

N -body simulations can be used to test the predictions of theoretical models on a wide variety of scales. On galactic scales, they can be used to test for the existence and abundance of galactic haloes. On intermediate scales, questions of clustering and peculiar velocities may be addressed. Finally, on large scales, the presence of voids, bubbles and filaments may be investigated.

The investigation of voids in N -body simulations is still at an early stage. Work done by Melott [Melott 1987] represents a first attempt at linking the simulations with the voids which are observed in the universe today.

One of the first problems encountered is the transition that must be made from statistics based on the mass distribution in the numerical models to statistics based on galaxy counts. Since the process of galaxy formation is not yet well understood, this transition can only be made in a rather ad hoc manner.

For CDM models, Melott invokes the concept of biasing. Only particles which are in regions overdense by a certain threshold above the mean density correspond to galaxies. Figure 8a shows the results of the CDM simulation for all the particles, while figure 8b gives only the biased subset.

For HDM models, only particles which are or have ever been in any overdense region are identified as galaxies. Again, this corresponds to a type of biasing. Figures 9a and 9b show the results for the HDM and biased HDM models respectively.

Melott finds that in the CDM models, void size is highly dependent on the biasing threshold, but this is not the case for HDM models. Melott also performs a "nearest-neighbour" type analysis on his data, calculating the distribution of the distance from each galaxy to its nearest neighbour. By doing this, he finds that the characteristic scale of voids is about twice as big in hot models as in the cold ones. Taking a 3σ biasing threshold limit, the maximum "radius" of a void in the cold models is found to be 560 h^{-1} km/s, while it is 1160 h^{-1} km/s in the hot models. If we take h = 0.4 as a lower bound, the observation of voids more than 2800 km/s across at their smallest axis could rule out the cold models. Surveying a sufficiently large volume without finding such voids could rule out the hot model.

These results are of course very preliminary ones. However, they do serve to illustrate how data on the size of voids, and more specifically a spectrum of void sizes, could put strong constraints on the type of theoretical model that could explain the structures in the universe today.

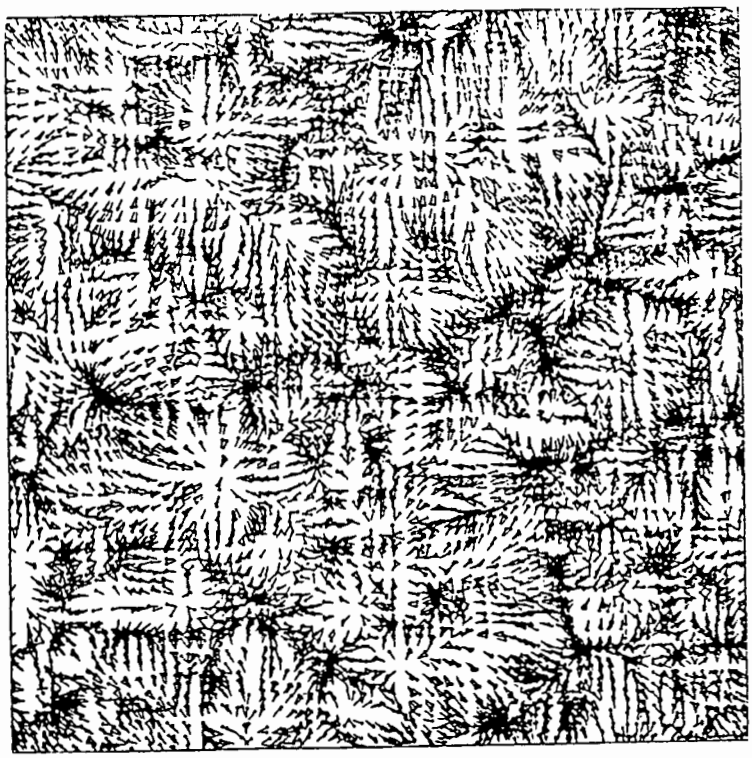

Figure 8a *Results of Melott's N-body simulations for cold dark matter models. This figure shows all particles. The arrows are the size of the dynamical resolution and point in the projected direction of motion.*

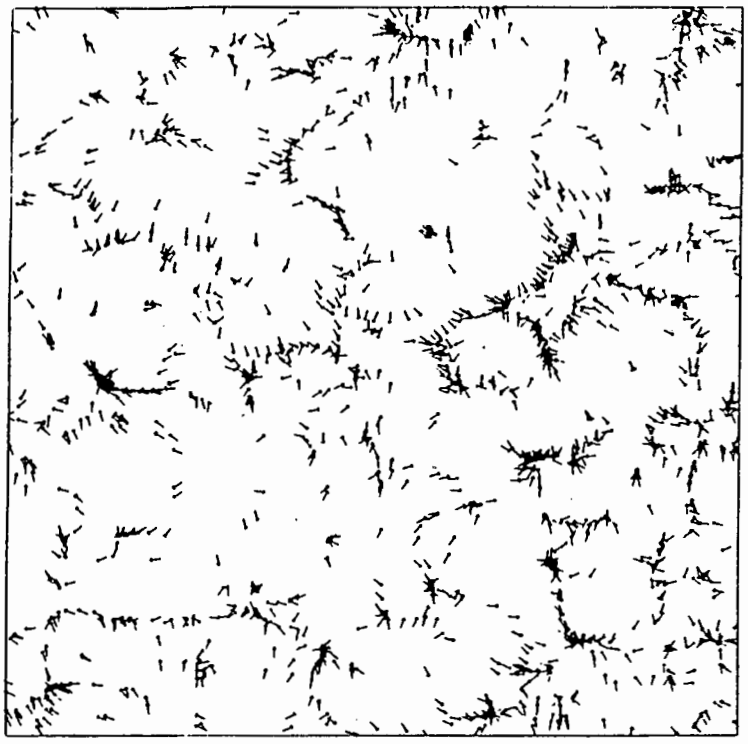

Figure 8b *The biased subset of the CDM simulation.*

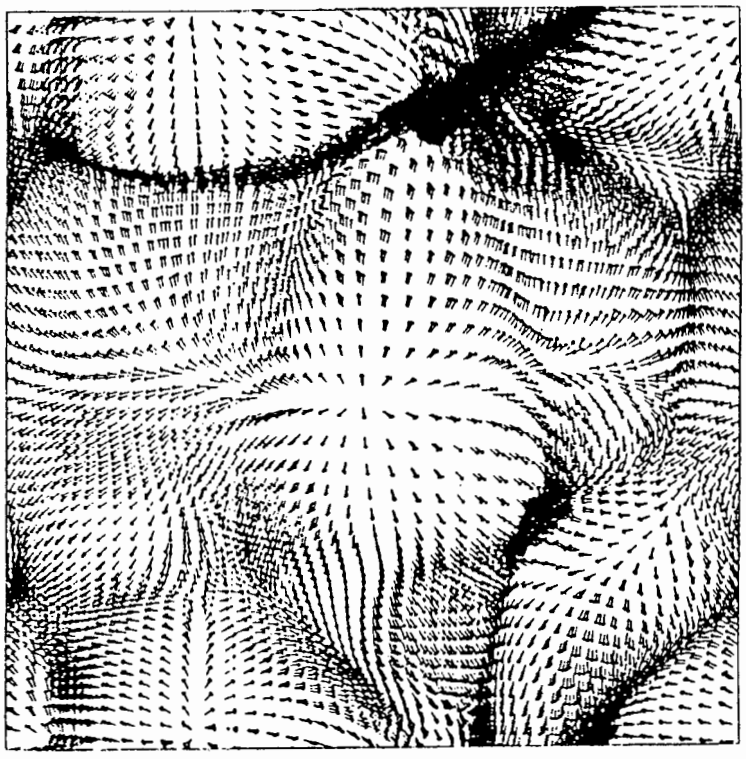

Figure 9a *Results of Melott's N-body simulations for neutrino models. This figure shows all partices.*

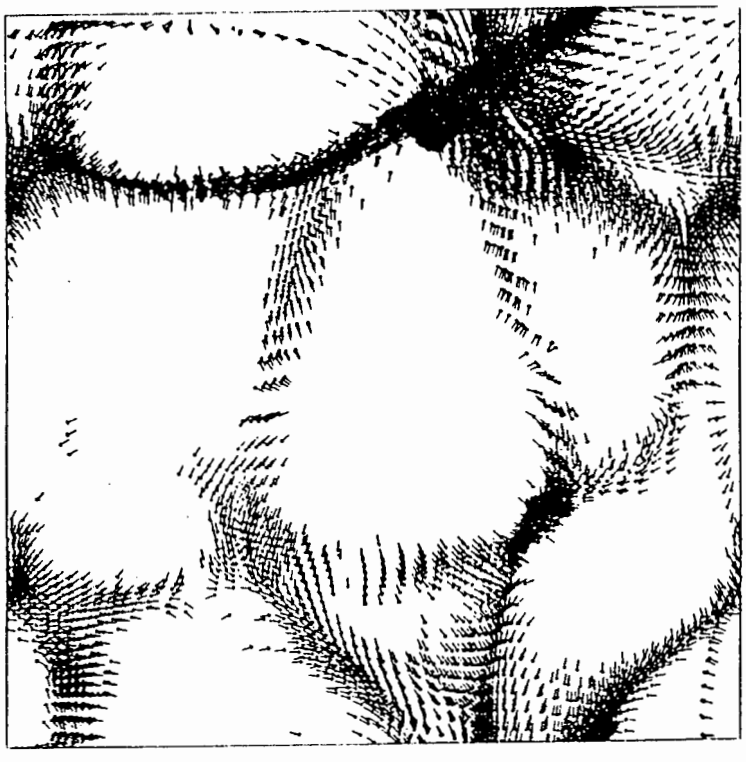

Figure 9b *The biased subset of the neutrino model simulation.*

b) The adhesion model

There are a number of disadvantages associated with N -body simulations. The main drawback is that the possibilities of this approach are restricted by the capabilities of modern computers, as the dynamical range in terms of the length of structures in the model increases very slowly with the growth of the number of particles: $l \propto \sqrt[3]{N}$. What this means is that the number of particles N in a simulation would have to be extremely large in order for structures on the largest scales to appear. It would therefore be useful to have an analytic theory of structure formation at late times.

Progress towards such an analytic theory has been made by Kofman and Shandarin [Kofman & Shandarin 1988] who have formulated a model of "adhesion". This model is a natural extension of the pancake theory developed by Zel'dovich.

According to Zel'dovich's theory, pancakes are the typical structures in HDM, having the size of superclusters of galaxies. In CDM models, the situation is more complicated. If the initial spectrum of density perturbations possesses a cutoff on small scales, the first objects to form at the non-linear stage are pancakes of the cutoff size. Later on gravitational instability continues as a process which is basically hierarchical clustering. Unfortunately, Zel'dovich's approximation is no longer valid quite quickly after the formation of the first pancakes. Therefore it cannot be used directly for the study of CDM models.

However, a rather simple modification of the Zel'dovich approach was suggested [Gurbatov et al 1985]. This new model is based on the phenomenon of gravitational adhesion or sticking which was found by means of numerical simulations [Doroshkevich et al 1980]. It is based on the fact that the pancakes remain rather thin in comoving coordinates. The numerical experiments show that the thickness of pancakes, after a short period of quite rapid growth, stabilizes and increases very slowly with time.

In the adhesion model pancakes, filaments and clumps are assumed infinitely thin. Instead of dealing with these objects, the models deals with surfaces, lines and points. This assumption results in the model dealing with the skeleton of the structure, rather than with the structure itself. However, it is claimed that the positions of these surfaces, lines and points are kept inside the real pancakes, filaments and clumps over the whole evolution of the structure.

The mathematical formalism of the adhesion theory will not be dealt with here. (See [Kofman et al 1989] for more details) The model has been tested against N- body simulations and the results have been found to compare very favourably with those of the numerical method.

It should be said, however, that the fundamental quantity that is dealt with in the adhesion model is not the matter density ρ, but the gravitational potential field Φ. Large scale structure present in the universe today is found to be intimately linked with the statistical properties of the gravitational potential perturbations at the onset of non-linearity. More specifically, it is also suggested [Kofman, preprint] that voids of galaxies form around high peaks of the initial Φ field. The higher the peak, the larger the void. Thus the statistics of observed voids are determined by the statistics of the high peaks of the gravitational potential, which, in turn, strongly depend on both the model of dark matter and the form of the spectrum of primordial perturbations.

Thus the study of the statistics of voids may provide a useful link between theory and astronomical observations via the model of adhesion.

CHAPTER II

STATISTICAL MEASURES FOR VOIDS IN THE GALAXY DISTRIBUTION

In principle it is possible to learn about the early universe and the origin of fluctuations from the present structure of the universe. In order to do this, we need to be able to quantify what up to now has been a purely descriptive view of the large-scale structure. Words such as "filaments", "bubbles" and "voids" need to be given a precise definition. Most importantly, we would like some statistical means of identifying key features in the galaxy distribution in order to be able to make some comparison with the predictions of theoretical models.

In this chapter, we will focus on statistical measures which have been developed to determine the presence of voids in the galaxy distribution. This will serve as an introduction to Chapter III, in which a new statistical method of identifying voids is developed by the author.

2.1) N-Point Correlation Functions

Since many catalogues list positions of galaxies, it is often useful to think of the matter distribution as a distribution of point-like objects. If differences among objects are ignored, it is only a question of the nature of the distribution of positions $\mathbf{r}_j$, and this can be described by the n-point correlation functions.

a) Two-point spatial correlation function $\xi(r)$

The probability that an object is found in the infinitesimal volume δV is

$$\delta P = n\,\delta V \qquad (1)$$

where the mean number density n is independent of position. The probability is proportional to the size of the volume element because doubling δV doubles the chance of finding an object.

The two-point correlation function ξ is defined by the joint probability of finding an object in both of the volume elements δV_1 and δV_2 at separation r_{12},

$$\delta P = n^2\,\delta V_1\,\delta V_2\,[1 + \xi(r_{12})] \qquad (2)$$

Consistent with homogeneity and isotropy, ξ has been written as a function of the separation alone. The factor n^2 makes the correlation function dimensionless. As in equation (1), the probability is proportional to $\delta V_1 \delta V_2$ because doubling either infinitesimal volume element doubles the chance of finding an object.

In a uniform random Poisson point process the probabilities of finding objects in δV_1 and δV_2 are independent so the joint probability is the product of the single point probabilities in equation (1):

$$\delta P = n^2 \, \delta V_1 \, \delta V_2$$

In this case $\xi \equiv 0$, the positions of the particles are uncorrelated. If the object positions are correlated, $\xi > 0$, if the positions are anti-correlated, $-1 \leq \xi < 0$.

Since the chance of finding an object in δV_1 is $n\delta V_1$, the conditional probability of finding an object in δV_2 given that there is an object in δV_1 is

$$\delta P(2/1) = n \, \delta V_2 \, [1 + \xi(r_{12})] \; .$$

Another way to put this is that if an object is chosen at random from the ensemble, the probability of finding that it has a neighbour at distance r in δV is

$$\delta P = n \, \delta V \, [1 + \xi(r)] \qquad (3)$$

b) Three-point and higher correlation functions

Following equation (3), one can define a three-point correlation function by the equation

$$\delta P = n^2 \delta V_b \delta V_c \, [1 + \xi(r_{ab}) + \xi(r_{bc}) + \xi(r_{ac}) + \zeta(r_{ab}, r_{bc}, r_{ca})] \qquad (4)$$

One can consider δP as the number of pairs of objects b and c, with separation r_{bc} contained within the volumes δV_b and δV_c at distances r_{ab} and r_{ac} from a randomly chosen member, a, of the catalogue. In other words, δP is proportional to the number of triplets of objects which form triangles with sides in some range of r_{ab}, r_{bc} and r_{ca}.

The first term in brackets in equation (4) is the contribution expected from a uniform random distribution. The next three terms are the contributions from the two-point correlation of the objects. That is, these terms allow for triangles formed by a correlated pair and a third, uncorrelated object. Finally, the last term is the contribution from triplets in which all three objects are correlated. Since the frequency of occurrence of triplets defining a given triangle is independent of how the labels a,b and c are assigned to the vertices, ζ is a symmetric function of its arguments r_{ab}, r_{bc} and r_{ca}. The entire quantity in square brackets in equation (4) is the three-point correlation function. The function ζ is referred to as the reduced part of the correlation function.

Higher order correlation functions can be defined in a similar way. It is clear that the correlation functions become increasingly complicated and difficult to evaluate as their order n increases. For this reason, the most analysis has been done using the simplest of these functions, the two-point correlation function.

c) Results of correlation function studies

As a result of the efforts of Peebles and co-workers [Peebles 1980], an approximate power law behaviour for the two-point correlation function over a certain range of scales has been derived:

$$\xi(r) = (r_0/r)^{\gamma} \text{ for } 0.1\,h^{-1}\text{Mpc} \leq r \leq 9\,h^{-1}\text{Mpc}\,;$$

$$\gamma = 1.77 + 0.04\ ;\quad r_0 = (4.3 + 0.3)h^{-1}\text{Mpc}$$

r_0 is referred to as the correlation length of the sample and $h = H_0/100\ \text{kms}^{-1}\ \text{Mpc}^{-1}$.

Another interesting result has been the investigation of the cluster-cluster (rather than galaxy-galaxy) two-point correlation function. This function has been found to have the same slope (γ = 1.8) as for galaxies, but the correlation is about 20 times larger [Bahcall & Soneira 1983; Klypin & Kopylov 1983].

However, the study of two-point correlation functions has its limitations. In many numerical simulations (see for example [Klypin & Shandarin 1983; Fry and Melott 1985]), it is found that the two-point function at any time is approximately a power-law function of separation, $\xi(r) \approx r^{-\gamma}$, but the power index γ evolves with time in the simulation. Thus it is not possible to use the shape of the two-point function alone to distinguish between models. Instead, the

logarithmic slope of the two-point function serves as an indicator that lets us identify the epoch corresponding to the "present" in a simulation. In the correct model, once this choice of present epoch has been made, all other measures of structure must agree with observations.

An obvious step is to investigate the behaviour of the three-point and perhaps four-point correlations as well. This has been done with some success (see for example [Fry and Melott 1985]). Hot and cold models are indeed distinguished to some degree by this measure. However, these correlation functions are difficult and time-consuming to evaluate and are subject to larger uncertainties. Moreover, even such relatively well-understood measures as the two-point function have been seen to exhibit a dependence on morphological type [Davis & Geller 1976; Giovanelli et al 1986] or on surface brightness [Davis & Djorgovski 1985].

It has become clear by now that there are aspects of the galaxy distribution that are not captured in low order correlations. One that has achieved much fame is a visual impression that has been variously characterized as "filamentariness", "texture", "bubbliness", "sponginess" and "foaminess". In the following sections, we will look at some attempts that have been made to quantify these striking visual impressions into a reproducible, objective, statistical measure.

2.2) The Void Probability Function

a) *Definitions and properties*

For a given distribution of objects (here galaxies) the count probability $\Phi_N(V)$ is defined as the probability of finding exactly N galaxies in a volume of size V, randomly chosen in the sample. The particular case N = 0 sets the void probability function (hereafter VPF) $\Phi_o(V)$.

It is a noteworthy result that the VPF can be related to the hierarchy of n-point reduced correlation functions w_n in the following way [White 1979]:

$$\Phi_o(V) = \exp\left[\sum_{i=1..\infty} (-n)^i/i! \int\ldots\int w_i(x_1,\ldots,x_i)\, dV_1\ldots dV_i \right]$$

where n is the mean density of the sample. Thus the VPF has the original property of involving the correlation functions of all orders in a symmetric way and therefore yields information that low-order correlation functions do not contain.

The VPF is a function of n, the density of the sample; V, the size of the volume involved and also, the shape of the sample. The V-dependence of the VPF is intuitive. The probability for a volume to be empty clearly increases as the volume decreases. Moreover,it is natural to expect that, for any volume V, the chance of being empty is bigger for a clustered sample than for a random one. In this sense, the VPF can be seen as a measure of clustering.

However, the VPF also depends on the average density n of the sample. For a denser sample, the probability of finding a void decreases. This stands in contrast to the situation for the two-point correlation function ξ. Two samples can be similarly clustered and take on identical values of the two-point correlation function even if the sample densities are quite different.

b) *Scaling*

The n-dependence and V-dependence of the VPF are not necessarily independent and some circumstances imply that they are connected. In such a case the properties of the galaxy distribution at a given scale would be bound to its properties at another scale. This distribution is said to obey some scaling property.

Such a scaling property appears in the simple case of a random distribution. The VPF in this case is given by

$$\Phi_0(n,V) = \exp(-nV) .$$

Clearly the VPF is a function of the scaling variable $p = nV$ only. Expressing the VPF as a function of n or of V expresses the same informational content. Moreover, for two samples with the same (random, in this case) distribution, but with different densities n_1 and n_2, both VPFs, as functions of V, can be related by this scaling property: their values at a volume V_1 for sample 1, and at a volume $V_2 = n_1 \cdot V_1/n_2$ for sample 2, are the same.

Hence there are two useful properties due to the scaling relation: 1) that n-dependence and V-dependence are related, and 2) that the values of the VPF can be compared even for two samples with different densities. This leads to the question of the existence of such a scaling for the real galaxy distribution.

It has been suggested by White [1979] and specified by Schaeffer [1984], that the real galaxy distribution could satisfy some scaling properties. Schaeffer showed in detail how a wide class of statistical models, the so-called hierarchical models, possess such properties. In these

models the function $x = \log(\Phi_o)/nV$ - the logarithm of the VPF normalized to its Poissonian value - becomes a power series in the scaling variable $q = nV<\xi>$ where

$$<\xi> = \int \frac{d^3r_1}{V_1} \frac{d^3r_2}{V_2} \quad \xi_{12}\,(r_1 - r_2)$$

Such a scaling property would open up the possibility of comparing different samples with different densities, or of exploring a non-homogeneous catalogue - both of which would be of great use in statistical studies of the galaxy distribution.

c) The void probability function and scaling in the CfA catalogue

Maurogordato and Lachièze-Rey [1987] derived the VPF for the CfA catalogue. Restricted to the Northern Hemisphere, this catalogue displays 1833 galaxies in a 6° by 117° strip and is complete down to a limiting magnitude of $m_b = 14.5$.

In order to calculate the VPF, Maurogordato and Lachièze-Rey (hereafter MLR) used the following procedure. The shape of the sampling volumes was restricted to a spherical one. Having chosen the value V for the volume of the sphere, a random point lying inside the boundaries of the catalogue was generated. This point was taken to be the centre of the sphere of volume V. The number of catalogue galaxies present inside the sphere was counted. This process was repeated for N_c different spheres of volume V. After having tested the N_c spheres, the number $N_o(V)$ of spheres that were empty of galaxies was noted. Thus the probability of an empty, spherical volume is estimated as

$$\Phi_o(V) = N_o(V) / N_c \,.$$

Edge effects were eliminated by decreasing the test field as the size of the spheres increased, so that no sphere could in any way cross the edge of the catalogue.

The results of this procedure are given in figure 10. The VPF of the CfA catalogue is compared to that of a random catalogue with the same characteristics (volume, shape, number of galaxies, and density). As expected, more voids are present in the CfA catalogue than in the random one. The average void size is also larger in the CfA catalogue.

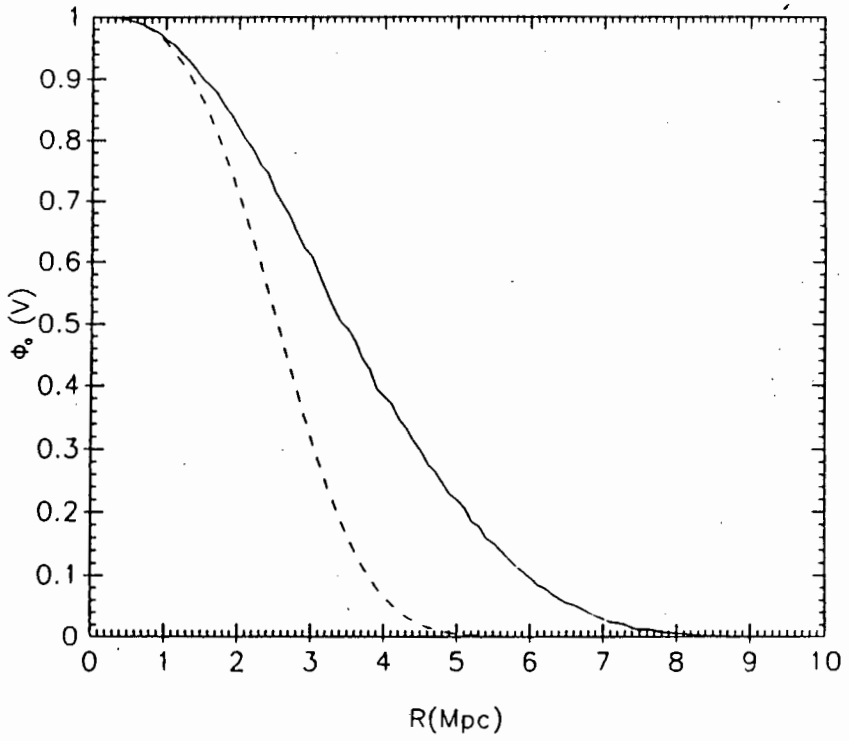

Figure 10 *The void probability funtion of the CfA catalogue. Solid line shows the VPF of the real catalogue. Dashed line is the VPF of a Poisson catalogue with the same characteristics as the real one.*

Checking the scaling properties implies the comparison of different samples which are similarly clustered, but with different average densities. MLR constructed these samples by artificially extracting them from the CfA catalogue, which was taken as the "parent" sample. A given fraction f of the galaxies present in the parent sample were selected by means of a random process. In this way "child" samples were generated for different values of f. The density of the child samples all differed, but the same clustering properties were present in each of them. In figure 11, $\log(\Phi_0(V))/nV$ is plotted against the proposed scaling variable $q = nV\langle\xi\rangle$ for each of the three child samples that were generated. It is seen that the three curves are superimposed with a great precision. Hence the scaling relation proposed by White and Schaeffer is indeed confirmed for the CfA catalogue.

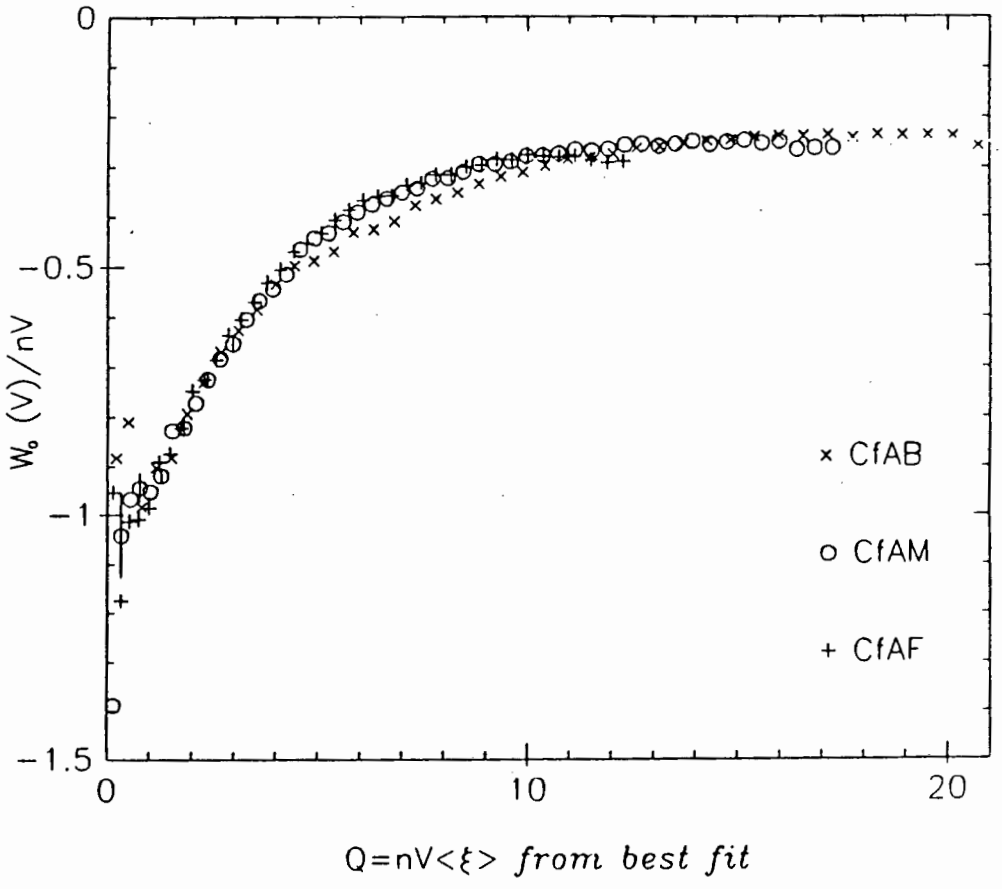

Figure 11 *The scaling relation is seen to be obeyed by the three child samples (labelled CfAB, CfAM and CfaF) derived from the CfA catalogue.*

d) Scaling in dynamical models as predicted by simulations

Fry et al [1989] have tested for the scaling of the VPF in numerical simulations of various theoretical models. The results are not entirely conclusive. The simulation results obey the hierarchical scaling in many cases, but not in all. In particular, neutrino models without biasing do not obey the scaling law. Cosmic string models exhibit scaling, but do not agree well with the galaxy data. Fry et al conclude that the comparison of numerical results with observations suggests that the initial fluctuation spectrum has a behaviour closest to that of cold dark matter models.

It should be noted that the VPF, although providing a measure of the "voidiness" of the galactic distribution, is not a tool for picking out and identifying individual voids in the universe. It also places no lower limit on the size of a void. It thus does not distinguish between voids on very small scales, which may just be the result of randomness in the galaxy distribution, and well-established voids on very large scales, which clearly must have been formed by some physical process. These are issues which will be addressed by the author in Chapter III.

2.3) Point Smoothing Analysis and the Topological Genus Parameter

One of the important problems in cosmology today is characterizing the nature of the topology of the large-scale structure in the universe. Up to about 1986, when Gott and his coworkers began their study of the topology of the galaxy distribution, there were two major competing views on the question of topology: the hierarchical clustering view [Soneira and Peebles 1978] and the cell structure of the universe view [Joeveer and Einasto 1978].

In the hierarchical clustering view, the high-density regions are seen as isolated clumps, while the low-density regions constitute a single connected region. In more colourful terms, hierarchical clustering is often said to result in a "meatball" topology. This kind of model is natural in a universe dominated by some form of cold dark matter.

The cell structure model arises in a "top-down" formation scenario, such a that in a neutrino-dominated universe, where superclusters form before the galaxies. This picture is one in which isolated voids exist in one connected high-density medium. The model is thus said to result in a "bubble" or "Swiss cheese" topology.

Gott et al [Gott, Melott, Dickinson 1986] pioneered a method of investigating the topology of the galaxy distribution in an objective and systematic way. In their 1986 paper, they dealt with a volume-limited cubical sample which formed part of the CfA catalogue. In order to investigate questions of topology, it is necessary to be able to construct continuous density contours in space. It is thus not appropriate to deal with the galaxy data itself, which is given in terms of a discrete point distribution. Gott et al resolved this problem by convolving the galaxy data with a Gaussian smoothing function of the form $\exp(-r^2/\lambda)$, where λ is known as the smoothing length. In this way, every point inside the cubical volume was assigned a density. Topological properties of the galaxy distribution could also be studied on different scales by changing the value λ of the smoothing length.

After smoothing the galaxy data, it was then possible to construct density contours. Gott et al separated their sample into high- and low-density regions, where the dividing line was chosen so that the total volume occupied by the high- and low-density regions was exactly equal. The high-density regions were thus defined as regions where the density was higher than the median value. The results of this procedure are given in figure 12. Figure 12a shows the high-density region and figure 12b shows the low-density region.

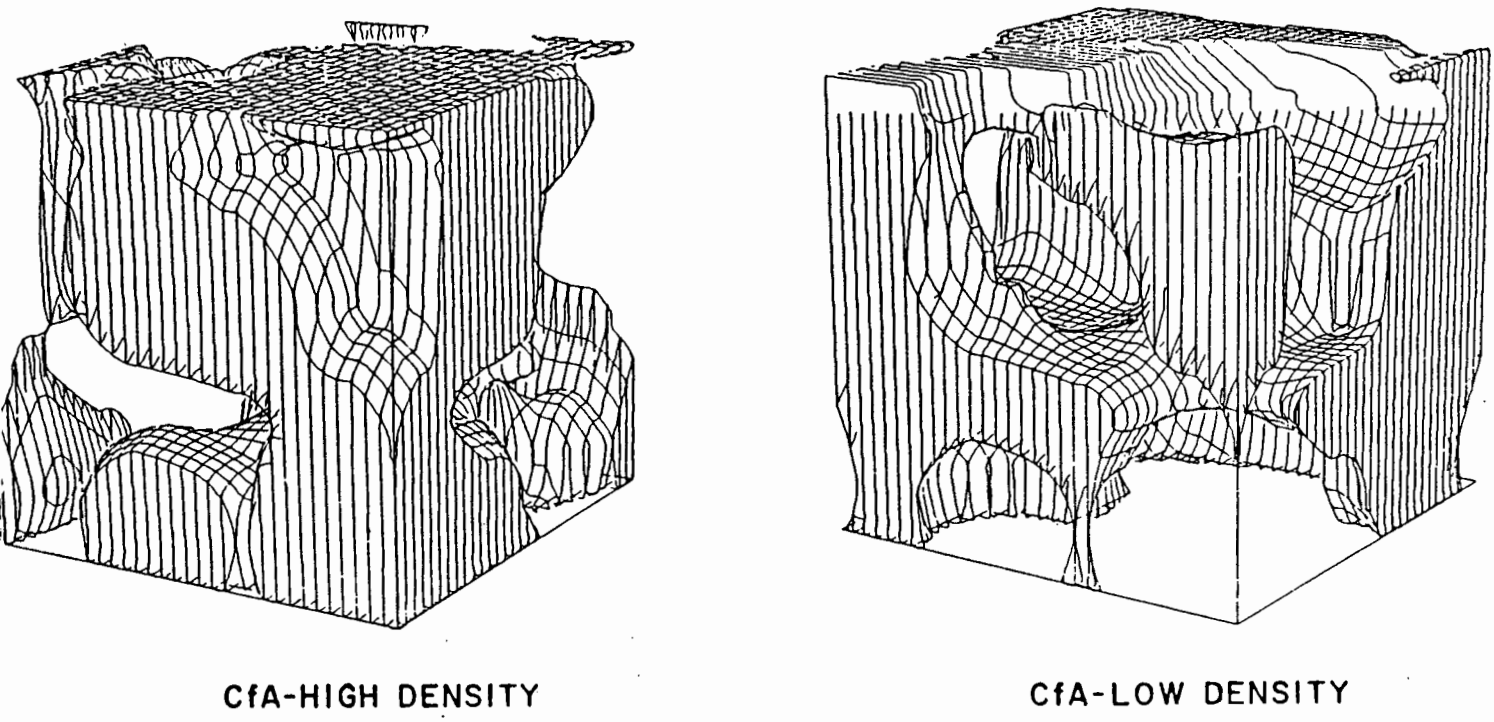

Figure 12 *CfA volume limited sample. Earth is at the bottom front corner. Cube side length is* $28.9h^{-1}$ *Mpc. (a) high-density region. (b) low-density region.*

Several comments can be made about this picture. First of all, the high-density parts form one connected region. Second, The low-density parts also form one connected region. Mathematically, this is known as a sponge. Sponges are characterized by many holes; chambers are connected by tunnels. Thus both high- and low-density regions are multiply connected and are also completely interlocking. It can also be seen that the high- and low-density regions are geometrically quite equivalent and indistinguishable from each other.

Gott et al point out that there are theoretical reasons for the universe showing a sponge-like structure. According to inflationary scenarios, the fluctuations which lead to galaxies and clusters are due to quantum fluctuations with a Zel'dovich power spectrum (see section 1.6). At any given scale such fluctuations will have a Gaussian distribution in their amplitudes and as many positive fluctuations as negative ones. During the linear regime, the growth rate of fluctuations is independent of their amplitudes, so the fluctuations will retain their Gaussian nature. Likewise, when the fluctuations are damped by adiabatic processes or free-streaming, positive and negative fluctuations are damped equally.

The end result of this is that if we examine the initial conditions present at recombination where everything is still in the linear regime, we will find that they are exactly symmetric with respect to positive and negative density fluctuations. The high-density regions must have the same topology as the low-density regions, because a simple change in sign of the original quantum fluctuations would have reversed their roles.

Thus the universe is expected to start off with a sponge-like topology. How this topology evolves will of course depend on what goes on during the non-linear era. To investigate this, one again needs to appeal to N-body simulations (see later).

In a following paper [Gott,Weinberg,Melott 1987], a mathematical formalism to characterize the topology of a contour surface is developed.

The genus of a contour surface is defined as

$$G_S = \text{(Number of holes)} - \text{(Number of isolated regions)}$$

where "hole" means a hole like that in a doughnut and where an isolated (i.e. compact) region may be above or below the threshold density. From the definition above, it is clear that a

sponge has a positive genus since its surface is all in one piece and it is multiply connected with many holes. On the other hand, a sample containing isolated clumps of matter would have a negative genus.

Using the Gauss-Bonnet theorem, it can be shown that G_s is related to the integral of the Gaussian curvature K over the contour surface,

$$G_s = \frac{-1}{4\pi} \int K \, dA \qquad (5)$$

The existence of equation (5) makes it possible to write a computer program which will measure the genus of a contour surface. Data, either from an observational sample or from a numerical simulation, is typically presented in a pixeled array. The data is smoothed and a density threshold chosen. The contour surface is then a corrugated one which follows the pixels. Since the faces of the pixels are flat and their edges are straight, the Gaussian curvature is concentrated in delta functions at the vertices. The computer program calculates the integral of the Gaussian curvature over the surface by simply adding the contribution from each vertex. For details of the computer program, see [Weinberg 1988].

The statistical tool that has been developed by Gott and his coworkers in order to measure the topology of the galaxy distribution is the *genus-threshold density relation.* This relation gives the dependence of genus on the fractional volume f enclosed by the contour. Hamilton, Gott and Weinberg [1986] have derived an analytic expression for this relation at the start of recombination in the case of random Gaussian fluctuations with power spectrum P(k). In this case

$$G_s = N (1 - \upsilon^2) \exp(-\upsilon^2/2) \qquad (6)$$

Here υ is the number of standard deviations by which the contour threshold density departs from the mean density, so that the volume fraction on the high-density side of the contour is

$$f = (2\pi)^{-\frac{1}{2}} \int_{\upsilon}^{\infty} \exp(-t^2/2) \, dt$$

N is a normalization constant which is positive and depends only on P(k). Notice that while the amplitude of the genus curve depends on N, the shape of the genus curve is independent of N, and hence the power spectrum P(k). Since N is positive, the median density contour, f = 0.5,

$\upsilon = 0$, is always spongelike with $G_s > 0$ regardless of the initial power spectrum. For $f < 0.16$, $\upsilon > 1$, G_s is negative and we see isolated clusters. For $f > 0.84$, $\upsilon < -1$, G_s is again negative and we see isolated voids.

Melott, Weinberg and Gott [1988] have investigated the genus-threshold relation for a wide variety of dynamically evolved models. What they find can be summarized as follows.

Hierarchical clustering models such as CDM and biased CDM models retain their initial random Gaussian topology when they are smoothed on scales larger than the correlation length. This is because fluctuations on scales larger than the correlation length are only now starting to come out of the linear regime. This is illustrated in figure 13. It can be seen that the genus curve of the evolved CDM model still corresponds very well to the theoretical relation given by equation (6) (dotted curve).

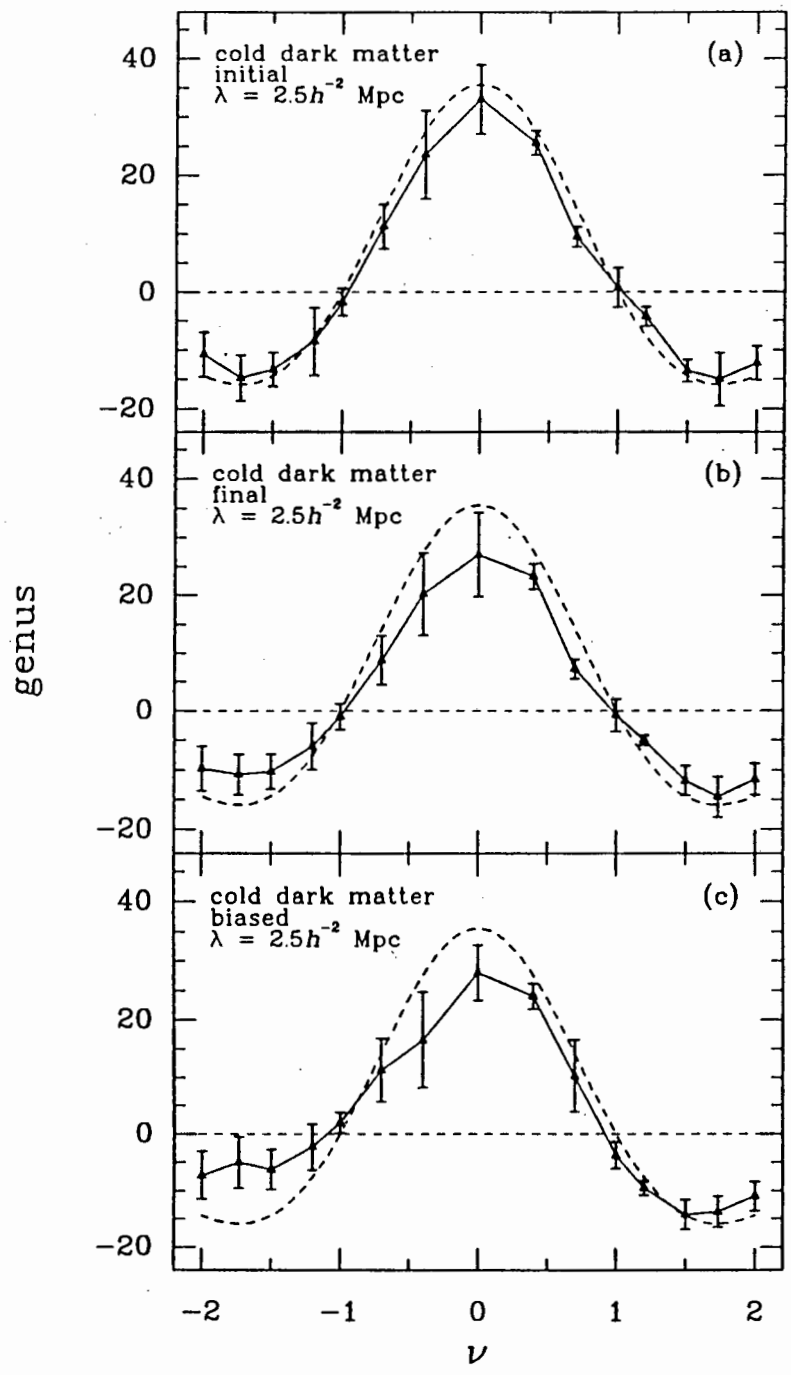

Figure 13 *The genus-threshold density relation fot the (a) initial, (b) final, and (c) biased conditions of the CDM model. Points represent the average results for four simulations. The broken line shows the theoretical prediction for this relation at the time of recombination.*

Simple "toy" models in which galaxies lie on the surface of bubbles or in isolated clusters have non-Gaussian topologies, which appear as asymmetries in the G_s (υ) curve. Bubble or Swiss cheese distributions show a strong preference for isolated voids and a shift of the peak of the G_s curve towards higher densities (see figure 14). Cluster or meatball distributions have the opposite asymmetry, with isolated clusters over a large range of threshold densities and a G_s curve that peaks below the median density.

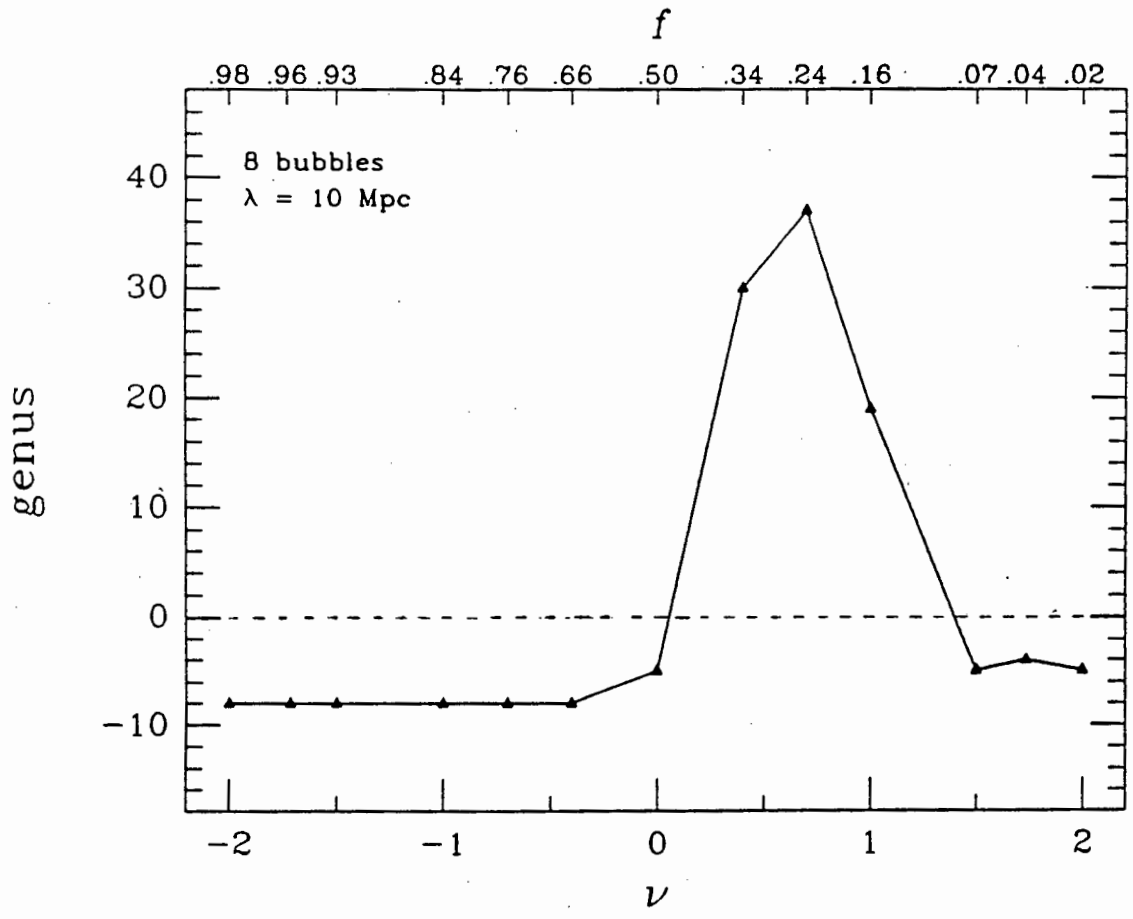

Figure 14 *The genus versus density enhancement curve for the bubble model. The flat portion on the left-hand side at a value G_s = -8 indicates the detection of eight isolated voids.*

HDM models, like CDM models, show a Gaussian topology when they are smoothed at the correlation length. However, they can be distinguished from the CDM models as follows. When smoothed at half the correlation length, dynamically evolved HDM models show a distinct bubble topology. CDM models, however, tend to go in the opposite direction, with some models showing a meatball topology at small smoothing lengths.

Explosion models and cosmic string models have non-Gaussian structure and tend to show Bubble and meatball topologies respectively.

In their most recent paper [Gott et al 1989], Gott and his collaborators apply the topology measuring algorithm to a number of observational data sets including the Abell cluster sample, the Giovanelli and Haynes sample, the CfA sample and the Thuan and Schneider dwarf sample.

On scales significantly larger than the correlation length, it is found that the topology is sponge-like and in agreement with the random Gaussian formula given in equation (6). When the topology is studied on scales of order of the correlation length, there is a small shift in the genus curve in the direction of a meatball topology. No evidence for bubbles was detected in the samples. Whenever shifts did occur, they were in a meatball direction.

Slight meatball shifts show up in CDM models smoothed at the correlation length due to a combination of biasing and sample effects, but this is not sufficient to explain the observational results. Nonetheless, Gott et al conclude that the CDM power spectrum predicts the observed trend of G_S with the smoothing length λ well, and overall, of models studied, the CDM model comes closest to fitting the data. While neutrino models cannot be ruled out, they fit the topology data less well than the CDM models.

2.4) A Fractal description of the Universe

The complicated geometry of superclusters and voids does not lend itself easily to a quantitative description. In the previous section, we discussed a way of describing structure by means of topology. Another method is to use a fractal description of this geometry.

The most widely used quantitative method that has been applied to the study of the large-scale distribution of the galaxies is the correlation analysis developed in detail by Peebles (see section 2.1). One of the interesting results of the correlation study was the discovery of the fact that the correlation length of the sample depends on the type of objects studied: for galaxies it is $5h^{-1}$Mpc [Davis & Peebles], but for clusters of galaxies it is $25h^{-1}$Mpc [Bahcall & Soneira].

Einasto, Klypin and Saar [1986] suggested that this behaviour of the correlation function may be due to the fact that the ratio of the volume occupied by systems of galaxies to the full volume of the sample (the filling factor) is observed to decrease with increasing depth of the samples. They demonstrated that in this case the value of the correlation function at small samples is inversely proportional to the filling factor of the sample.

The tendency of the filling factor to decrease with increasing sample size can be described naturally if we suppose that the distribution of galaxies in space is fractal, as suggested by Mandelbrot [1982]. The basic property of a fractal distribution is its self-similarity, which leads to a systematic dependence of the mean density of a sample and its filling factor on the sample size. Self-similarity is also consistent with the observation (see for example [Szalay & Schramm 1985]) that the distribution of galaxies is mirrored by that of galaxy clusters. This means that one would not be able distinguish between a picture of a galaxy catalogue and a picture of a cluster catalogue, just as would be expected if the universe had a fractal structure.

It should be said that the fractal description of the universe does not yet have any strong motivation from a physical model of large-scale structure formation. Vicsek and Szalay [1987] have developed a model which simulates galaxy formation in the explosion scenario using a cellular-automaton-type stochastic process. Their model results in a fractal structure over a certain range of scales. Further work must still be done, however, in order to gauge the validity of this approach.

Fractal structure is defined as follows. If the cumulative number of galaxies, N(R), in a system of galaxies varies with the distance from any galaxy in the system, R, as

$$N(R) = R^D$$

then the distribution of galaxies is said to be fractal with an effective dimension D. Jones et al [1988] developed a method of determining the effective dimension of a sample by using a box-

counting method by dividing the volume into cells of size l and counting the number of occupied cells $N(l)$. The plot of $\log(N(l))$ versus $\log(1/l)$ yields a straight line, its slope being the fractal dimension of the sample:

$$D(l) = \frac{d[\ \log N(l)\ ]}{d[\ \log (1/l)\ ]}$$

Analysis of the value of the quantity D for various samples of galaxies has led to some controversy over the validity of a simple fractal description of the universe. Einasto et al [1988] explore the possibility of a mixture of fractal sets in the data and propose a multifractal formalism to describe the observations.

Attempts have also been made to investigate the self-similarity of the large-scale structure via the investigation of voids in the galactic distribution. Einasto et al [1989] claim to find evidence that the mean void diameter in a sample is proportional to the size of the sample. Another possibility might be to compare the shape of the spectrum of void sizes of the galaxy distribution to that of the galaxy cluster distribution. In order to accomplish this, the techniques presented in Chapter III might well prove to be useful.

CHAPTER III

VOIDS IN THE DISTRIBUTION OF GALAXIES: AN ASSESSMENT OF THEIR SIGNIFICANCE

3.1) The Need for a Catalogue of Voids

One approach of investigating structure in the universe is to use the high-density peaks of the galaxy distribution, i.e. the rich clusters of galaxies, as tracers of the large-scale structure. In order to do this, a complete sample of clusters over a large volume of space is required. Three extensive catalogues of rich clusters are available: The Abell [1958] catalogue of rich clusters; the "Catalogue of Galaxies and Clusters of Galaxies" by Zwicky et al [1961-1968]; and the catalogue of clusters by Schectman [1985] determined from the Shane & Wirtanen [1967] galaxy counts.

Abell and Zwicky both identified clusters as density enhancements on the Palomar Sky Survey plates, but they used quite different selection criteria for the inclusion of clusters in their catalogues. Schectman identified clusters from the Shane & Wirtanen galaxy counts, using still another selection algorithm of density enhancement. The obvious next step, therefore, is to use a completely automated procedure of identifying clusters by computer algorithms that search data tapes of computer-scanned images. Such "objective" catalogues are being prepared by several groups (eg Maddox et al [1988])

This thesis, however, is concerned with a completely different approach - the study of voids in the distribution of galaxies. Chapters I and II have attempted to show how the study of voids can provide a new perspective on large-scale structure that compliments the one gained by studying clusters and superclusters of galaxies. It has also been stressed that the statistical properties of voids may provide important links between astronomical observations and theories of large-scale structure formation. An obvious question to ask, therefore, is whether there are catalogues of voids akin to the Abell, Zwicky and Schectman catalogues of rich clusters.

In the Northern Hemisphere, a small number of individual voids have been studied quite carefully. The most famous of these is the Bootes void which was discovered by Kirshner et al [1981]. While constructing a deep survey of the distribution of galaxies in six, small, well-

separated fields in the two Galactic caps, Kirshner and his collaborators discovered that the redshift distributions in each of the three Northern fields showed an identical 6000 km/s gap. A redshift survey was then undertaken to test the hypothesis of the existence of a large void in the region [Kirshner et al 1987]. The conclusion is that there is a large, roughly spherical void, of radius 62 Mpc, centred at $\alpha = 14^h50$, $\delta = 46^\circ$ and V = 15500 km/s. Other voids that have been well studied include the Coma void [Gregory & Thompson 1978] and the Hercules void [Tarenghi et al 1979].

However, there has been no systematic search for voids in the Northern Hemisphere. Therefore, no database currently exists that could be used by astrophysicists who wish to consider voids as indicators of large-scale structure in the universe.

In the Southern Hemisphere, a more thorough survey of voids has been accomplished. In an early catalogue of galaxies south of declination -30°, compiled by Fairall [1984], a list of about six major voids evident in the data is given. This list is updated in the Southern Redshifts Catalogue and Plots, compiled by Fairall and Jones [1988]. Twelve major voids in the galaxy distribution can now be identified. These are all striking voids which have been picked out by means of a visual inspection of the galaxy data. Again, this is not really satisfactory as we would ideally prefer a more objective way of identifying voids in the galaxy distribution - a method in which judgement would not be left up to the human eye.

One of the primary goals of this project, therefore, was to devise an algorithm for the purpose of picking out and identifying voids in the galaxy distribution. A method was then developed to assess the "significance" of all the voids that were found. (What exactly is meant by "significance" will be made clear later.) The end result of this procedure is a catalogue of voids of galaxies - the first of its kind in the field of extragalactic astronomy. It is believed that this catalogue represents a database that will be of value to both observers, who wish to know where voids are in order to probe their structure and properties more thoroughly, and to theorists, who wish to solve the problem of the origins of structure in the universe.

3.2) What is a Void?

Characteristics of voids

Before we can begin our search for voids, we need to know exactly what it is we are looking for. Some uncertainty does exist as to the precise definition of a void - whether a void should be defined as a region that is completely empty of galaxies, or whether a void is merely an underdense region in the sample under investigation.

Choosing the definition of a void as an underdense region means that a threshold density for voids must rather arbitrarily be decided on. Moreover, the establishment of a threshold density leads to voids whose boundaries are dependent on the data sample in use. Different data samples give different overall coverage of galaxies and have different selection effects in direction, all of which could affect the boundaries of the void in question. Using this definition thus means that the volumes and positions of voids could vary quite a lot according to the sample of galaxies that is being used.

On the other hand, all major redshift surveys up to the present have shown that voids contain a central, nearly spherical region which is completely empty of galaxies. This central region does not vary appreciably according to what data sample is used, provided that the data sample provides a reasonable coverage of the sky. There is also evidence that as redshifts accumulate in the catalogue, only the boundary walls of the void are affected. The central region of the void remains empty of galaxies.[Fairall 1989]

So if we do decide to believe that voids contain a truly empty central portion, it would make sense to discard the definition of a void as merely an underdense region, simply because of the ambiguities associated with having to choose a threshold density.

For these reasons, voids will be considered as regions that are empty of galaxies throughout this analysis. In other words, voids occur in regions where the matter density was too low for galaxy formation to have taken place (assuming, of course, that galaxies have not moved appreciably since the time of their formation). This definition is simple, physically pleasing, and makes the search for voids a lot easier than it would be otherwise. It has also been motivated by observational considerations as described above.

It should be noted that this definition may result in the split of what has in the past conventionally been regarded as a single void into a number of smaller "subvoids". This would occur as a result of the presence of one or more galaxies in the interior of the region in question. Nonetheless it will be shown in the following sections that significantly large regions which are completely empty of galaxies are still found in the galaxy data, even where the galaxy density is quite high.

Some constraint must clearly be placed on the shape of a void. Otherwise the entire distribution of galaxies could be considered to be embedded in one single, large, interconnected void. This is because galaxies, on a cosmic scale, are essentially point-like objects. Studies of visually identified voids have shown that the shape of these voids can be well approximated by fitting an ellipsoid or a sphere to the galaxies on the boundaries of the voids [Matravers & Maurellis, 1990]. In other words, the "bubbles" in the galactic distribution (see the Introduction) are very nearly spherical or ellipsoidal in shape. A measure of the volume of the void is then given by the volume of the approximating sphere or ellipsoid.

Another important consideration is the size of the void. Even if the distribution of galaxies is completely random, many voids will be found if the void diameter is taken to be comparable to the average intergalactic separation length. This is a very important matter and it will discussed in more detail in the section entitled "The Significance of Voids".

3.3) The Search for Voids

i) The data

The first data set that was used was "The Southern Redshifts Catalogue" compiled by Fairall and Jones [1988]. This catalogue consists of optical redshifts for galaxies south of declination -17.5°.

The data was restricted to a rectangular volume given by

$$-9000\ \text{km/s} \le x \le 9000\ \text{km/s}$$
$$-9000\ \text{km/s} \le y \le 9000\ \text{km/s}$$
$$-9000\ \text{km/s} \le z \le 9000\ \text{km/s}$$

where x, y and z are Cartesian coordinates given by the familiar transformation rule

$$x = V \cos(\alpha) \sin(90^\circ - \delta)$$
$$y = V \sin(\alpha) \sin(90^\circ - \delta)$$
$$z = V \cos(90^\circ - \delta)$$

where V represents the recessional velocity of the galaxy, δ the declination, and α right ascension converted to degrees. Thus the positive x-axis is directed towards R.A. 0 hours and declination 0° and the positive y-axis is directed towards R.A. 6 hours and declination 0°. The positive z-axis is directed towards declination 90°.

This catalogue was later merged with the 1987 version of Huchra's ZCAT (private communication to A.P.Fairall) in order to find Northern Hemisphere voids. Once again a rectangular volume was chosen. Choosing the size of the rectangular volume was a matter of judgement. Beyond a redshift about 10 000 km/s, the data seemed a bit too sparse to warrant a search for voids. However, as a final step, larger rectangular volumes(-16000 km/s $\leq$ x,y,z $\leq$ 16000 km/s) were experimented with in order to find the true volumes of voids located at the edges of the data set, and to extend the void spectrum to larger void sizes.

ii) Control of Data

It should be noted that the data sets mentioned above are not "controlled" data sets. In other words, the redshifts that appear in the "Southern Redshifts Catalogue" and ZCAT were accumulated from many different sources. It is thus a distinct possibility that certain regions of the sky are undersampled in comparison to other regions. This irregularity in sampling is a factor that must be taken into account when the significance of a void that has been found is assessed.

Fairall [1989] comments that the greatest justification for using as many redshifts as possible is to increase the quantity of the data. In the Northern sky the fact that foamlike structures did not show up in the original CfA survey [Davis et al 1981] and yet did appear later in the CfA "slice of the universe" [de Lapparent et al 1986] is an indication that quantity of data is vital for determining the true large-scale structure of the universe. That is not to say that a proper quality - i.e. a magnitude-limited sample - should not be the aim, but its cost is time. The CfA

"slice of the universe" is based on quality data, yet its foamlike structures can even be seen in a much earlier and sparser version of Huchra's ZCAT (1983) - provided that all available redshifts are used. [Fairall et al 1985]

Finally, there are strong indications that voids remain empty even as more and more redshifts are added to the catalogue. All the voids that were identified in the first version of the plots of the Southern skies [Winkler 1983] are confirmed in the 1988 version [Fairall & Jones]. No void has been "filled up" with galaxies as a result of the addition of more redshifts.

It was decided that all available redshifts would be used in undertaking the search for voids in the galaxy distribution. Complete samples of the quality of de Lapparent et al's "slice of the universe" simply do not exist on large enough scales and very big samples of galaxies are needed in order to produce a respectable-sized catalogue of voids. It thus seemed necessary to use all available redshifts in order to accomplish the primary goal that was set. Recall also that the definition of a void that was chosen is a region that is completely empty of galaxies. It is then worthwhile to use all redshifts in order to determine the boundaries of a void in a conservative a manner as possible.

The price that must be paid for using all redshifts is, as mentioned, an uncertainty in the significance of the void that has been found. The possibility that the existence of the void is due to undersampling in a particular direction in the sky must always be considered. This is an issue that is discussed and, it is hoped, partially resolved in the following sections.

iii) The "Voidsearch" Algorithm

As a first step, a cubical gridding was performed on the data set. All cubes containing one or more galaxies were marked "on", and those cubes which were empty of galaxies were marked "off". Cubes in regions obscured by the Milky Way ($-10^\circ \leq b \leq 10^\circ$, b is galactic latitude) and cubes falling outside the declination limits of the data set were also marked "on". The purpose of this was to prevent the program from finding false voids in regions not covered by the data sample.

As a first approximation, the program searched for aggregates of "off" cubes. It was decided that the program would look for cubical-shaped aggregates. This was done for two reasons. Firstly, a cube is the easiest shape to search for, because of the way the gridding was done.

Secondly, a spherical or nearly-spherical void contains an embedded cube whose volume is close to that of the actual void. Searching for cubical voids, therefore, is not very much different to searching for spherical ones.

An important question is the size of the cubical gridding. The smaller the length of the gridding, the higher the resolution of the algorithm, and the smaller the minimum size of a void which can be found. One absolute lower limit on void size corresponds to the mean intergalactic separation length of catalogue galaxies of small redshift. In other words, the diameter of a void must be greater than the average separation between galaxies in the densest region of the catalogue. This length has been estimated to be about 400-500 km/s. The gridding length is thus taken to be 200 km/s, so that the smallest void considered will consist of an aggregate of four grid cubes.

From now on, the aggregate of "off" cubes found by the program will be referred to as the base void. To approximate the actual shape of the void more closely, the program examined the grid cubes in the immediate neighbourhood of the base void. More specifically, the program attempted to append a series of "adjacent faces" onto each of the six outer surfaces of the base void. What is meant by an "adjacent face", is a single-layered, rectangular grouping of "off" cubes, equal to in area or smaller than the surface onto which it is to be added. Figure 15 is a diagrammatical representation of the process just described. This process is particularly tailored to finding spherical or ellipsoidally-shaped voids.

An additional constraint was later imposed: that each adjacent face have area no less than two-thirds that of the surface onto which it was to be added. The purpose of this was to prevent the approximating void from having long, finger-like extensions leading into other voids, instead of a roughly ellipsoidal shape (see figure 16). For the purpose of finding a void spectrum, it is more convenient to regard voids as being isolated, compact objects that do not interconnect. Although it may be argued that Gott's spongelike structure (see section 2.3) is being artificially suppressed here, this procedure permits individual voids to be distinguished and a meaningful measure of volume to be applied to each void.

The program looked for the largest base voids first, progressing down in size to the smaller voids. Each time a base void was found, adjacent faces were then added to fill out its shape. The volume occupied by both base void and adjacent faces was then marked as being filled In this way, smaller voids would not later be found inside the larger ones.

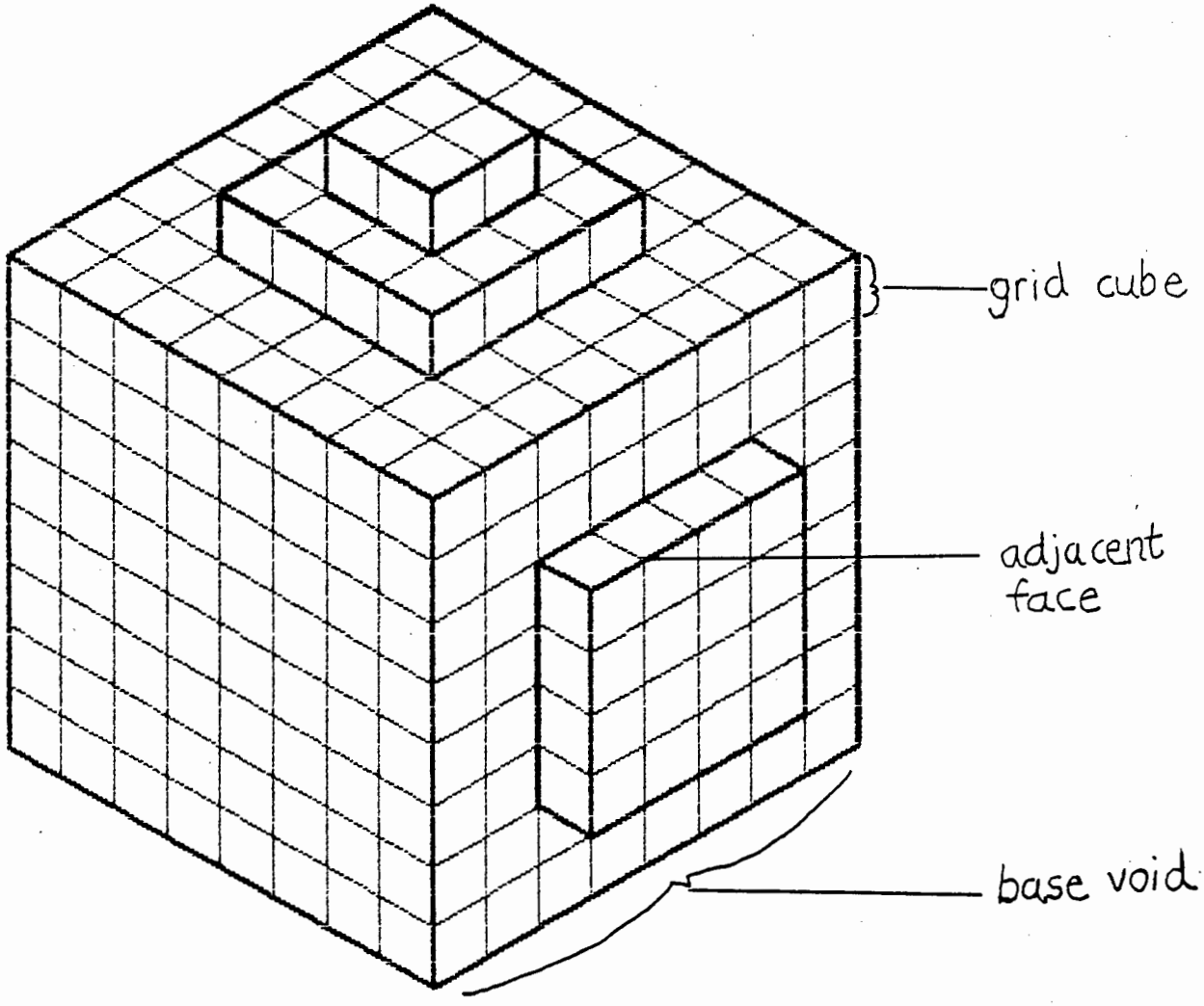

Figure 15 *An illustration of the procedure of locating voids in the "Voidsearch" algorithm. A sample cubical base void is depicted here, together with adjacent faces.*

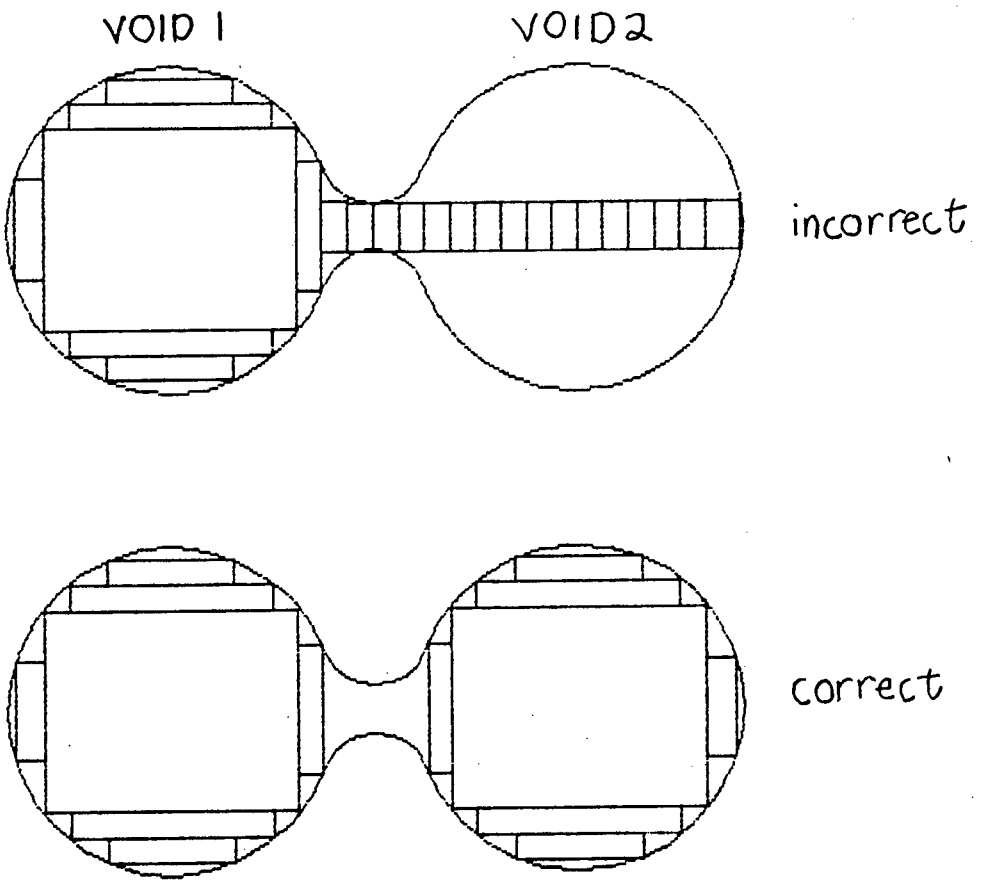

Figure 16 *An illustration of why constraints must be placed on the minimum size of an adjacent face.*

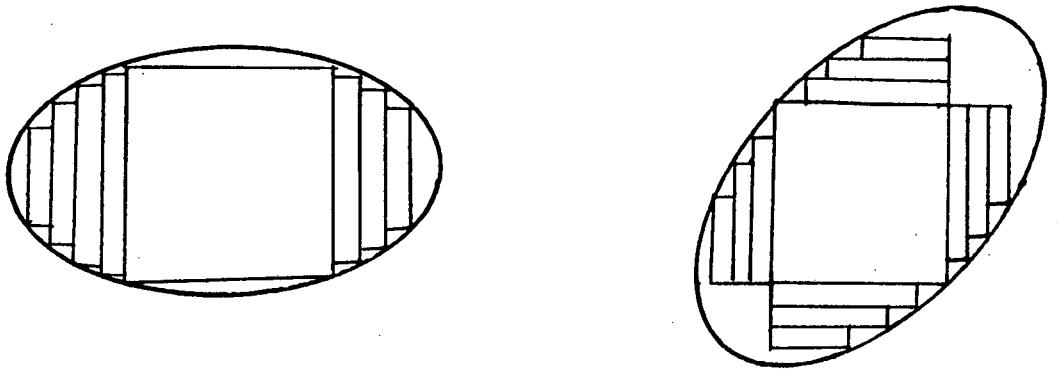

Figure 17 *Void fitting for an ellipsoidal void. Left: The fit is good if the void is aligned along a coordinate axis. Right: The fit is not as good if the void is orientated at an angle to the axis. However, the two base voids are almost the same sizes*

The question might be asked whether the fact that adjacent faces are only searched for along three preferred directions, i.e. those of the x, y and z-axes, does not make the void-finding procedure unduly sensitive to the way the data is orientated. In other words, if the data set were to be rotated through some angle Θ, would the same voids still be found?

Clearly if the void is spherical or very nearly spherical, a rotation of the data set will not make any difference. If the void is more ellipsoidal a situation like that depicted in figure 17 emerges. If the void is aligned along either of the x, y or z-axes, the fit is seen to be very good. If the void is aligned at some angle to these axes, the fit is a good bit worse, but still not unacceptable. However, it can be seen that the Voidsearch algorithm finds almost the same sized base void in each case. In the following sections, it will be seen that it is the significance of the base void that determines the significance of the void itself. Hence a rotation of the data set will not affect the measures of significance in our analysis to any considerable extent.

A listing of the "Voidsearch" program appears in the Appendix.

3.4) The Significance of Voids

What is meant by a "significant" void? If the density of galaxies is high enough to produce a marked contrast between the void and its surroundings, the void may be judged visually to be significant.If the density of galaxies is low, visual judgement of the significance of a void becomes very much more dubious. It is well known that the human eye will pick out voids in even a random distribution of points of low enough density.

The above discussion is particularly relevant to the search for voids in real galaxy catalogues. The density of galaxies in these catalogues falls off very quickly with increasing redshift. At high redshifts, it is not clear if the distribution of galaxies in the catalogue is a good indicator of the underlying large-scale structure. In fact at high redshifts, the catalogue distribution often seems to resemble a purely random one. In addition, directional selection effects may result in voids appearing simply as a result of an undersampling of galaxy redshifts in a certain part of the sky.

Some test of significance is thus needed that can be applied to each void found by the algorithm described in the previous section. The significance of a void will clearly depend on two parameters - its size and the mean density of its surroundings. The significance also depends on the shape of the void in question. However, by sticking to one shape (cubes in this case), this complication can be avoided..

Let us suppose, for argument's sake, that we have a box of galaxies of mean density n and that the mean density does not vary too appreciably according to what subsection of the box we consider (i.e. there are no selection effects operating inside the box). Suppose that we have located a cubical void of volume V inside it.

Let us now generate another box of galaxies of mean density n, but this time, let the galaxies be distributed randomly within the box.

Then we can calculate the probability of finding a cubical void of volume V inside this second box as being:

$$P = (nV)^3 / V * \exp(-nV) \qquad (1)$$

[Otto et al 1986]

If P is very small ($P << 1$), we say that our cubical void is significant. The fact that P is small means that the void must have been formed by some physical mechanism. The existence of the void does not fit the random distribution hypothesis, and thus cannot be dismissed as being merely a consequence of a lack of data in the box.

The above argument describes the essence of the test of significance that was used.. However, it was not chosen to follow Politzer, Preskill and Wise's analytical approach to calculating void probabilities. This was because the data set in use has rather complex boundaries resulting from the exclusion of the region between -10° and 10° in galactic latitude. Formula (1) has to be modified for edge effects introduced by the boundaries of the data set. Also, the mean density varies quite markedly throughout the catalogue, both as a result of the decrease in data with increasing redshift, and as a result of directional selection effects. It was therefore decided that probabilities would be calculated by means of computer simulations using random catalogues.

3.5) The Random Catalogue Simulations

The aim was to produce a random catalogue that incorporated the observational selection effects of the galaxy catalogue itself. Obviously, not all observational selection effects can be accounted for, but a thorough analysis of the data was performed in order to search for general trends in selection. What was found is as follows:

1) The most important selection effect is the decrease in galaxy density with increasing redshift. (See figure 18)

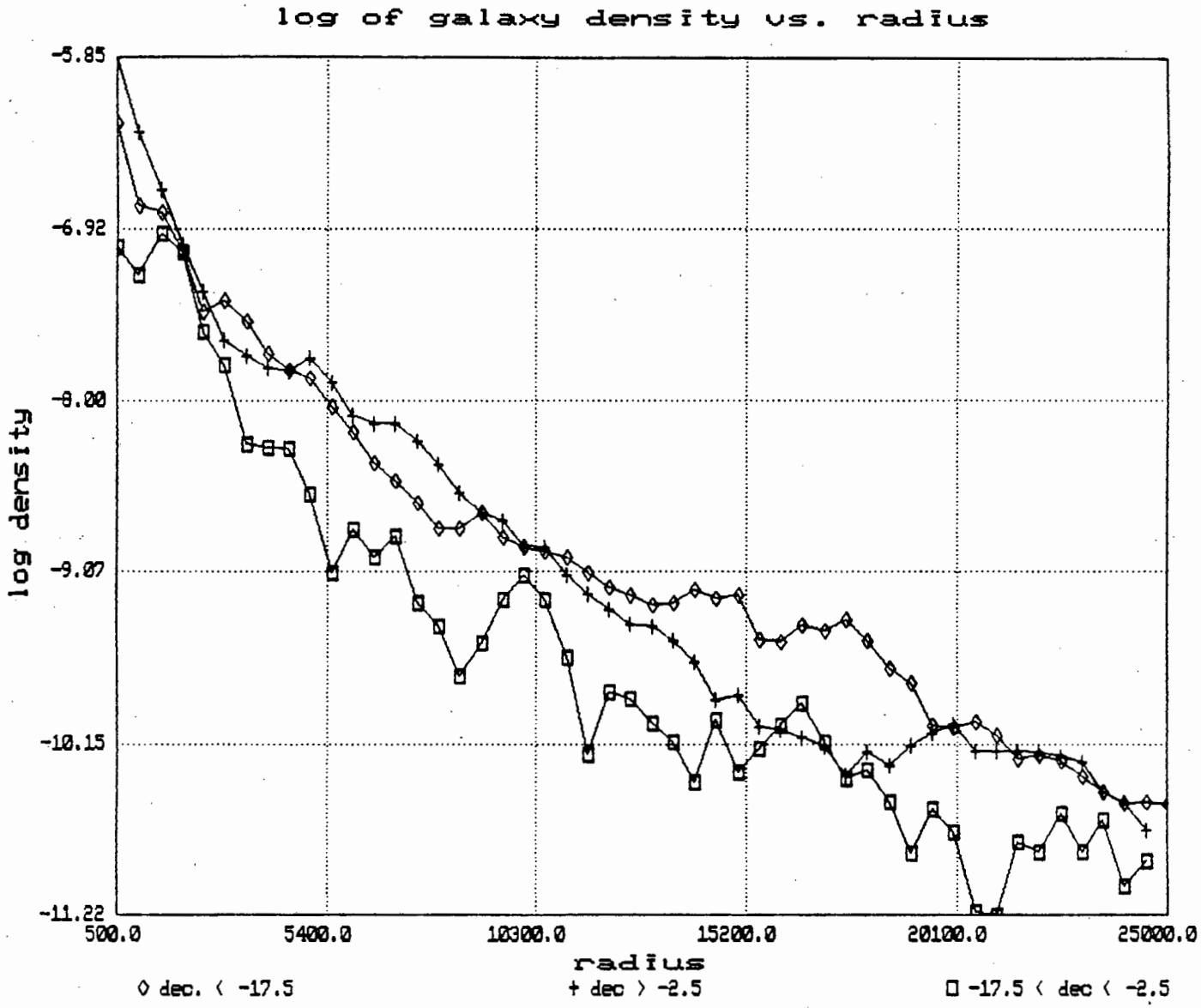

Figure 18 *Log of galaxy density plotted against radial distance from the earth for the three regions: $\delta < -17.5^\circ$, $-17.5^\circ < \delta < -2.5^\circ$ and $\delta > -2.5^\circ$. Radial distance is given in km/s and density is in units of [no. of galaxies/$(km/s)^3$]*

2) There is a selection effect in galactic latitude. As galactic latitude approaches 0°, there is an increasing extinction in galaxy number. This is of course due to obscuration by the Milky Way.

3) There are selection effects in declination. In the Northern Hemisphere, regions of high declination tend to be undersampled in comparison to the region $0^\circ < \delta < 35^\circ$. It is suspected that this effect may be attributed to the fact that most observatories are situated at middle latitudes, and there is a tendency for astronomers to concentrate their observations in the overhead direction.The same effect is present in the Southern Hemisphere data. There is also a very sharp underdensity of data near $\delta = -90^\circ$. However, this is probably the result of a large, well-known void situated there.

4) When the Southern Redshifts Catalogue is merged with ZCAT, there is a marked underdensity of data in the region between -2.5° and -17.5° in declination.This region is a traditional "no man's land", as Southern Hemisphere observers have bounded their catalogues at $\delta = -17.5^\circ$ and Northern Hemisphere observers have bounded theirs at $\delta = -2.5^\circ$. This region of the sky has thus not been properly catalogued yet. The author's thesis supervisor (Fairall) is presently part of a joint effort to obtain redshifts in this area. When this task is completed, Northern and Southern redshifts will be able to be merged to give a more realistic picture of the entire sky.

5) The Southern and Northern Hemisphere catalogues have different density vs. redshift functions. This is entirely expected.

In generating the random catalogues, the following procedure was used. Galaxies were generated into concentric radial shells of width 500 km/s out to a limiting redshift of 25000 km/s. Into each radial shell, the same number of galaxies were placed at random as occurred in the corresponding shell of the real catalogue. This was done separately for the Northern Hemisphere, the Southern Hemisphere and the intervening "no man's land". In this way, the density vs. redshift functions of the real catalogues could be mimicked in the random catalogues.

Each time a galaxy was generated, it was subjected to a certain probability of extinction according to the value of its galactic latitude and declination. These probabilities were given in

look-up tables in the program, rough values for which were obtained from the analysis of the real galaxy catalogues. By experimenting with different values in the look-up table, random catalogues were obtained with much the same selection effects as the real ones.

The next step was to run the Voidsearch algorithm on a rectangular sub-volume of each of the 100 random catalogues that were generated, and to compare the average distribution of voids to that of the real universe.

It has been suggested by Lynden-Bell (private communication) that an alternative way of generating a random catalogue with the same directional selection effects as a real galaxy catalogue would be to randomly juggle the redshifts within the real catalogue itself. In other words, random catalogues would be generated by picking the directions in the sky of real galaxies, and reassigning the redshifts randomly from the redshift catalogue. This would move the galaxies radially, but would keep all the directional selection effects of the real catalogue.

Unfortunately, this suggestion has come too late for the results to be included in this thesis. However,a discussion and comparison of the two methods of generating random catalogues will be included in a future publication.

3.6) Results of the Random Simulations

As has been discussed previously, whether a void is significant or not depends upon its volume and upon the density of its surroundings. It has also been seen that density is correlated very strongly with redshift and to a lesser extent, declination.

An illuminating way of studying the void distribution is to divide the voids into different groups or "classes" according to their volume, and the declination of their centres. The dimension of the base void is used to determine which volume class a given void belongs to. Five declination classes are also defined : $\delta < -25^\circ$; $-25^\circ < \delta < 0^\circ$; $0^\circ < \delta < 30^\circ$; $30^\circ < \delta < 60^\circ$ and $60^\circ < \delta < 90^\circ$. We will refer to these declination classes as A, B, C, D and E respectively. Then each void can be characterized by an ordered pair consisting of a number and a letter. The number refers to the size of the base void, and the letter refers to which declination group the void belongs to. For example, a void labelled (6,C) would have a base void six grid units in length, and would have a centre lying between 0° and 30° in declination.

The purpose of the division of voids in this manner is to "factor out", in a sense, the dependence of void significance on volume and declination. We can now concentrate on the distribution in redshift space of voids of a given volume and declination class. In figures 19 - 21, histograms of Number of Voids vs. Redshift are plotted. Each figure corresponds to a different class of voids: figure 19, voids labelled by (3,C); figure 20, (6,D); figure 21, (5,A). The solid line corresponds to the real distribution of voids, while the dotted line corresponds the average void distribution of all the random catalogues.

In each case, we see that the real distribution is shifted to the left with respect to the random one. What this means is that in the real catalogue, voids of a given size occur at lower redshift than they do in the random catalogues. In other words, there exist voids which occur at galaxy densities high enough, so that the probability of finding such voids at the corresponding redshift in a random catalogue is very small indeed.

In each of figures 19 - 21, two regions in the graph of the real void distribution have been shaded in. Region I, marked by horizontal shading, corresponds to voids in the region where the random probability distribution is zero. Since a total of 100 random simulations were performed, this means that these voids occur in the random catalogues with probability less than 1%. Region II, marked by vertical shading, corresponds to the region where there is an overdensity of voids in the real distribution as compared to the random one. Voids which occur in region I are called significant. The redshift which marks the right-hand boundary of region I,is called the cut-off redshift for significant voids. Once again it must be stressed that this cut-off redshift is different for each class of voids and must be determined separately.

In region II, the distribution of galaxies is a lot more "voidy" than in the random catalogues. However, it is not possible to pinpoint any individual void as being significant. The random "noise", caused by the lack of observational data, is quite high. This is what prevents us from finding significant voids in this region.

Beyond the redshift which marks the right-hand boundary of region II, the real distribution joins the random one. The lack of observational data here is so great, that the galaxy distribution cannot be thought to trace the bubbly structure at all.

It is worthwhile to include a special discussion of figure 19 at this point. This is because figure 19 shows a typical distribution of a class of small voids in the real galaxy catalogue as compared to the average distribution of the same class in the random catalogues. It should be

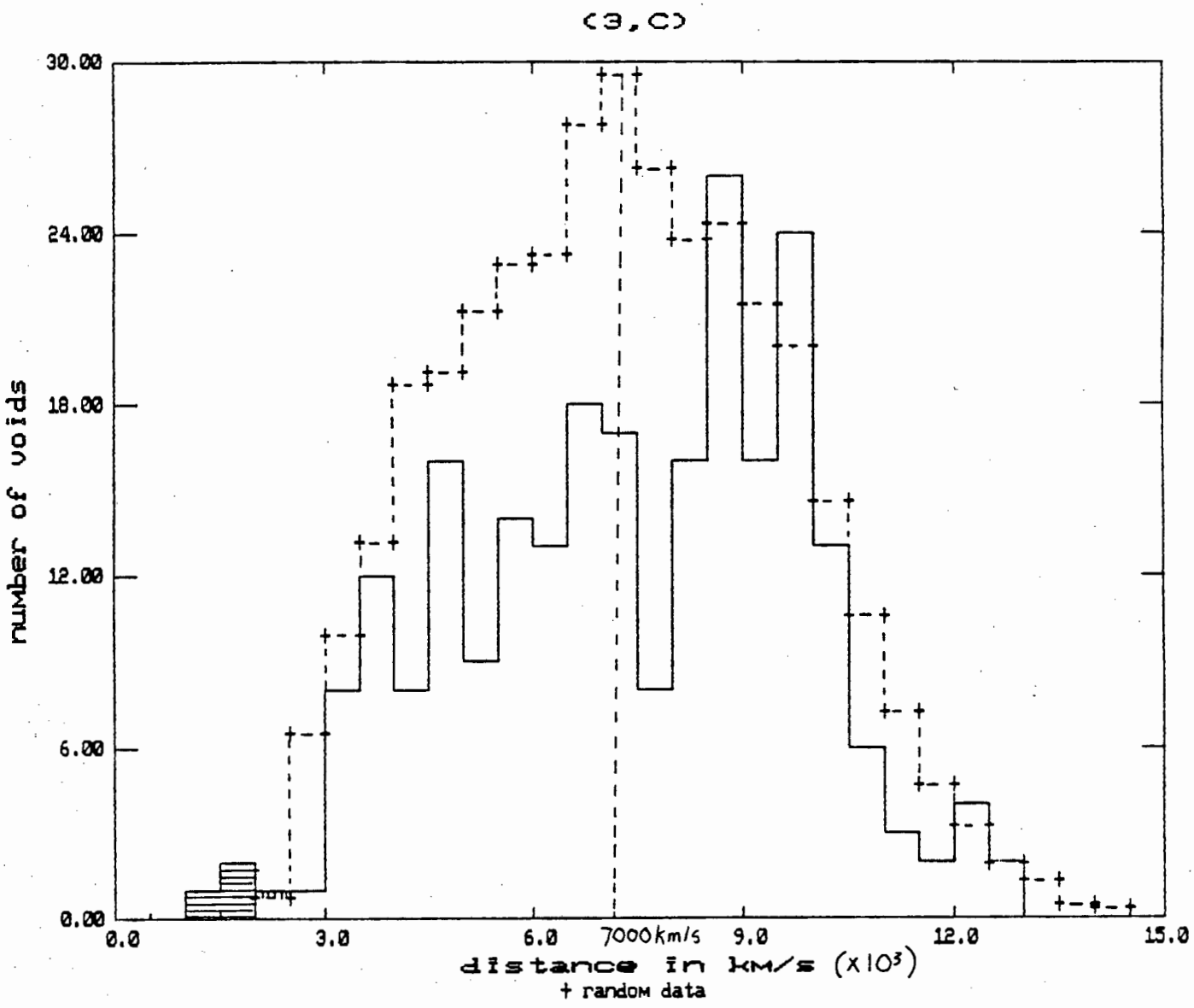

Figure 19 *The histogram of the void distribution for the real galaxy catalogue as compared to the histogram for the average random catalogue distribution. The shadings are explained in the text. This figure shows the distribution of voids falling in class (3,C).*

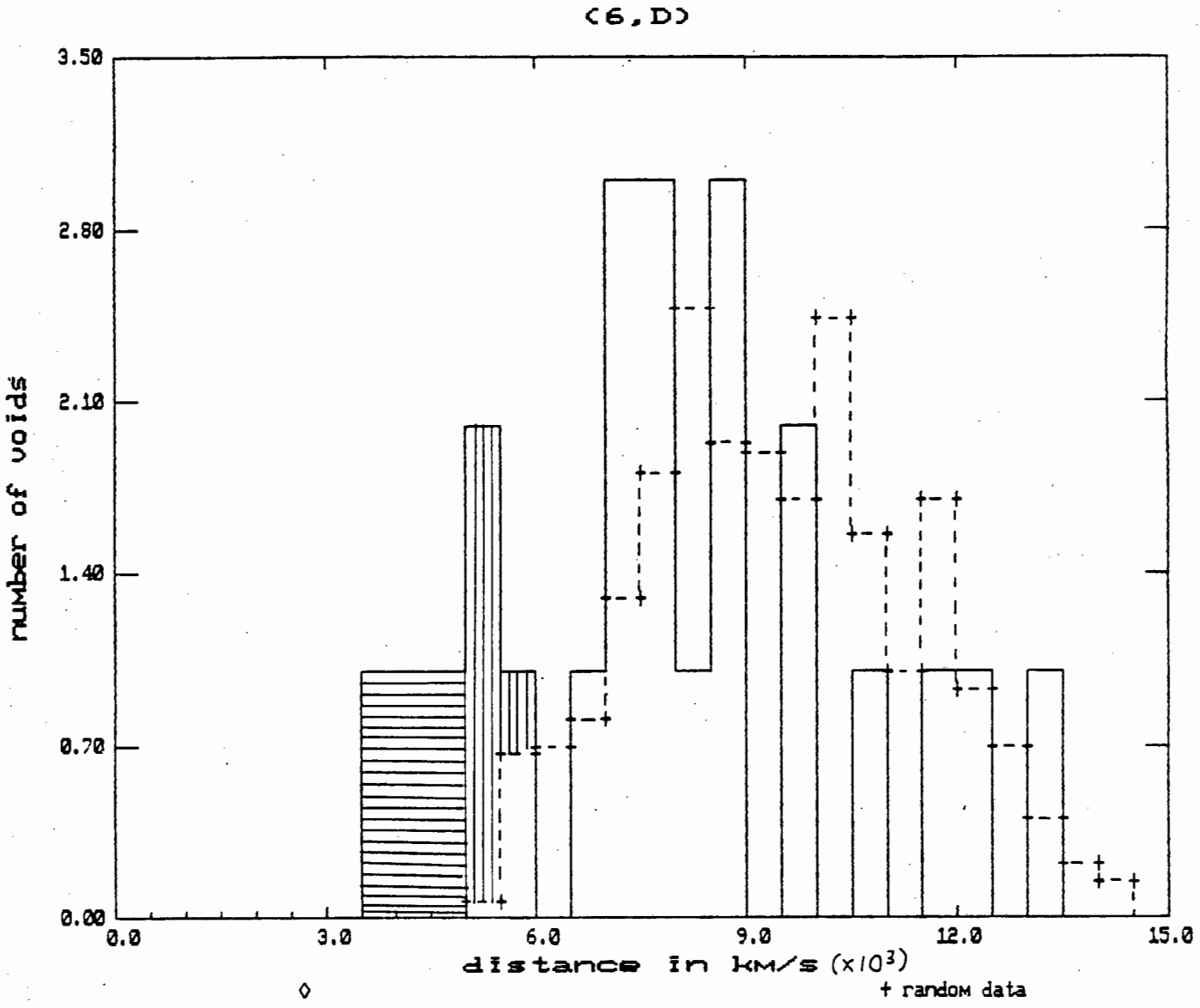

Figure 20 *As in figure 18, but for voids in class (6,D).*

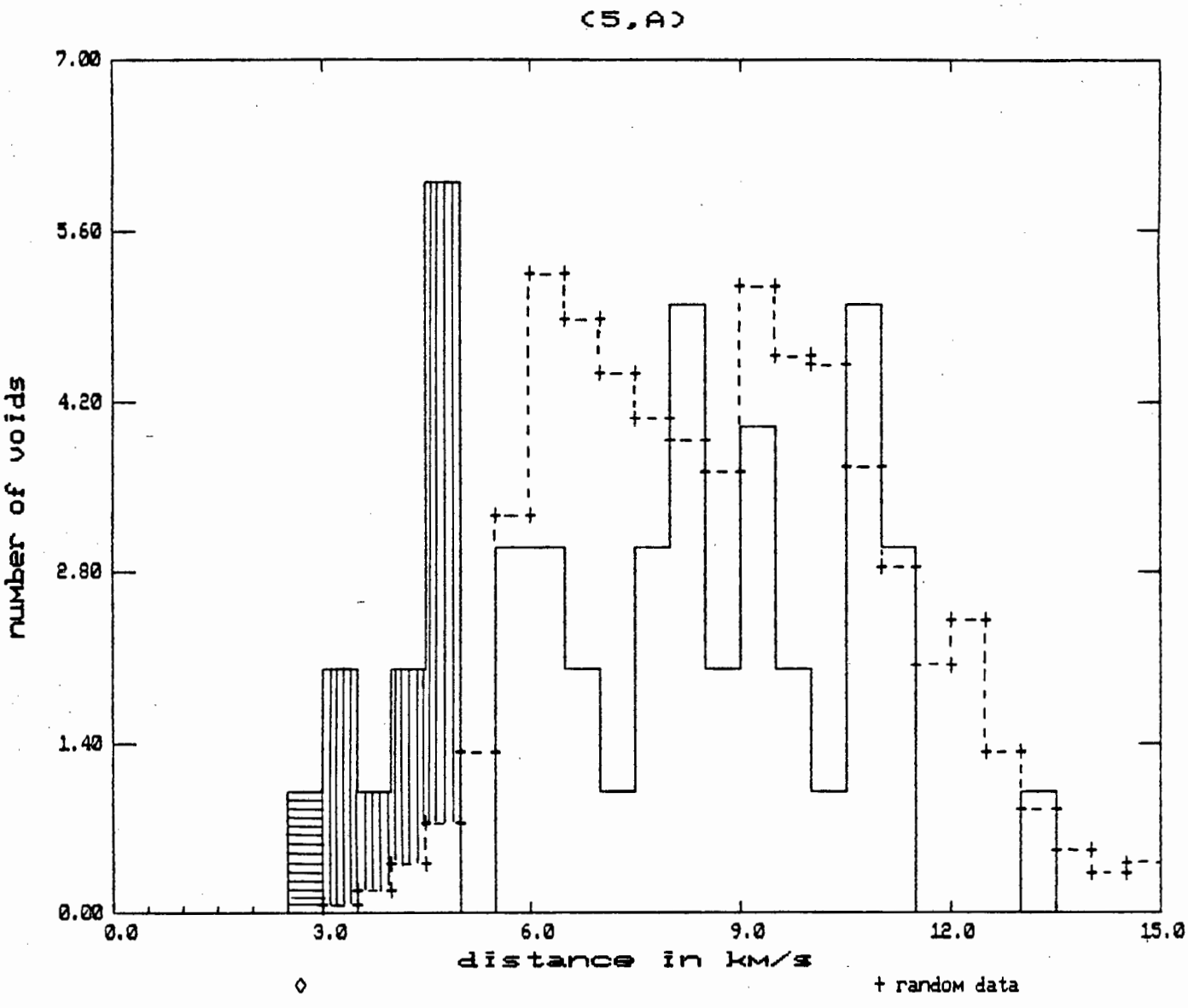

Figure 21 *As in figure 18, but for voids in class (5,A).*

noted that the shape of the average distribution of the random catalogues is more or less symmetric about the line corresponding to distance = 7000 km/s. The shape of the real catalogue distribution is, however, skewed quite distinctly to the right.

This can be explained by the fact that in the real galaxy catalogue, the larger voids are occurring at smaller redshifts than in the random ones. The presence of these large voids thus leaves less "room" for small voids to be found at low redshifts. This is why the small void distribution for the real catalogue dips below the average random one for redshifts between 3000 and 8000 km/s in figure 19.

Figure 19 is thus interesting from two points of view. First of all, it illustrates that small voids are found at lower redshifts in the real catalogue than in the random ones. Secondly, it contains information that relates directly to the distribution of the larger voids in both the real and random catalogues.

In the following subsections, the results of the random simulations will be presented for three data sets:

1) The Southern Redshifts Catalogue (1988 version)
2) The Southern Redshifts Catalogue (1985 version)
3) The merged ZCAT and Southern Redshifts Catalogue (1988)

3.6.1) The Southern Redshifts Catalogue (1988 version)

4236 galaxies out to a limiting redshift of 16 000 km/s were taken from this catalogue .

Fairall [Fairall & Jones 1988] has performed an extensive visual analysis of the Southern Hemisphere galaxy distribution. He has identified thirteen candidates for voids and has given them the names: Sagittarius, Microscopium, Eridanus, Southern Eridanus, Octans, Hydra, Sculptor, Apus, Columba, Capricornus, Fornax, Hydrus and Ara.

In Table 1 , a list of the significant voids found in the Southern Redshifts Catalogue is presented. A void is considered significant if it occurs in the random catalogue simulations with probability less than 1%. All the candidate voids appear except for Fornax, Hydrus and Ara. Voids corresponding to Fornax, Hydrus and Ara were found by the Voidsearch algorithm, but they were not deemed to be significant. Of the three, Fornax was the most significant, with a random probability of 16%.

cube size	edge count	total size	dist. (km/s)	r.a .	decl.	name/ comments
3	12	39	1109	20.4	-39.1	Sagittarius
4	44	108	1939	19.5	-38.2	Joins onto Sagittarius
4	32	96	1844	18.0	-77.5	Octans
6	384	600	3311	2.5	-46.5	Eridanus
7	294	637	4836	21.5	-76.4	Apus
8	638	1150	4280	20.0	-30.9	Micro-scopium
8	64	576	4055	3.0	-69.6	Southern Eridanus
8	549	1061	5188	6.0	-27.6	edge of data set
9	1244	1973	5429	11.8	-29.8	Hydra
10	1000	2000	5064	23.6	-33.6	Sculptor
13	1868	4065	8449	15.4	-29.0	edge of data set
13	1690	3887	8296	19.4	-64.7	Apus extension?
14	615	3359	7413	10.2	-86.5	Apus extension?
16	1813	5909	8122	5.2	-36.2	Columba
16	2009	6105	9735	19.7	-29.4	Capricornus

Table 1

A list of highly significant (<1% chance of ocurrence in a random catalogue) voids found in the Southern Redshifts Catalogue [Fairall & Jones 1987] .
Cube size refers to the number of grid cubes (size 200 km/s) along the edge of the cubical base void.
Edge count refers to the number of grid cubes in all the adjacent faces.
Total size is the total number of grid cubes in the entire void.
R.a. and decl. are the right ascensions and declinations of the centres of the cubical base voids.

In Table 2 , a list of the regions which have an overdensity of voids as compared to the random catalogues is given. The void overdensity factor δV is defined as follows:

$$\delta V = n \text{ (real)} / n \text{ (random)}$$

where n (real) is the number of voids in the region in the real catalogue, and n (random) is the average number of voids in the random catalogues.

An overdensity of voids δV that is less than one means that more voids were present between the given redshift limits in the average random catalogue than in the real one. This corresponds to a region where the real distribution has dipped below the random one, as explained in the previous section.

TABLE 2

cube size	dist range (km/s)	δV - void enhancement factor
2	500 - 1000	3.75
	1000 - 1500	2.22
	1500 - 2000	< 1
	2000 - 2500	< 1
3	1000 - 1500	∞
	1500 - 2000	10.96
	2000 - 2500	< 1
	2500 - 3000	1.43
	3000 - 3500	1.32
	3500 - 4000	< 1
	4000 - 4500	< 1
4	1500 - 2000	∞
	2000 - 2500	4.87
	2500 - 3000	1.92
	3000 - 3500	1.16
	3500 - 4000	< 1
	4000 - 4500	< 1
5	3000 - 3500	7.31
	3500 - 4000	< 1
	4000 - 4500	< 1
6	3000 - 3500	∞
	4000 - 4500	10.56
	4500 - 5000	10.00
	5000 - 5500	1.98
	5500 - 6000	< 1
	6000 - 6500	< 1
7	4500 - 5000	∞
	5000 - 5500	47.40
	5500 - 6000	5.9
	6000 - 6500	1.8
	6500 - 7000	< 1
	7000 - 7500	< 1

cube size	dist range (km/s)	δV - void enhancement factor
8	4000 - 4500	∞
	5000 - 5500	∞
	5500 - 6000	< 1
	6000 - 6500	13.60
	6500 - 7000	< 1
	7000 - 7500	< 1
9	5000 - 5500	∞
	6000 - 6500	< 1
	6500 - 7000	< 1

Table 2

A listing of the regions where there is an overdensity of voids in the Southern Redshifts Catalogue as compared to random catalogue simulations.

An overdensity of ∞ indicates that no voids of that size were located in the region in any of the one hundred random simulations.

$\delta V < .1$ indicates that there are more voids present on average in the random catalogues than in the real galaxy catalogue.

3.6.2)The Southern Redshifts Catalogue (1985 version)

This is an earlier version of the previous catalogue with about half as many galaxy redshifts in it. It is also bounded at $\delta = -30^{\circ}$ as opposed to $\delta = -17.5^{\circ}$ for the 1988 version.

The purpose of analyzing this catalogue is to see how void significance evolves as a galaxy catalogue is built up. In Table 3 , all voids that have random probability less than 15% are presented. The two polar voids, Octans and Apus, are the only Fairall voids with random probability less than 1%. Other Fairall voids, namely Sagittarius, Sculptor, Microscopium, Eridanus, Southern Eridanus, Hydra, and Columba are present, but at fairly high random probabilities. These probabilities may be exaggerated, as the $\delta = -30^{\circ}$ boundary of the catalogue means that some of these voids are cut off, and a true measure of their volume is not obtained. However, what is clear is that almost all the voids which are found with random probabilities less than about 15% do not "disappear" when more redshifts are added to the catalogue. They are present again in the 1988 version, and at a higher significance too.

TABLE 3

cube size	edge count	total size	dist. (km/s)	r.a .	decl.	name/ comments	random prob.
4	66	130	2450	0.4	-34.9	Sagittarius	10%
5	125	250	2179	3.9	-74.5	Octans	< 1%
6	371	587	4176	19.4	-35.1	Micro-scopium	14%
6	186	402	3709	3.0	-40.3	Eridanus	6%
6	325	541	3655	16.8	-80.0	Octans/ Apus	6%
6	362	578	4530	2.7	-62.0	Southern Eridanus	14%
7	107	450	4511	23.0	-36.8	Part of Sculptor	4%
7	646	989	3559	6.5	-49.3	edge of data set	2%
8	355	867	5790	14.7	-36.0	edge of data set	10%
9	1907	2636	6755	22.5	-35.3	Sculptor	12%
14	3483	6227	7002	12.0	-88.4	Apus	< 1%
14	3807	6551	8355	4.4	-38.5	Columba	5%

Table 3

A list of significant voids found in the 1985 version of the Southern Redshifts Catalogue. These voids are all found in a random catalogue with probabilty less than 15%.

3.6.3)The merged ZCAT and Southern Redshifts Catalogue

This catalogue consists of 17929 galaxies out to a limiting redshift of 30 000 km/s. It includes all the galaxies listed in the Southern Redshifts Survey.

This is the data set that is used to obtain the void spectrum described in the next chapter. Table 4 is a list of all voids, out to a limiting redshift of about 15 000 km/s, that were found with random probability less than 15%.

Southern Hemisphere voids listed in Table 1 appear again in this list. However, Southern voids which were previously found near the edges of the data set, may have had their volumes and positions shifted as a result of the merger of the two catalogues.

In the analysis of this data set, two griddings were used. Firstly a fine gridding (200 km/s) was used to search for the smaller voids out to a limiting redshift of about 9500 km/s. Then the grid size was doubled to 400 km/s and voids out to limiting redshift of 15 000 km/s were located. This was done in order to save computer time. In addition, it was not considered necessary to use a high-resolution procedure to locate the larger voids.

Care was also taken in order to ensure that the largest, and hence most distant voids occurred well within the rectangular boundaries of the data set. By doing this, we sought to make sure that true estimates of the volumes and densities of voids would be obtained. The artificial truncation of voids due to obscuration by the Milky Way is, however, a problem that was not addressed. This factor may influence the volume estimates of a number of voids listed in Table 4.

Special attention is called to four particular voids. These voids are labelled by the numbers (88), (89),(90) and (93) in the right-hand column of Table 4. These are large voids that have exceptionally high significance. In other words, the probability of finding such voids in random catalogue simulations is well below 1%. If we assume that each base void is embedded in a surrounding sphere which is empty of galaxies, voids (88), (89) and (90) would each have diameters of $50h^{-1}$ Mpc and void (93) would have a diameter of $62h^{-1}$ Mpc (where $h = H_0/100\ kms^{-1}\ Mpc^{-1}$). These are thus voids which are comparable in size to the "great" void in Boötes ($62h^{-1}$ Mpc in diameter), which was discovered by Kirshner et al [Kirshner 1987]. These voids are also significantly closer than the Boötes void, which would make them easier to study in detail.

An attempt was made to examine voids (88) and (89) a bit more closely. This was thought to be especially necessary, since these voids occur in the "no man's land" marking the boundary of the Southern and Northern galaxy catalogues. A few hundred recently acquired, unpublished redshifts in the vicinity of the two voids were added in by hand, and it was found that they remained unscathed. No new galaxies were found to lie near the centre of the voids.

TABLE 4

cube size	edge count	total size	dist. (km/s)	r.a .	decl.	void ref no
2	4	12	1000	20.5	0.0	1
3	12	39	1797	10.3	-22.9	2
3	12	39	1145	23.0	-5.0	3
3	39	66	1338	5.1	-4.3	4
3	29	56	1706	20.7	3.4	5
3	47	74	1396	8.2	21.0	6
3	57	84	1905	4.5	15.2	7
3	6	33	1658	22.6	32.9	8
4	16	80	2245	7.8	-78.5	9
4	0	64	2040	18.0	-78.7	10
4	28	92	2474	4.9	-53.9	11
4	73	137	2683	10.2	0.0	12
4	32	96	2425	13.6	4.7	13
4	60	124	2683	15.4	17.3	14
4	60	124	2010	17.2	23.5	15
4	0	64	1497	1.2	32.3	16
4	92	156	2623	21.9	27.2	17
4	60	124	2482	7.2	40.1	18
5	180	305	3192	4.5	-76.2	19
5	40	165	2629	0.9	-34.8	20
5	85	210	3217	4.8	-27.8	21
5	20	145	2105	21.3	-19.4	22
5	110	235	2704	21.0	6.4	23
5	0	125	3217	0.8	8.9	24
5	174	299	3267	8.1	12.4	25
5	120	245	3913	17.1	13.3	26
5	50	175	3984	14.7	16.0	27
5	80	205	3254	10.0	35.7	28
6	120	336	3726	6.3	-53.6	29
6	110	326	3742	2.8	-44.0	30
6	356	572	3487	21.0	-13.3	31
6	108	324	2683	3.4	17.3	32
6	0	216	4907	17.8	11.8	33
6	158	374	3567	0.3	38.1	34
6	515	731	4418	7.5	46.4	35
6	294	510	5404	0.0	39.0	36
6	144	360	4833	16.0	48.1	37
6	130	346	5466	14.1	50.2	38
7	35	378	5996	21.6	-71.9	39
7	403	746	3872	16.9	-4.4	40
7	126	469	4102	15.0	-1.4	41
7	781	1124	5451	13.2	9.5	42
7	331	674	5996	3.2	14.5	43
7	224	567	6593	22.0	16.7	44

TABLE 4

cube size	edge count	total size	dist. (km/s)	r.a .	decl.	void ref no
7	378	721	4476	11.2	37.1	45
7	332	675	4034	19.9	75.2	46
8	528	1040	6378	15.1	3.6	47
8	168	680	6753	2.0	17.2	48
8	615	1127	7122	14.6	21.3	49
8	56	568	3965	17.7	44.9	50
8	244	756	4956	14.7	68.2	51
8	416	928	5950	9.9	50.6	52
8	458	970	5646	11.1	73.0	53
9	850	1579	6173	23.3	-19.9	54
9	216	945	6147	22.0	2.8	55
9	888	1617	6327	4.5	13.7	56
9	352	1081	7675	15.7	20.6	57
9	951	1680	5827	16.8	32.1	58
9	706	1435	8335	23.2	39.5	59
9	436	1165	7469	12.1	63.8	60
10	941	1941	7400	22.9	-40.4	61
10	1959	2959	7291	4.2	-11.1	62
10	474	1474	7365	21.0	3.1	63
10	172	1172	8991	16.6	18.1	64
10	1000	2000	7305	15.6	52.6	65
10	996	1996	7068	19.0	58.1	66
11	1260	2591	5723	15.9	-15.2	67
11	1439	2770	8258	0.8	11.9	68
11	1546	2877	9945	14.3	17.0	69
12 +	2160	3888	9067	19.4	-67.9	70
12 +	1120	2848	8275	16.1	5.5	71
12 +	0	1728	8980	0.7	5	72
12 +	240	1968	9675	22.1	19.3	73
12 +	480	2208	9330	3.5	31.0	74
12 +	976	2704	8030	0.8	40.4	75
14 +	616	3360	7097	6.1	-40.4	76
14 +	3640	6384	10157	5.8	-14.8	77
14 +	2656	5400	9319	20.0	-13.7	78
14 +	2592	5336	7826	1.5	-13.3	79
14 +	1664	4408	10574	20.8	7.6	80
14 +	1904	4648	10931	2.5	7.4	81
14 +	5032	7776	8679	3.9	82.3	82
16 +	2440	6536	13452	18.2	-59.6	83
16 +	8520	12616	10072	23.5	-16.1	84
16 +	384	4480	11737	2.4	-62.4	85
16 +	7080	11176	12937	4.7	8.9	86
16 +	3984	8080	11960	7.2	39.5	87

cube size	edge count	total size	dist. (km/s)	r.a .	decl.	void ref no
18 +	6200	12032	10619	14.9	-16.4	88
18 +	2520	8352	10498	9.2	-3.3	89
18 +	6664	12496	10498	18.1	31.0	90
20 +	8680	16680	15748	0.2	-62.7	91
20 +	12936	20936	15321	13.2	16.7	92
22 +	29169	39816	13815	13.2	-87.4	93
22 +	5456	16104	14248	23.7	-13.8	94
22 +	29849	40496	14237	20.1	75.8	95

Table 4

A list of 95 significant voids (<15% probability of finding void in a random catalogue) for the merged Southern Redshifts Catalogue and ZCAT. (Note: For locating cubical base voids size 12 and larger, the grid size was doubled to 400 km/s. This was done in order to save computer time. The resolution of the void-finding procedure is thus cut by a half for the larger voids. This is indicated by a "+" in the table above)

3.7) Discussion of the Results

In the 1988 version of the Southern Redshifts Catalogue, the majority of the significant voids that were found were those that had already been identified visually as candidate voids. The analysis presented in this chapter has thus served to confirm their validity. It can be stated that it is very highly probable that these voids are real - that they are not the artefacts of a lack of data in any region. The visual analysis of the Southern Redshifts Catalogue accomplished by Fairall and Jones [1988] has therefore been tested numerically and has been found to be quite sound.

The time evolution of the Southern Redshifts catalogue has also been studied. By time evolution, we mean the evolution of the picture of large-scale structure given by the catalogue as more and more redshifts are added to it. It has been seen that most voids which were found in the 1985 catalogue with random probability less than 15%, occur again in the 1988 catalogue. In other words, there is definite evidence that voids tend to remain empty and change only slightly in volume as redshifts accumulate. For this reason, the author believes that the procedure developed in this chapter allows one to predict the existence and position of a void, and to get a rough measure of its volume, even in regions where there is a sparsity of observational data.

In the Northern Hemisphere, no previous systematic search for voids has been made. Table 4 is therefore a type of catalogue of voids. Of course, as more data becomes available, the catalogue will have to be altered. Meantime, it is believed, this catalogue can serve as a predictive tool for the volume and position of voids "hidden" by a lack of observational data.

An attempt was made to correlate some of the voids given in Table 4 with voids that are evident in the CfA "slice of the universe". In figure 22, the positions and numbers of five voids which appear in Table 4 are indicated on the CfA plot. The numbers shown are the "void reference numbers" listed in the right-hand column of Table 4.

Positions of possible voids have also been indicated in the "Redshift Plots of Huchra's Z Catalogue" [Fairall et al 1985]. In figure 23, the slice corresponding to right ascension 10 hours is shown. Six voids present in Table 4 can be located in this slice and their positions and identities are once again indicated by the void reference numbers.

Finally, four potentially interesting voids have been identified. These voids are unusually large, close by, and statistically very significant. Because of the implications that large voids hold for large-scale structure formation theories (see section 1.17) , the author regards the discovery of these voids as important and worthy of further investigation

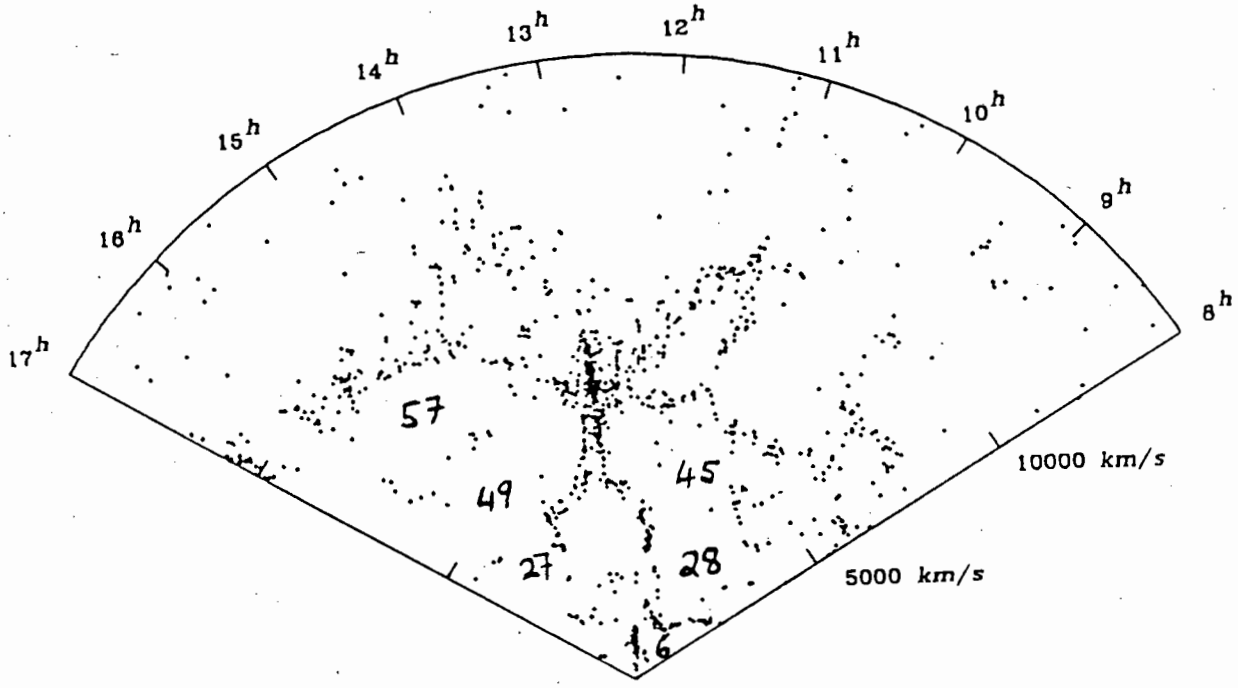

Figure 22 *Voids appearing in Table 4 that are found in the CfA "slice of the universe". The numbers in the diagram refer to the void reference numbers in the right-hand column of Table 4.*

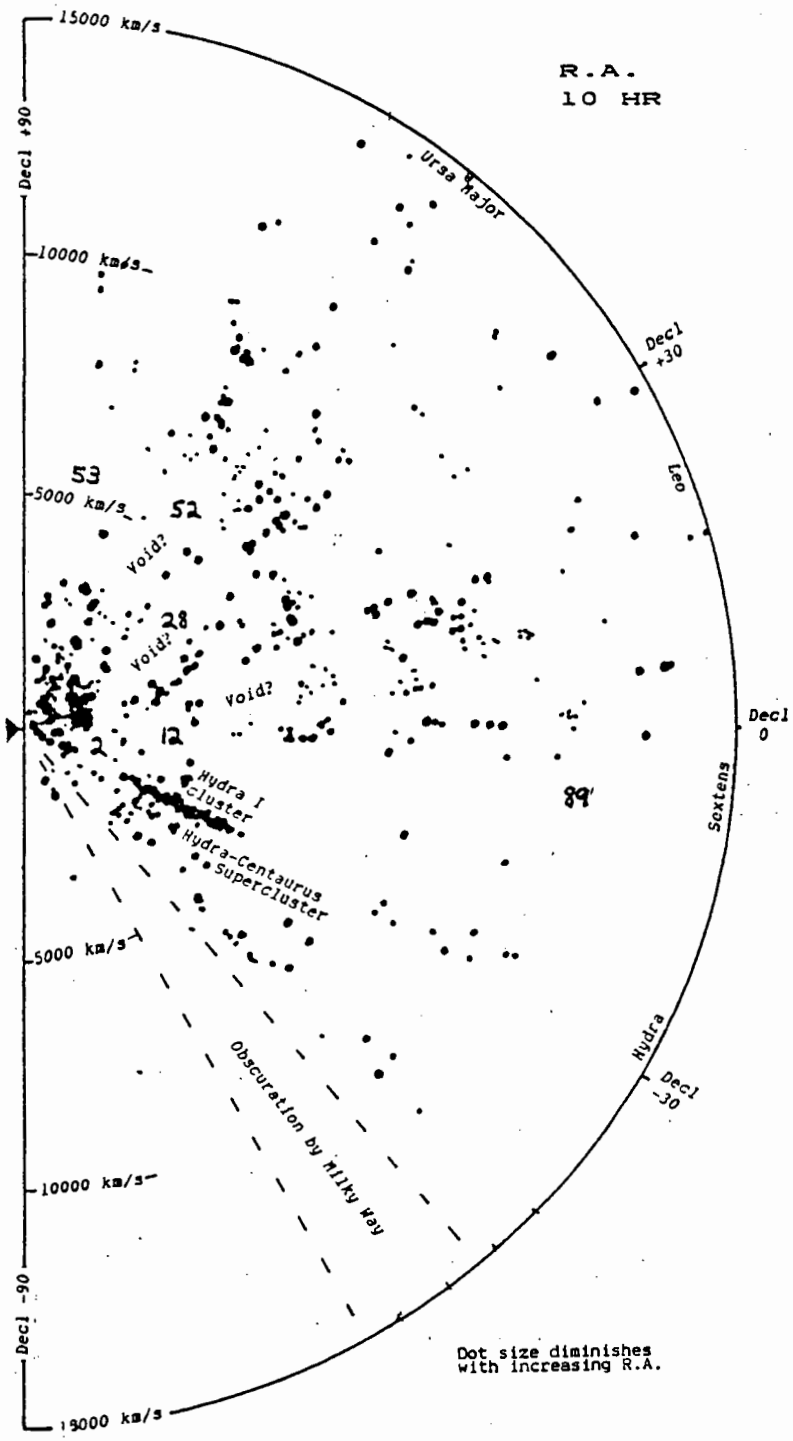

Figure 23 *Voids Appearing in Table 4 that are found in the R.A. = 10 slice of the "Redshift Plots of Huchra's Z Catalogue".*

CHAPTER IV

THE VOID SPECTRUM

4.1) The Void Spectrum

The analysis of the random catalogue simulations has provided us with cut-off redshift for each class of void. Voids located at redshifts less than the cut-off value for their class are considered to be significant.

It is now straightforward to obtain a number density for each volume class of voids. To do this, one must calculate the total volume in which significant voids of a given volume class may occur. This volume is bounded by five different cut-off redshifts, corresponding to the five different declination classes discussed previously. One calculates the volume by adding up the volume of these five wedge-shaped pieces. The number density is then given by the number of significant voids that were found in the volume class, divided by the volume just calculated.

Figure 24 is a graph of the log (number density) versus volume class. Figure 25 is the number density normalized by the volume occupied by the voids of each given class. It is related to the graph of figure 24 through a simple multiplication by the factor s^3, where s is the side length of the base void of the given volume class. In other words, figure 25 is a plot of the relative volume occupied by voids of each volume class.

We refer to figure 25 as our void spectrum. It shows the relative percentage of space occupied by each volume class of voids. It has a number of interesting features. Firstly, it is peaked at a base void side length of 4, corresponding to a distance of 800 km/s. If it is assumed that the cubical base void is embedded inside an empty sphere, we can calculate that these cubes correspond to spherical voids of diameter $11.2h^{-1}$ Mpc. This would indicate that whatever the physical mechanism is that is responsible for the formation of voids,it should favour voids of around $11h^{-1}$ Mpc.

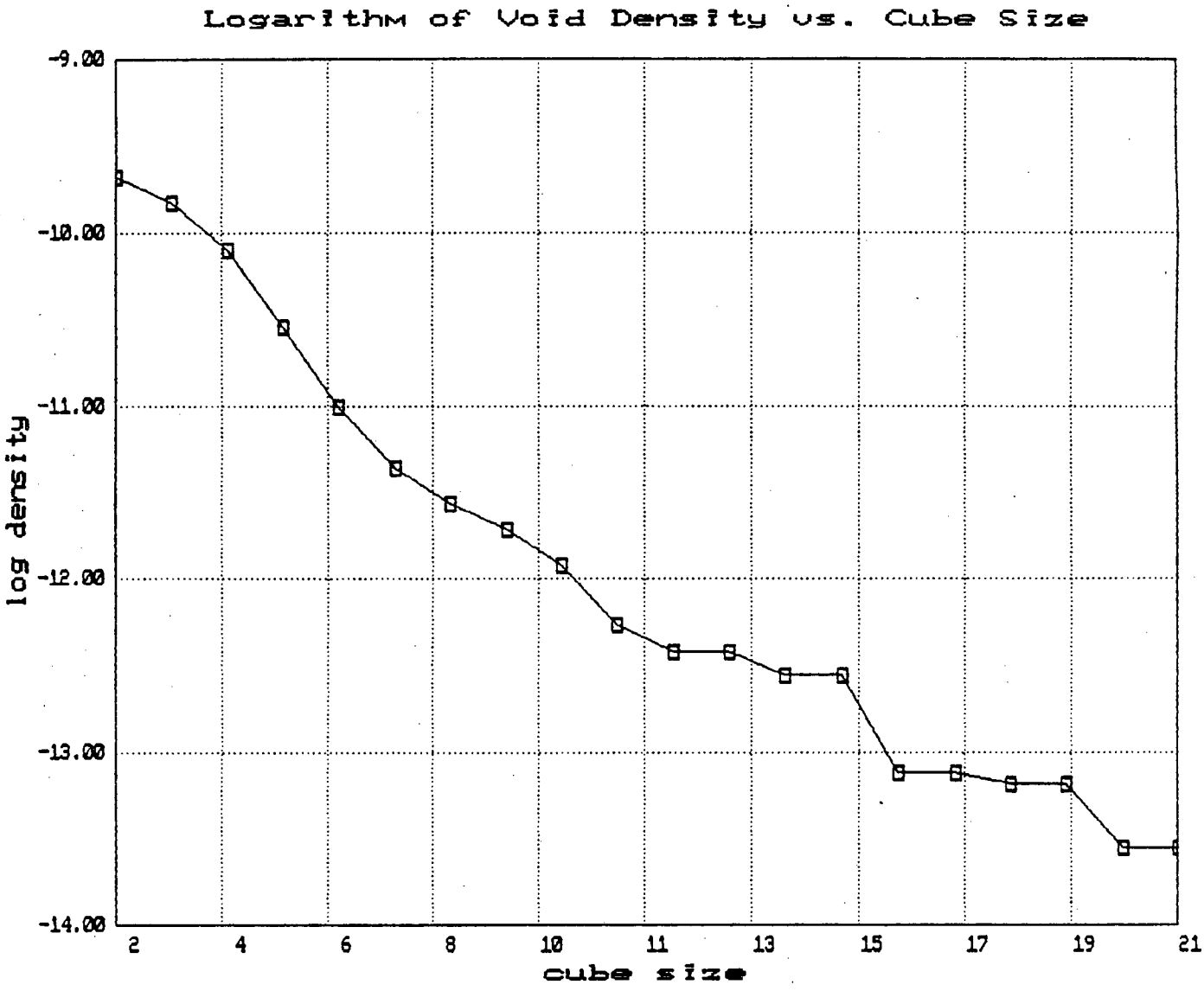

Figure 24 *A plot of the logarithm of void density versus void size. Density is given in units of [no. of voids/(km/s)^3] and void size is given as the number of grid cubes along the edge of the base void.*

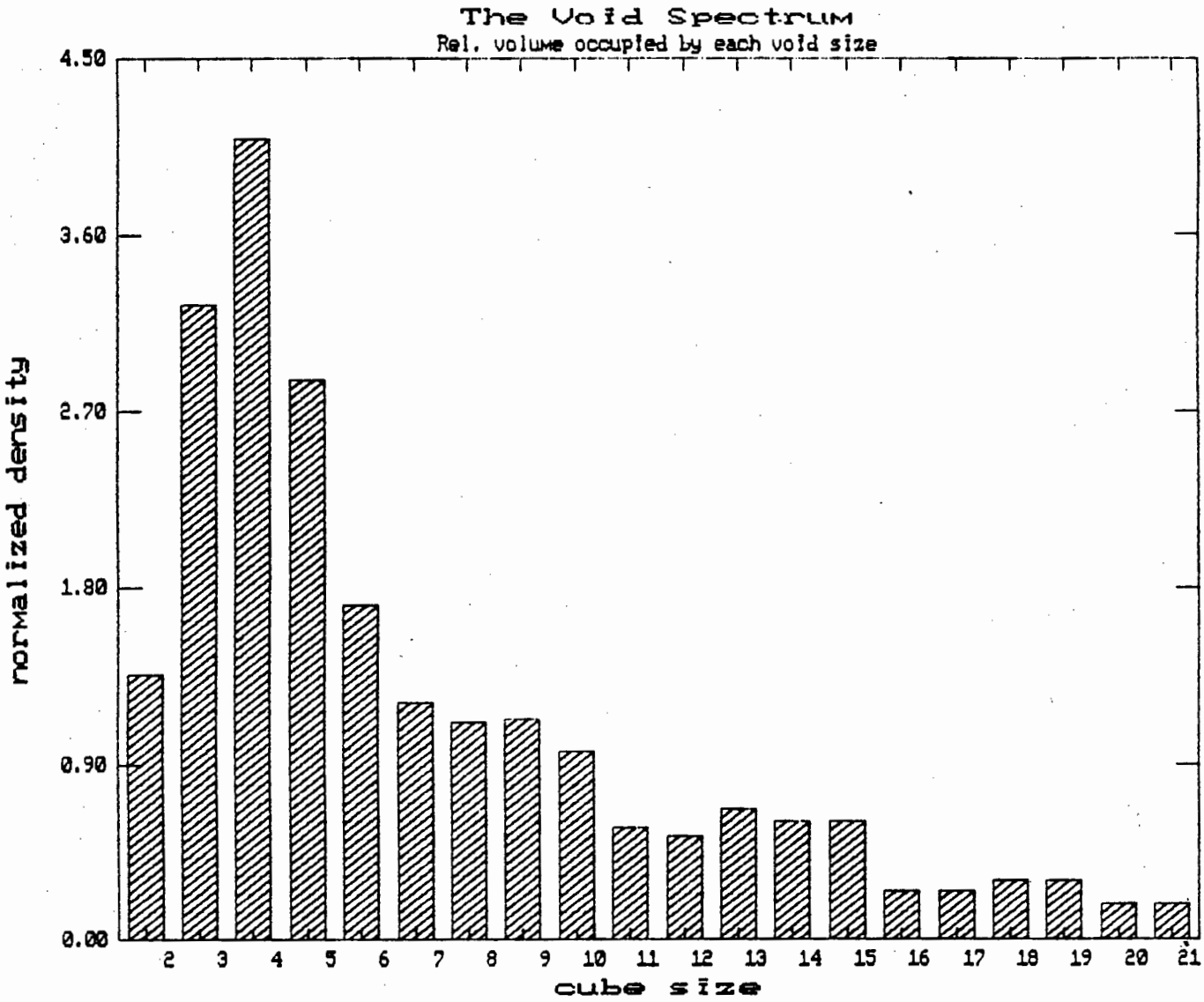

Figure 25 *The void spectrum derived from the galaxy data. The numbers on the y-axis depict the relative percentage of the total volume occupied by each size class of void.*

For comparison, the void spectrum of a Poisson catalogue is plotted in figure 26. This spectrum was obtained using the following procedure. A random catalogue of uniform density was generated into a rectangular volume. The "Voidsearch" algorithm was then used to locate all voids within the catalogue. Number densities were estimated by dividing the number of voids in a given volume class by the volume of the entire rectangular region of the catalogue. Normalized densities are plotted against volume class in figure 26.

As expected, the void spectrum of the Poisson catalogue is flat up to a limiting void size which is simply the result of the finite volume of the catalogue. It is thus clear that a Poisson catalogue does not have a preferred void size. This is , of course, a well-known analytical result. This situation is completely different to the one depicted in figure 25. It is therefore very clear that the distribution of galaxies is not at all a random one.

The second interesting feature are the long tails of the distributions in figures 24 and 25. We have only considered base voids up to 4600 km/s in length, corresponding to spherical voids up to $64.5h^{-1}$ Mpc in diameter. Up to this point, there is no sign of any upper limit to void volume. The frequency of the occurrence of voids in the upper volume range may well prove useful as a point of comparison between our analysis of the observational data and the predictions of the theoretical models.

It is possible to make an estimate of the percentage of all space occupied by voids in the size ranges that have been considered. The percentage of all space occupied by cubical base voids of side lengths between 2 and 20 grid cubes comes out at 22.6%. If it is assumed that the base voids are embedded inside spherical voids, the percentage is more like 33%. It is interesting that these figures are in agreement with an independent estimate made by Fairall [1984]. Nonetheless this still does not allow for deviations from sphericity which might well increase this figure by more than a factor of two. However, a lower bound of 1/3 can cearly be placed on the fraction of all space that is occupied by the empty inner cores of voids in the universe.

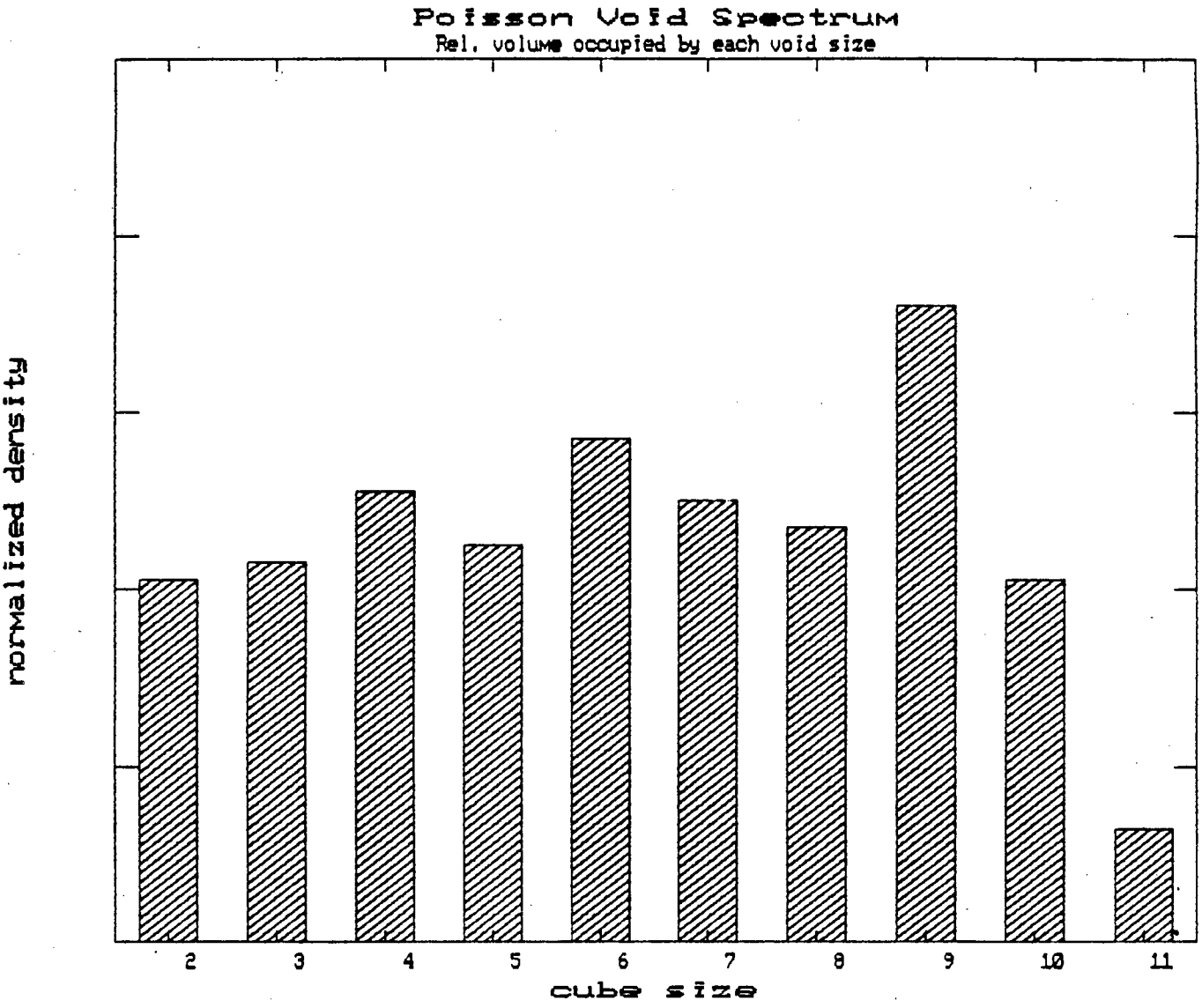

Figure 26 *The void spectrum for a Poisson catalogue of uniform density (i.e. no selection effects present)*

4.2) Summary and Recommendations

A thorough search for voids has been performed throughout the entire sky and out to a redshift of 15 000 km/s. The significance of the voids that were found has been tested by means of numerous random catalogue simulations. Only voids which were found to occur with very small probability in the random catalogues were considered significant.

This analysis has led to a number of interesting results which can be summarized as follows:

1) Confirmation of the validity of visually identified voids in the Southern Redshifts Catalogue.

2) Evidence that statistically significant voids remain empty as more redshifts are added to a galaxy catalogue.

3) Construction of the first "catalogue" of statistically significant voids throughout the whole sky and out to a limiting redshift of 15 000 km/s.

4) Identification of four very large (comparable in size to the Bootes void) , statistically significant voids which occur at relatively low redshift.

5) Construction of a spectrum of sizes of statistically significant voids which shows a definite peak for voids of diameter $11h^{-1}$ Mpc. The void spectrum also shows no sign of a cut-off in void size for diameters up to $64h^{-1}$ Mpc.

6) Placement of a lower bound of 1/3 on the total fraction of all space that is occupied by the inner, empty cores of voids.

Recommendations for future work

The author intends to extend this analysis to various other data sets, including the forthcoming "Catalogue of Radial Velocities of Galaxies" compiled by Palumbo et al. Another possibility would be to extract a void size spectrum from later versions of ZCAT that are due to be published.

One obvious next step would be to apply the author's "Voidsearch" algorithm to data from N - body simulations of theoretical large-scale structure formation models. In this way, the observational void spectrum could be compared to the spectra predicted by the various theories of structure formation. This procedure would involve the application of many of the techniques discussed in section 1.17. One of the most important problems would be deciding how to go from the particle statistics of the simulation to galaxy statistics - a step which is necessary in order to make the link to observational data.

Unfortunately, the author was not in a position to complete this analysis ,as it would have required the co-operation and collaboration of overseas astrophysicists who have written the highly involved N -body simulation codes. The logistics of this would have placed this project well beyond the scope and time constraints of a Masters degree thesis.

Nonetheless it is sincerely hoped that this analysis will be completed in the future as it is believed that the void spectrum in figure 25 represents an important link between theory and observations.

REFERENCES

Abell G.O. (1958): Astrophys J. Suppl. **3**,211

Bahcall N.A., Soneira R.M. (1983): Astrophys. J. **270**, 20

Bond J.R., Szalay A.S. (1983): Astrophys. J. **274**, 443

Brandenburger R., Kahn R., (1984): Phys. Lett. **141B**, 317

Centrella J., Melott A.L. (1983): Nature **305**, 196

Chincarini G., Rood H.J. (1980): Sky Telesc. (May) p364

Cowsik R. (1986) in "Cosmic Pathways", ed. Cowsik, pp. 289-310 (Tata McGraw Publishers)

Davies R.D., Lasenby A.N., Watson R.A., Daintree E.J., Hopkins J., Beckman J., Sanchez-Almeida J., Rebolo R. (1987): Nature **326**, 462

Davis M., Geller M. (1976): Astrophys. J. **288**, 15

Davis M., Huchra J.P., Lathan D.W., Tonry L.J. (1982): Astrophys. J. **253**, 423

Davis M., Peebles P.J.E. (1983): Astrophys. J. **267**, 465

Davis M., Djorgovski S. (1985): Astrophys. J. **299**, 15

De Lapparent V., Geller M.J., Huchra J.P. (1986): Astrophys. J. letters **302**, L1

Doroshkevich A.G., Kotok E.V., Novikov I.D., Polyudov A.N., Shandarin S.F., Sigov Yu.S. (1980): Mon.Not.R.Astron.Soc. **192**, 321

Doroshkevich A.G., Shandarin S.F., Zel'dovich Ya.B. (1982): Comments Astrophys. **IX**, 265

Efstathiou G., Davis M., Frenk C.S., White S.D.M. (1985): Astrophys. J. Suppl **57**, 241

Einasto J., Klypin A.A., Saar E. (1986): Mon.Not.R.Astron.Soc. **219**, 457

Einasto J., Einasto M., Saar E., Jones B.J.T., Martinez V. (1988) in "Large Scale Structure of the Universe", p 241, eds Audouze et al, (Kluwer,Dordrecht)

Einasto J., Einasto M., Gramman M. (1989): Mon. Not.R.Astron.Soc. **238**, 155

Ellis J., Hagelen J.S., Nanopoulos D.V., Olive K., Srednicki M. (1984): Nucl. Phys. B **238**, 453

Fairall A.P. (1984): Publ. Dept. Astr. Univ. Cape Town, no 6.

Fairall A.P. and undergraduate students (1985): Publ. Dept. Astr. Univ. Cape Town, no. 8

Fairall A.P., Jones A. (1988): Publ. Dept. Astr. Univ. Cape Town, No. 10

Fairall A.P. (1989) in "The Proceedings on Morphological Cosmology", eds Flin & Duerbeck, p141, (Springer Verlag)

Frenk C.S., White S.D.M., Davis M. (1983): Astrophys. J. **271**, 417

Fry J.N., Melott A.L. (1985): Astrophys. J. **292**, 395

Fry J.N., Giovanelli R., Haynes M.P., Melott A.L., Scherrer R.J. (1989): Astrophys. J. **340**, 11

Giovanelli R., Haynes M., Chincarini G.L. (1986): Astrophys. J. **311**, 6

Gott J.R., Melott A.L., Dickinson N. (1986): Astrophys. J. **306**, 341

Gott J.R., Weinberg D.H., Melott A.L. (1987): Astrophys. J. **317**, 1

Gott J.R., Miller J., Thuan T.X., Schneider S.E., Weinberg D.H., Gammie C., Polk K., Vogeley M., Jeffrey S., Bhavsar S.P., Melott A.L., Giovanelli R., Haynes M.P., Tully R.B., Hamiltom A.J.S. (1989): Astrophys. J. **340**, 625
Gregory S.A., Thompson L.A. (1978): Astrophys. J. **222**, 784
Gregory S.A., Thompson L.A., Tifft W.A. (1980): Astrophys. J. **243**, 411
Gurbatov S.N., Saichev A.I., Shandarin S.F. (1989): Mon.Not.R.Astron.Soc. **236**, 385
Haynes M.P., Giovanelli R. (1986): Astrophys. J. letters **306**, L55
Huchra J.P., Davis M., Latham D.W., Tonry L.J. (1983): Astrophys. J. Suppl. **53**, 89
Ipser J., Sikivie P. (1983): Phys. Rev. Lett. **50**, 925
Jeans J. (1902): Phil. Trans. Roy. Soc. **199A**, 49
Jeans J. (1928): "Astronomy and Cosmogony", (Cambridge Univ. Press)
Joeveer M., Einasto J. (1978) in I.A.U. Symposium 79, "The Large Scale Structure of the Universe", eds. Longair and Einasto, p241, (Dordrecht, Reidel)
Jones B.J.T., Martinez V., Saar E., Einasto J. (1988): Astrophys. J. letters **332**, L1
Kirshner R.P., Oemler A., Schechter P.L., Shectman S.A. (1981): Astrophys. J. letters **248**, L57
Kirshner R.P., Oemler A., Schechter P.L., Shectman S.H. (1987): Astrophys. J., **314**, 493
Klypin A.A., Kopylov A.I. (1983): Sov.Astron.Lett. **9**, 75
Klypin A.A., Shandarin S.F. (1983): Mon.Not.R.Astron.Soc. **204**, 89
Kofman L.A., Shandarin S.F. (1988): Nature **334**, 129
Kofman L.A. (1989) in "Cracow Summer School on Cosmology", (Springer,Berlin)
Kofman L.A., Pogosyan D., Shandarin S.F. (1990): Mon.Not.R.Astron.Soc. **242**, 200
Krauss L.M. (1986): Scientific American **255**,
Lifshitz E. (1946): J. Phys. USSR **10**, 116
Maddox S.J., Efstathiou G., Loveday J. (1988) in I.A.U. Symp. no. 130, "Evolution of Large Scale Structure in the Universe", eds. Audouze and Szalay, (Dordrecht,Reidel)
Mandelbrot B.B. (1982): "The Fractal Geometry Of Nature", (Freeman and Co.)
Matravers D., Maurellis A. (1990) in "Proceedings on Large Scale Structures and Peculiar Motions", eds Latham & da Costa, (Astron. Soc. of the Pacific)
Maurogordato S., Lachieze-Rey M. (1987): Astrophys J. **320**, 13
Melott A.L. (1987): Mon.Not.R.Astron.Soc. **228**, 1001
Melott A.L., Weinberg D.H., Gott J.R. (1988): Astrophys. J. **328**, 50
Ostriker J.P., Peebles P.J.E. (1973): Astrophys. J. **186**, 467
Otto S., Politzer H.D., Preskill J., Wise M.B. (1986): Astrophys J. **304**, 62
Peebles P.J.E. (1980): "The Large-Scale Structure of the Universe", (Princeton University Press)
Press W.H., Davis M. (1982): Astrophys. J. **259**, 449

Primack J.R., Blumenthal G.R. (1983) in "Formation and Evolution of Galaxies And Large Structures in the Universe", eds. Audouze and Tran Thanh Van, pp 163-183, (Reidel, Dordrecht)
Rees M. (1987): Nature **326**, 455
Rubin V.C., Burstein D., Ford W.K., Thonnard M. (1985): Astrophys. J. **289**, 81
Schaeffer R. (1984): Astron. Astrophys. **134**, L15
Shane C.D., Wirtanen C.A. (1967): Publ. Lick Obs. **22**, 1
Shapiro P.R., Struck-Marcell C., Melott A.L. (1983): Astrophys. J. **275**, 413
Shectman S. (1985): Astrophys J. Suppl. **57**, 77
Silk J. (1968): Astrophys. J. **168**, 459
Soneira R.M., Peebles P.J.E. (1978): Astronom. J. **83**, 845
Stecker F.W., Shafi Q. (1983): Phys. Rev. Lett **50**, 928
Szalay A., Schramm D. (1985): Nature **314**, 718
Tarenghi M., Tifft W,G., Chincarini G., Rood H.J., Thompson L.A. (1979): Astrophys. J. **234**, 793
Tifft W.G., Gregory S.A. (1976): Astrophys J. **205**, 696
Tully R.B. (1982): Astrophys. J. **257**, 389
Tully R.B. (1986): Astrophys. J. **303**, 25
Urson J.M., Wilkinson D.T. (1984): Nature **312**, 417
Vicsek T., Szalay A.S. (1987): Phys. Rev. Lett. **58**, 2818
Weinberg D.H. (1988): Pub. A.S.P. **100**, 1373
Weinberg S. (1971): Astrophys. J. **168**, 175
Weinberg S. (1972): "Gravitation and Cosmology - Principles and Applications of the General Theory of Relativity", (John Wiley & Sons)
White S.D.M. (1979): Mon.Not.R.Astron.Soc. **186**, 145
Winkler H. (1983): Mon.Not.Astr.Soc.Southern Africa **42**, 74
Zel'dovich Ya.B. (1970): Astron. Astrophys. **5**, 84
Zel'dovich Ya.B., Novikov I.D. (1983): "Relativistic Astrophysics vol. 2 - The Structure and Evolution of the Universe", (Univ. of Chicago Press)
Zwicky F., Herzog E., Wild P., Karpowicz M., Kowal C.T. (1961-1968): "Catalog of Galaxies And Clusters of Galaxies", vols. 1-6, (Calif. Inst. of Techn., Pasadena)

APPENDIX

Program "VOIDSEARCH"

```
************************************************************************
*                        MAIN PROGRAM                                  *
* Searches through 200 km/s gridding to find all voids bigger than     *
* four blocks square (200 by 200 by 200 km/s)                          *
************************************************************************

      INTEGER  BLOCK(90,90,90), DATA(90,90,90), COUNT (25)
      OPEN (16, NAME = 'NEWALLVOIDS.DAT',STATUS = 'NEW')
      DO 10 J = 1,25
        COUNT(J) = 0
   10 CONTINUE
      CALL ZERO (BLOCK)
      CALL READ (DATA)
      DO 20 NSIZE = 21,2,-1
        PRINT*, 'NSIZE:', NSIZE
        CALL SELECT (NSIZE,BLOCK,DATA,COUNT)
   20 CONTINUE
      CLOSE (16, STATUS = 'KEEP')
      STOP
      END

************************************************************************
*                    SUBROUTINE ZERO                                   *
* Subroutine initializes array BLOCK to zero. Array BLOCK will         *
* contain data identifying the location and size of the voids          *
************************************************************************

      SUBROUTINE ZERO (BLOCK)
      INTEGER BLOCK(90,90,90)
      DO 60 J = 1,90
        DO 40 K = 1,90
          DO 20 L = 1,90
            BLOCK(L,K,J)=0
   20     CONTINUE
   40   CONTINUE
   60 CONTINUE
      RETURN
      END

************************************************************************
*                      SUBROUTINE READ                                 *
* Subroutine to read contents of  files containing the gridded data    *
* into the array DATA. Each element of the array DATA contains either  *
* a 1 , 0 or -1, corresponding to galaxy, no galaxy or forbidden zone  *
************************************************************************

      SUBROUTINE READ (DATA)
      INTEGER DATA(90,90,90)
      CHARACTER*30 NAME(90)
      DATA (NAME(I), I = 1,45) / 'SYS$SCRATCH:GUINIGRID.DAT;1',
```

```
     + 'SYS$SCRATCH:GUINIGRID.DAT;2','SYS$SCRATCH:GUINIGRID.DAT;3',
     + 'SYS$SCRATCH:GUINIGRID.DAT;4','SYS$SCRATCH:GUINIGRID.DAT;5',
     + 'SYS$SCRATCH:GUINIGRID.DAT;6','SYS$SCRATCH:GUINIGRID.DAT;7',
     + 'SYS$SCRATCH:GUINIGRID.DAT;8','SYS$SCRATCH:GUINIGRID.DAT;9',
     + 'SYS$SCRATCH:GUINIGRID.DAT;10','SYS$SCRATCH:GUINIGRID.DAT;11',
     + 'SYS$SCRATCH:GUINIGRID.DAT;12','SYS$SCRATCH:GUINIGRID.DAT;13',
     + 'SYS$SCRATCH:GUINIGRID.DAT;14','SYS$SCRATCH:GUINIGRID.DAT;15',
     + 'SYS$SCRATCH:GUINIGRID.DAT;16','SYS$SCRATCH:GUINIGRID.DAT;17',
     + 'SYS$SCRATCH:GUINIGRID.DAT;18','SYS$SCRATCH:GUINIGRID.DAT;19',
     + 'SYS$SCRATCH:GUINIGRID.DAT;20','SYS$SCRATCH:GUINIGRID.DAT;21',
     + 'SYS$SCRATCH:GUINIGRID.DAT;22','SYS$SCRATCH:GUINIGRID.DAT;23',
     + 'SYS$SCRATCH:GUINIGRID.DAT;24','SYS$SCRATCH:GUINIGRID.DAT;25',
     + 'SYS$SCRATCH:GUINIGRID.DAT;26','SYS$SCRATCH:GUINIGRID.DAT;27',
     + 'SYS$SCRATCH:GUINIGRID.DAT;28','SYS$SCRATCH:GUINIGRID.DAT;29',
     + 'SYS$SCRATCH:GUINIGRID.DAT;30','SYS$SCRATCH:GUINIGRID.DAT;31',
     + 'SYS$SCRATCH:GUINIGRID.DAT;32','SYS$SCRATCH:GUINIGRID.DAT;33',
     + 'SYS$SCRATCH:GUINIGRID.DAT;34','SYS$SCRATCH:GUINIGRID.DAT;35',
     + 'SYS$SCRATCH:GUINIGRID.DAT;36','SYS$SCRATCH:GUINIGRID.DAT;37',
     + 'SYS$SCRATCH:GUINIGRID.DAT;38','SYS$SCRATCH:GUINIGRID.DAT;39',
     + 'SYS$SCRATCH:GUINIGRID.DAT;40','SYS$SCRATCH:GUINIGRID.DAT;41',
     + 'SYS$SCRATCH:GUINIGRID.DAT;42','SYS$SCRATCH:GUINIGRID.DAT;43',
     + 'SYS$SCRATCH:GUINIGRID.DAT;44','SYS$SCRATCH:GUINIGRID.DAT;45'/
       DATA (NAME(M), M=46,90)/
     + 'SYS$SCRATCH:GUINIGRID.DAT;46','SYS$SCRATCH:GUINIGRID.DAT;47',
     + 'SYS$SCRATCH:GUINIGRID.DAT;48','SYS$SCRATCH:GUINIGRID.DAT;49',
     + 'SYS$SCRATCH:GUINIGRID.DAT;50','SYS$SCRATCH:GUINIGRID.DAT;51',
     + 'SYS$SCRATCH:GUINIGRID.DAT;52','SYS$SCRATCH:GUINIGRID.DAT;53',
     + 'SYS$SCRATCH:GUINIGRID.DAT;54','SYS$SCRATCH:GUINIGRID.DAT;55',
     + 'SYS$SCRATCH:GUINIGRID.DAT;56','SYS$SCRATCH:GUINIGRID.DAT;57',
     + 'SYS$SCRATCH:GUINIGRID.DAT;58','SYS$SCRATCH:GUINIGRID.DAT;59',
     + 'SYS$SCRATCH:GUINIGRID.DAT;60','SYS$SCRATCH:GUINIGRID.DAT;61',
     + 'SYS$SCRATCH:GUINIGRID.DAT;62','SYS$SCRATCH:GUINIGRID.DAT;63',
     + 'SYS$SCRATCH:GUINIGRID.DAT;64','SYS$SCRATCH:GUINIGRID.DAT;65',
     + 'SYS$SCRATCH:GUINIGRID.DAT;66','SYS$SCRATCH:GUINIGRID.DAT;67',
     + 'SYS$SCRATCH:GUINIGRID.DAT;68','SYS$SCRATCH:GUINIGRID.DAT;69',
     + 'SYS$SCRATCH:GUINIGRID.DAT;70','SYS$SCRATCH:GUINIGRID.DAT;71',
     + 'SYS$SCRATCH:GUINIGRID.DAT;72','SYS$SCRATCH:GUINIGRID.DAT;73',
     + 'SYS$SCRATCH:GUINIGRID.DAT;74','SYS$SCRATCH:GUINIGRID.DAT;75',
     + 'SYS$SCRATCH:GUINIGRID.DAT;76','SYS$SCRATCH:GUINIGRID.DAT;77',
     + 'SYS$SCRATCH:GUINIGRID.DAT;78','SYS$SCRATCH:GUINIGRID.DAT;79',
     + 'SYS$SCRATCH:GUINIGRID.DAT;80','SYS$SCRATCH:GUINIGRID.DAT;81',
     + 'SYS$SCRATCH:GUINIGRID.DAT;82','SYS$SCRATCH:GUINIGRID.DAT;83',
     + 'SYS$SCRATCH:GUINIGRID.DAT;84','SYS$SCRATCH:GUINIGRID.DAT;85',
     + 'SYS$SCRATCH:GUINIGRID.DAT;86','SYS$SCRATCH:GUINIGRID.DAT;87',
     + 'SYS$SCRATCH:GUINIGRID.DAT;88','SYS$SCRATCH:GUINIGRID.DAT;89',
     + 'SYS$SCRATCH:GUINIGRID.DAT;90'/
      DO 100 J = 1,90
        OPEN (9, FILE = NAME(J), STATUS = 'OLD')
        DO 90 K = 1,90
          DO 80 L = 1,90
            READ (9,71) NUM
71          FORMAT (I3)
            IF (NUM .EQ. -1) THEN
              DATA (L,K,J) = -1
```

```
            ENDIF
            IF (NUM .GE. 0) THEN
              IF (NUM .EQ. 0) THEN
                DATA (L,K,J) = 0
              ELSE
                DATA (L,K,J) = 1
              ENDIF
            ENDIF
   80     CONTINUE
   90   CONTINUE
        CLOSE (9, STATUS = 'KEEP')
  100 CONTINUE
      RETURN
      END


*************************************************************************
*                  SUBROUTINE SELECT                                    *
* Subroutine calls routines to find square voids of a given size.       *
* The subprogram calls edge-filling routines in order to approximate    *
* the shape of the void more closely. The routine also keeps track of   *
* how many 200 by 200 by 200 km/s blocks there are in each void and     *
* its adjoining faces. Void information is written to file 16.          *
*************************************************************************

      SUBROUTINE SELECT (NSIZE,BLOCK,DATA,COUNT)
      INTEGER DATA(90,90,90), BLOCK(90,90,90),COUNT(25),FLAG,ECNT
      INTEGER TOTSIZ, X, Y, Z
      DO 580 L = 1, 90-NSIZE+1
        DO 560 K = 1,90-NSIZE+1
          DO 540 J = 1,90-NSIZE+1
            FLAG = 1
            CALL FINDBX(J,K,L,NSIZE,FLAG,BLOCK,DATA)
            IF (FLAG .EQ. 1) THEN
              CALL FILLBX (J,K,L,NSIZE,BLOCK)
              COUNT(NSIZE-1) = COUNT(NSIZE-1) + 1
              ECNT = 0
              CALL EDGES(J,K,L,NSIZE,BLOCK,DATA,ECNT)
              TOTSIZ = NSIZE*NSIZE*NSIZE+ECNT
              X = (J-1)*200 -9000 + NSIZE*100
              Y = (K-1)*200 -9000 + NSIZE*100
              Z = (L-1)*200 -9000 + NSIZE*100
              DIST = SQRT(REAL(X)*REAL(X) + REAL(Y)*REAL(Y) +
     +                                      REAL(Z)*REAL(Z))
              RY = REAL(Y)
              RX = REAL(X)
              IF (RX .NE. 0.0) THEN
                PHI = ATAN2D(RY,RX)
              ELSEIF (RY .GT. 0) THEN
                PHI = 90.
              ELSE
                PHI = 270.
              ENDIF
              RA= MOD(PHI+360.,360.)/15.
```

```
              DEC = 90. - ACOSD(REAL(Z)/DIST)
              WRITE(16,538) NSIZE,ECNT,TOTSIZ,X,Y,Z,DIST,RA,DEC
  538         FORMAT (I7,3X,I9,3X,I9,3X,I6,2X,I6,2X,I6,1X,F9.1,3X,
     +                F4.1,3X,F5.1)
            ENDIF
  540     CONTINUE
  560   CONTINUE
  580 CONTINUE
      RETURN
      END

*********************************************************************
*                SUBROUTINE FINDBX                                  *
* Subroutine to find a square void of a given size. The X,Y and Z   *
* coordinates refer to the bottom left hand corner of the cube.     *
*********************************************************************

      SUBROUTINE FINDBX (NX,NY,NZ,NSIZE,NFL,BLOCK,DATA)
      INTEGER DATA(90,90,90), BLOCK(90,90,90)
      DO 180 J = NZ, NZ + NSIZE -1
        DO 160 K = NY, NY + NSIZE -1
          DO 140 L = NX, NX + NSIZE -1
            IF ((DATA(L,K,J) .NE. 0).OR.(BLOCK(L,K,J).NE. 0)) THEN
              NFL = 0
              RETURN
            ENDIF
  140     CONTINUE
  160   CONTINUE
  180 CONTINUE
      RETURN
      END

*********************************************************************
*                  SUBROUTINE FILLBX                                *
* Subroutine to mark an area which has found to be an empty square void*
* Routine fills the appropriate elements of array BLOCK with numbers  *
* corresponding to the size of the square void.                       *
*********************************************************************

      SUBROUTINE FILLBX (NX,NY,NZ,NSIZE,BLOCK)
      INTEGER BLOCK(90,90,90)
      DO 134 J = NZ, NZ + NSIZE -1
        DO 133 K = NY, NY + NSIZE -1
          DO 132 L = NX, NX + NSIZE -1
             BLOCK(L,K,J)= NSIZE
 132     CONTINUE
 133   CONTINUE
 134 CONTINUE
      RETURN
      END
```

```
*************************************************************************
*                    SUBROUTINE EDGES                                   *
* Subroutine to add on adjoining faces to a previously found square     *
* void. Routine attacks one face of the cube at a time. Adjoining faces*
* are added until no adjoining face larger than two thirds the area of *
* the previous face can be found.                                       *
* Routine makes use of FACE and FILLEG. FACE locates the largest        *
* adjoining face and FILLEG decides whether the adjoining face should   *
* be marked in the void array BLOCK.                                    *
*************************************************************************
      SUBROUTINE EDGES (NX,NY,NZ,NSIZE,BLOCK,DATA,ECNT)
      INTEGER DATA(90,90,90), BLOCK(90,90,90),FLAG,ECNT
      NT1 = NSIZE
      NT2 = NSIZE
      NUMB = 1
      FLAG = 1
      N1 = NX
      N2 = NY
* the bottom or lower z=const face
  500 IF ((NT1.GT.0).AND.(FLAG.EQ.1).AND.((NZ-NUMB).GT.0))THEN
        CALL FACE (N1,N2,NZ-NUMB,3,NT1,NT2,NA,NB,NC,DATA)
        IF ((NT1.GT.0).AND.(NT2.GT.0))THEN
          CALL FILLEG (NA,NB,NC,NT1,NT2,3,BLOCK,FLAG,ECNT)
          NUMB = NUMB + 1
          N1 = NA
          N2 = NB
          GOTO 500
        ENDIF
        GO TO 505
      ENDIF
  505 NT1 = NSIZE
      NT2 = NSIZE
      NUMB = 1
      FLAG = 1
      N1 = NX
      N2 = NY
* the top or upper z=const face
  510 IF ((NT1.GT.0).AND.(FLAG.EQ.1).AND.((NZ+NUMB+NSIZE-1).LE.30))THEN
        CALL FACE (N1,N2,NZ+NUMB+NSIZE-1,3,NT1,NT2,NA,NB,NC,DATA)
        IF ((NT1.GT.0).AND.(NT2.GT.0))THEN
          CALL FILLEG (NA,NB,NC,NT1,NT2,3,BLOCK,FLAG,ECNT)
          NUMB = NUMB + 1
          N1 = NA
          N2 = NB
          GOTO 510
        ENDIF
        GO TO 515
      ENDIF
  515 NT1 = NSIZE
      NT2 = NSIZE
      NUMB = 1
      FLAG = 1
      N2 = NY
```

```
      N3 = NZ
* the left or smaller x=const face
  520 IF ((NT1.GT.0).AND.(FLAG.EQ.1).AND.((NX-NUMB).GT.0))THEN
        CALL FACE (NX-NUMB,N2,N3,1,NT1,NT2,NA,NB,NC,DATA)
        IF ((NT1.GT.0).AND.(NT2.GT.0))THEN
          CALL FILLEG (NA,NB,NC,NT1,NT2,1,BLOCK,FLAG,ECNT)
          NUMB = NUMB + 1
          N2 = NB
          N3 = NC
          GOTO 520
        ENDIF
        GO TO 525
      ENDIF
  525 NT1 = NSIZE
      NT2 = NSIZE
      NUMB = 1
      FLAG = 1
      N2 = NY
      N3 = NZ
* the right or larger x=const face
  530 IF ((NT1.GT.0).AND.(FLAG.EQ.1).AND.((NX+NUMB+NSIZE-1).LE.30))THEN
        CALL FACE (NX+NUMB+NSIZE-1,N2,N3,1,NT1,NT2,NA,NB,NC,DATA)
        IF ((NT1.GT.0).AND.(NT2.GT.0))THEN
          CALL FILLEG (NA,NB,NC,NT1,NT2,1,BLOCK,FLAG,ECNT)
          NUMB = NUMB + 1
          N2 = NB
          N3 = NC
          GOTO 530
        ENDIF
        GO TO 535
      ENDIF
  535 NT1 = NSIZE
      NT2 = NSIZE
      NUMB = 1
      FLAG = 1
      N1 = NX
      N3 = NZ
* the front or smaller y=const face
  540 IF ((NT1.GT.0).AND.(FLAG.EQ.1).AND.((NY-NUMB).GT.0))THEN
        CALL FACE (N1,NY-NUMB,N3,2,NT1,NT2,NA,NB,NC,DATA)
        IF ((NT1.GT.0).AND.(NT2.GT.0))THEN
          CALL FILLEG (NA,NB,NC,NT1,NT2,2,BLOCK,FLAG,ECNT)
          NUMB = NUMB + 1
          N1 = NA
          N3 = NC
          GOTO 540
        ENDIF
        GO TO 545
      ENDIF
  545 NT1 = NSIZE
      NT2 = NSIZE
      NUMB = 1
      FLAG = 1
      N1 = NX
```

```
      N3 = NZ
* the back or larger y= const face
  550 IF ((NT1.GT.0).AND.(FLAG.EQ.1).AND.((NY+NUMB+NSIZE-1).GT.0))THEN
        CALL FACE (N1,NY+NUMB+NSIZE-1,N3,2,NT1,NT2,NA,NB,NC,DATA)
        IF ((NT1.GT.0).AND.(NT2.GT.0))THEN
          CALL FILLEG (NA,NB,NC,NT1,NT2,2,BLOCK,FLAG,ECNT)
          NUMB = NUMB + 1
          N1 = NA
          N3 = NC
          GOTO 550
        ENDIF
        GO TO 555
      ENDIF
  555 RETURN
      END

*************************************************************************
*                        SUBROUTINE FACE                                *
* Subroutine to determine whether a previously found square void has    *
* an adjoining face.The routine will find the biggest square adjoining *
* face (or its rectangular extension) larger than two thirds           *
* the area of the previous face that was found.                        *
*************************************************************************

      SUBROUTINE FACE (NX,NY,NZ,N,NT1,NT2,NA,NB,NC,DATA)
      INTEGER DATA(90,90,90)
      INTEGER FCE(25,25),FLAG
* N tells you whether the face is orientated in the x,y or z direction.
* One must read in the data accordingly.FCE stores the data for the face
* to be tested.
      IF (N .EQ. 1) THEN
        J1 = NX
        J2 = NX
        K1 = NY
        K2 = NY + NT1 - 1
        L1 = NZ
        L2 = NZ + NT2 - 1
      ELSEIF (N .EQ. 2) THEN
        J1 = NX
        J2 = NX + NT1 - 1
        K1 = NY
        K2 = NY
        L1 = NZ
        L2 = NZ + NT2 - 1
      ELSE
        J1 = NX
        J2 = NX + NT1 - 1
        K1 = NY
        K2 = NY + NT2 - 1
        L1 = NZ
        L2 = NZ
      ENDIF
      DO 380 L = L1,L2
        DO 360 K = K1, K2
```

```
          DO 340 J = J1,J2
            IF (N .EQ. 1) FCE(K-K1+1,L-L1+1) = DATA(J,K,L)
            IF (N .EQ. 2) FCE(J-J1+1,L-L1+1) = DATA(J,K,L)
            IF (N .EQ. 3) FCE(J-J1+1,K-K1+1) = DATA(J,K,L)
  340     CONTINUE
  360   CONTINUE
  380 CONTINUE
* Initialize values of variables describing the adjoining face so that
* zeroes are returned if no adjoining face is found.
      MXDIM = 0
      MXSIZ = 0
      MYSIZ = 0
      MX = 0
      MY = 0
* From each block of FCE which contains no galaxies, search for a
* boundary of a square -- search to the right and also upwards
* (considering the lower left-hand corner as the origin)
      DO 420 K = 1, NT2-1
        DO 410 J =1, NT1-1
          IF (FCE(J,K) .EQ. 0) THEN
            NUMX = 1
            NUMY = 1
  390       IF ((J+NUMX.LE.NT1).AND.(FCE(J+NUMX,K).EQ.0))THEN
              NUMX = NUMX + 1
              GOTO 390
            ENDIF
  392       IF ((K+NUMY.LE.NT2).AND.(FCE(J,K+NUMY).EQ.0))THEN
              NUMY = NUMY+1
              GOTO 392
            ENDIF
* Search for the biggest square contained within the boundaries, if the
* boundaries allow for a square 400 by 400 km/s or larger and if the
* size of the boundaries indicates that a square larger than previously
* found one might exist.
            IF ((NUMX.GE.2).AND.(NUMY.GE.2).AND.
     +                                      (NUMX*NUMY.GT.MXDIM))THEN
              DO 396 NM = 2, MIN(NUMX,NUMY)
                FLAG = 0
                DO 395 M = K, K+NM-1
                  DO 393 L = J, J+NM-1
                    IF (FCE(L,M) .NE. 0) THEN
                      FLAG = 1
                      NSQ = NM - 1
                      GOTO 397
                    ENDIF
  393             CONTINUE
  395           CONTINUE
  396         CONTINUE
  397         IF (FLAG .EQ. 0) NSQ = MIN (NUMX,NUMY)
* If a square 400 by 400 km/s or larger is found, search for its largest
* rectangular extension.
  400         IF (NSQ .GE. 2) THEN
                IF (MXDIM .EQ. 0) THEN
                  MXDIM = NSQ*NSQ
```

```
                MXSIZ = NSQ
                MYSIZ = NSQ
                MX = J
                MY = K
              ENDIF
              IF (NUMX .GT. NSQ) THEN
                NFRR = 0
                DO 403 M = K, K+NSQ-1
                  DO 402 L = J+NSQ, J+NUMX-1
                    IF (FCE(L,M) .NE. 0) THEN
                      NNX = L-J
                      NNY = NSQ
                      NFRR = 1
                      IF (NNX*NNY .GE. MXDIM) THEN
                        MXDIM = NNX*NNY
                        MXSIZ = NNX
                        MYSIZ = NNY
                        MX = J
                        MY = K
                      ENDIF
                      GOTO 404
                    ENDIF
402               CONTINUE
403             CONTINUE
                IF ((NFRR .EQ. 0).AND.(NUMX*NSQ .GE. MXDIM))THEN
                  MXDIM = NUMX*NSQ
                  MXSIZ = NUMX
                  MYSIZ = NSQ
                  MX = J
                  MY = K
                ENDIF
              ENDIF
404           IF (NUMY .GT. NSQ) THEN
                NFDR = 0
                DO 406 M = K+NSQ, K+NUMY-1
                  DO 405 L = J, J+NSQ-1
                    IF (FCE(L,M) .NE. 0) THEN
                      NNX = NSQ
                      NNY = M-K
                      NFDR = 1
                      IF (NNX*NNY .GE. MXDIM) THEN
                        MXDIM = NNX*NNY
                        MXSIZ = NNX
                        MYSIZ = NNY
                        MX = J
                        MY = K
                      ENDIF
                      GOTO 410
                    ENDIF
405               CONTINUE
406             CONTINUE
                IF ((NFDR .EQ. 0).AND.(NUMY*NSQ .GE. MXDIM))THEN
                  MXDIM = NUMY*NSQ
                  MXSIZ = NSQ
```

```
                    MYSIZ = NUMY
                    MX = J
                    MY = K
                  ENDIF
                ENDIF
              ENDIF
            ENDIF
          ENDIF
  410   CONTINUE
  420 CONTINUE
* NA,NB and NC are the coordinates of the corner of the face closest to
* the origin
      IF (N .EQ. 1) THEN
        NA = NX
        NB = NY + MX -1
        NC = NZ + MY -1
      ELSEIF (N .EQ. 2) THEN
        NA = NX + MX -1
        NB = NY
        NC = NZ + MY -1
      ELSE
        NA = NX + MX -1
        NB = NY + MY -1
        NC = NZ
      ENDIF
* NT1 and NT2 are the dimensions of the adjoining face (zero if one cannot
* be found)
      A1 = REAL(MXSIZ)* REAL (MYSIZ)
      IF (MIN(NT1,NT2) .GE. 12) THEN
        A2 = REAL(NT1)*REAL(NT2)*0.75
      ELSE
        A2 = REAL(NT1)*REAL(NT2)*0.66
      ENDIF
      IF (A1 .GE. A2)THEN
        NT1 = MXSIZ
        NT2 = MYSIZ
      ELSE
        NT1 = 0
        NT2 = 0
      ENDIF
      RETURN
      END

*************************************************************************
*                  SUBROUTINE FILLEG                                    *
* Subroutine decides whether a previously found adjoining face ought    *
* to be marked in the array BLOCK. This depends on whether there is     *
* overlap between the area occupied by the adjoining face and element   *
* already marked in the array BLOCK.                                    *
*************************************************************************

      SUBROUTINE FILLEG (NA,NB,NC,NT1,NT2,N,BLOCK,FLAG,ECNT)
      INTEGER BLOCK(90,90,90), FLAG ,ECNT
      IF (N .EQ. 1) THEN
```

```
        J1 = NA
        J2 = NA
        K1 = NB
        K2 = NB + NT1 -1
        L1 = NC
        L2 = NC + NT2 -1
      ELSEIF (N .EQ. 2) THEN
        J1 = NA
        J2 = NA + NT1 -1
        K1 = NB
        K2 = NB
        L1 = NC
        L2 = NC + NT2 -1
      ELSE
        J1 = NA
        J2 = NA + NT1 -1
        K1 = NB
        K2 = NB + NT2 -1
        L1 = NC
        L2 = NC
      ENDIF
      FLAG = 1
      DO 680 L = L1,L2
        DO 660 K = K1,K2
          DO 640 J = J1,J2
            IF (BLOCK(J,K,L) .NE. 0) THEN
              FLAG = 0
              GOTO 700
            ENDIF
  640     CONTINUE
  660   CONTINUE
  680 CONTINUE
* if adjoining face is not in an already occupied area, fill in the adjoining
* face in array BLOCK and increment the edge count.
  700 IF (FLAG .EQ. 1) THEN
        DO 760 L = L1,L2
          DO 740 K = K1,K2
            DO 720 J = J1,J2
              BLOCK(J,K,L) = 1
  720       CONTINUE
  740     CONTINUE
  760   CONTINUE
        ECNT = ECNT + NT1*NT2
      ENDIF
      RETURN
      END
```